

Comparison of Simplified Models of Urban
Climate for Improved Prediction of Building
Energy Use in Cities

by

Michael A. Street

B.S., Physics, Morehouse College (2011)

Submitted to the Department of Architecture
in partial fulfillment of the requirements for the degree of

Master of Science in Building Technology

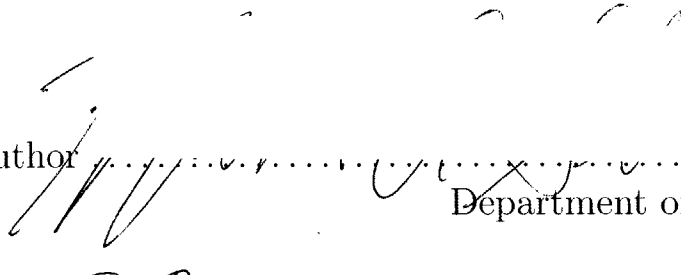
at the

MASSACHUSETTS INSTITUTE OF TECHNOLOGY

June 2013

© Massachusetts Institute of Technology 2013. All rights reserved.

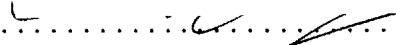
Signature of Author



Department of Architecture

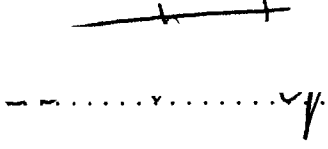
May 10, 2013

Certified by

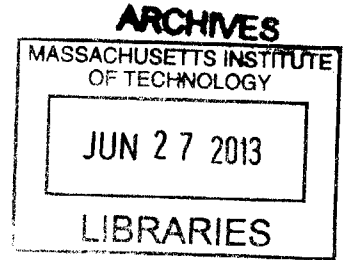


Christoph Reinhart
Associate Professor
Thesis Supervisor

Accepted by



Takehiko Nagakura
Associate Professor
and Chair of Department Committee on Graduate Students



Thesis Readers

Christoph Reinhart

Associate Professor, Department of Architecture

John Ochsendorf

*Professor, Department of Architecture and
Department of Civil and Environmental Engineering*

Les Norford

Professor, Associate Head, Department of Architecture

Comparison of Simplified Models of Urban Climate for Improved Prediction of Building Energy Use in Cities

by

Michael A. Street

Submitted to the Department of Architecture
on May 10, 2013, in partial fulfillment of the
requirements for the degree of
Master of Science in Building Technology

Abstract

Thermal simulation of buildings is a requisite tool in the design of low-energy buildings, yet, definition of weather boundary conditions during simulation of urban buildings suffers from a lack of data that accounts for the UHI effect. To overcome barriers preventing the use of more representative climate data in building thermal simulations, this thesis evaluates two recently developed methods for generating urban weather files from a rural station. The two methods examined are computationally inexpensive. The first method is the urban weather generator (UWG) a model developed by Bueno *et al.* and the second is a temperature alteration algorithm developed by Crawley 2008. Actual weather data is used to validate the modeled urban data. Actual and modeled weather data is then used in simulation of a typical single-family and small office building to quantify normalized energy use metrics of urban buildings. Applying the UWG to appropriate rural weather data reduces the error associated with energy prediction of an urban single-family building by nearly half (21% to 13%). If the Crawley algorithm is applied to rural data, the resulting weather data will produce simulation results that are lower (- 8%) and upper limits (+ 11%) to the actual urban energy simulation results. For applications that either require feedback with the urban design or have extensive data on the urban morphology we recommend the use of the UWG with a radius of 500 m. For applications that lack urban site data and are order of magnitude estimations, the Crawley algorithm generally is able to provide extremes of the predicted EUI.

Thesis Supervisor: Christoph Reinhart
Title: Associate Professor

Acknowledgments

Without the support of funding from the MIT Presidential Fellowship and the MIT Energy Initiative, this work and my education, would not have been possible. For that I am deeply grateful.

To my committee, Christoph, John, and Les, you each provided considerable guidance and assistance. Thank you for all the time each of you invested in overseeing my matriculation. The knowledge I have gained in these short two years has been immense and I appreciate your individual efforts in fostering my success. Bruno, thank you as well for the many conversations and emails that aided my first steps.

To my family, Marcia A. Phifer, Lloyd C. Street, Mom, Dad, Steve, Cassandra, your love and support was a calming presence in an otherwise rough sea.

Anton, Sabs, Tomo we keep each other sane. Keep fighting.

Special thanks to these groups of individuals for their unwavering loyalty, faith, and support: The *Apotheotic* 21, Academy of Courageous Minority Engineers, MSRP.

'Onward and Upward..'

Contents

List of Figures	11
List of Tables	17
1 Introduction	19
1.1 Purpose	20
1.2 The Urban Heat Island Effect	20
1.2.1 Energetic Basis & Analysis Methods	21
1.2.2 Implications for Building Energy Use	24
2 Literature Review	27
2.1 Simple Modeling Tools in Urban Climate Assessment	28
2.1.1 Empirical Models	28
2.1.2 Physical Models	31
2.2 Advanced Modeling Tools in Urban Climate Assessment	32
2.2.1 Emergence of Tractable Urban Climate Models	34
2.3 Needs & Current Limitations	36
3 Methodology	37
3.1 Site Descriptions	37
3.2 Experiment 1: UHI Quantification	39
3.3 Experiment 2: UHI Impact on Building EUI	44
3.4 Experiment 3: Simulated vs. Actual Weather Elements	44

3.5	Experiment 4: Building EUI & Simulated Weather	47
3.6	Experiment 5: Parametric Analysis of UWG	48
3.7	Summary	49
4	Results & Discussion	51
4.1	Experiment 1: UHI Quantification	51
4.2	Experiment 2: UHI Impact on Building EUI	58
4.3	Experiment 3: Simulated vs. Actual Weather Elements	62
4.4	Experiment 4: Building EUI & Simulated Weather	66
4.5	Experiment 5: Parametric Analysis of UWG	74
4.6	Summary	78
5	Conclusions	83
5.1	Key Findings	83
5.2	Future Work	85
A	EPW Tutorial	89
A.1	Weather Elements	89
A.1.1	Mining & Processing	90
A.1.2	Data Sources	90
A.1.3	User Functions	94
A.1.4	Demo: EPW from online data	102
A.1.5	Demo: Solar Data for EPW File	113
B	Whole Building Models	119
B.0.6	Single-Family Building	119
B.0.7	Small Office Building	123
C	References	127

List of Figures

1-1	Spatial distribution of the air-temperature across a city in section (a) and plan (b) view. The peak air-temperature occurs at the center of the ‘island’ as wind traverses from the city edge at A to B.(<i>Figure from Oke</i>)	22
3-1	Map of the Boston, MA metropolitan area and locations of each of the weather stations used to collect data. Each site’s local geography and proximity to the urban station may be seen. From left to right: Rural, Urban, TMY. Aerial photograph from Microsoft’s Bing Maps	39
3-2	Boston Logan International Airport is shown. We see just to the right the coastline of the larger peninsula and a number of runways. Aerial photograph from MassGIS (Office of Geographic Information (MassGIS), 2011).	40
3-3	The urban context is shown. We see that there are not many tall buildings, but the overall density and urban fabric is much more built up than at either reference station. Aerial photograph from MassGIS (Office of Geographic Information (MassGIS), 2011).	41
3-4	Hanscom Air Force base is shown. Again there are a number of runways that differ from a grassy rural area, but there are neither large geographic obstructions nor bodies of water. Aerial photograph from MassGIS (Office of Geographic Information (MassGIS), 2011).	42

3-5	The KMACAMBR4 PWS weather station is shown with instruments mounted above a residential building in central Cambridge, MA. Image by the author.	43
4-1	T-test results for the urban versus rural comparison of mean peak, night-time temperature for each month of the year 2011. The 80% confidence interval is the dashed line. Only months from KBED fall within the 95% confidence interval.	53
4-2	Dry-bulb temperature residuals between KBED and KMACAMBR4. The maximum urban-rural temperature difference is 5.7°C when all 8760 hours of the EPW file are considered. Outliers are excluded from selection of the maximum temperature difference	54
4-3	Distribution of dry-bulb temperature residuals between KBED and KMACAMBR4. All 8760 hours of the EPW file are considered for calculation of mean and standard deviation. For improved robustness the median is also calculated.	54
4-4	Dry-bulb temperature residuals between KBOS and KMACAMBR4. The maximum urban-rural temperature difference is 3.1°C when all 8760 hours of the EPW file are considered. Outliers are excluded from selection of the maximum temperature difference	55
4-5	Distribution of dry-bulb temperature residuals between KBOS and KMACAMBR4. All 8760 hours of the EPW file are considered for calculation of mean and standard deviation. For improved robustness the median is also calculated.	55
4-6	Dry-bulb temperature residuals between KBOS and KMACAMBR4. The maximum urban-rural temperature difference is 2.9°C when only night and low-wind speed hours of the EPW file are considered. Outliers are excluded from selection of the maximum temperature difference	56

4-7	Distribution of dry-bulb temperature residuals between KBOS and KMACAMBR4. Only night and low-wind speed of the EPW file are considered for calculation of mean and standard deviation. For improved robustness the median is also calculated.	56
4-8	Dry-bulb temperature residuals between KBOS and KMACAMBR4. The maximum urban-rural temperature difference is 2.9°C when only night and low-wind speed hours of the EPW file are considered. Outliers are excluded from selection of the maximum temperature difference	57
4-9	Distribution of dry-bulb temperature residuals between KBOS and KMACAMBR4. Only night and low-wind speed of the EPW file are considered for calculation of mean and standard deviation. For improved robustness the median is also calculated.	57
4-10	Variation in a single-family building’s simulated total EUI, heating EUI, and cooling EUI based on the source of weather data for simulation. The goal is to predict EUI at the Urban site, but typically only data from rural sites is available. Cooling EUI is two orders of magnitude less than heating EUI for this cold, moist climate.	60
4-11	Variation in a small office building’s simulated total EUI, heating EUI, and cooling EUI based on the source of weather data for simulation. The goal is to predict EUI at the Urban site, but typically only data from rural sites is available.	61
4-12	A summer design week comparison between the urban station and two modeled stations with KBED as the input rural station.	64
4-13	A winter design week comparison between the urban station and two modeled stations with KBED as the input rural station.	64
4-14	A summer design week comparison between the urban station and two modeled stations with KBOS as the input rural station.	65
4-15	A winter design week comparison between the urban station and two modeled stations with KBOS as the input rural station.	65

4-16	Changes in the simulated total EUI for a single-family building with variation of EPW values. KBED as the rural base.	67
4-17	Changes in the simulated total EUI for a small office building with variation of EPW values. KBED as the rural base.	67
4-18	Changes in the simulated total EUI for a single-family building with variation of EPW values. KBOS as the rural base.	68
4-19	Changes in the simulated total EUI for a small office building with variation of EPW values. KBOS as the rural base.	68
4-20	Changes in the total EUI for a single-family building. The rural station is KBED and the dashed lines are the limits imposed by the rural and urban values.	70
4-21	Changes in the total EUI for a small office building. The rural station is KBED and the dashed lines are the limits imposed by the rural and urban values.	71
4-22	Changes in the total EUI for a single-family building.	72
4-23	Changes in the total EUI for a small office building.	73
4-24	Evolution of the EUI for a single-family building for various iterations of the UWG. KBED as the rural base.	76
4-25	Evolution of the EUI for a small office building for various iterations of the UWG. KBED as the rural base.	76
4-26	Evolution of the EUI for a single-family building for various iterations of the UWG. KBOS as the rural base.	77
4-27	Evolution of the EUI for a small office building for various iterations of the UWG. KBOS as the rural base.	77
A-1	Websites that store PWS information facilitate direct access of weather data through web addresses that house comma separated value files. Each address is defined by a station and date string.	92

A-2	All weather elements were processed via the same algorithm, in which the data frequency was determined and then missing elements were filled with the previous element carried forward. Sub-hourly data was first filled and an hourly average was then applied to produce the EPW.	93
A-3	Average Monthly dry-bulb temperature at KBED in 2011.	108
A-4	Average Monthly dry-bulb temperature of the Boston TMY3 file. . .	109
A-5	Hourly dry-bulb temperature recorded at the weather station monitored by the Sustainable Design Lab @ MIT.	111
A-6	Average monthly dry-bulb temperature recorded at the weather station monitored by the Sustainable Design Lab @ MIT through 2013-05-05. Monthly maximum and minimum dry-bulb temperatures are identified by the red and blue lines, respectively.	112
A-7	Hourly Direct Normal Irradiance and Diffuse Horizontal Irradiance for a summer week in 2011 collected from an urban weather station. . . .	118
B-1	Single-Family building used for EnergyPlus simulations.	122
B-2	Schematic diagram of the single zone single family building heating and cooling system. Dehumidification occurs at the zone level and the fan is in a ‘blow-through’ configuration.	122
B-3	Small Office building used for EnergyPlus simulations.	125
B-4	Schematic diagram of the five zone small office building heating and cooling system. Zone air returns through a shared return path and passes through an outdoor air mixing box prior to being supplied to each zone.	125

List of Tables

3.1	Inputs to the UWG with Cambridge specific urban geometric parameters. Other parameters from UWG validation in Toulouse, France.	46
3.2	An ‘x’ indicates, which urban variables are placed into each airport EPW to create the experimental weather files.	48
4.1	Average peak, night-time dry-bulb temperature for each month of 2011 at each weather data site. The statistical significance of urban versus rural temperature differences is plotted in Fig. 4-1.	53
4.2	Normalized energy metrics for the single-family building under three separate simulation cases. The target values are those predicted from observed Urban weather data.	60
4.3	Normalized metrics of the small office building under three separate simulation cases. The small office building responds weakly to climatic variables when compared to the single-family building. KBOS and Urban weather data predict nearly identical values of the EUI.	61
4.4	Annual (<i>A</i>), summer (<i>S</i>) and winter (<i>W</i>) statistical analysis of modeled weather files: UWG (<i>U</i>), $\Delta\text{DB}=1^{\circ}\text{C}$ (1) and $\Delta\text{DB}=5^{\circ}\text{C}$ (5).	63
4.5	Normalized energy metrics for the single-family building with both urban weather schemes and KBED as the rural station.	70
4.6	Normalized energy metrics for the small office building with both urban weather schemes and KBED as the rural station.	71
4.7	Normalized energy metrics for the single-family building with both urban weather schemes and KBOS as the rural station.	72

4.8	Normalized energy metrics for the small office building with both urban weather schemes and KBOS as the rural station.	73
4.9	Change in urban parameters with increasing radius.	75
4.10	Each model's advantages and limitations is summarized above. A core limitation of the UWG is the inability to handle input weather data that is not strictly rural.	81
B.1	Simulation parameters for each EnergyPlus building model used in this study.	126

Chapter 1

Introduction

Thermal and daylight simulations of buildings have become common analysis tools for the design of new construction and assessment of building retrofits. Analytic building models developed for simulation have the ability to guide key decisions about building form, orientation, structure, envelope and mechanical system. The various combinations of these systems define the building's operational performance. Yet despite advances in technical capability to simulate whole-building thermal loads, there is a growing understanding that climate assumptions used during analysis and design to predict performance may be inadequate (Oxizidis *et al.*, 2007).

Current thermal simulation practice generally relies on either typical meteorological year (TMY) data for predicting a building's average performance or actual meteorological year (AMY) data for calibrating building models to observed data. However, there is cause for concern because these widely used TMY files, which serve as the basis for building design and evaluation, originate from long-term weather data stations outside of urban areas, typically at airports (Wilcox and Marion, 2008). Since many building sites tend to be urban, using weather data from a rural site introduces a bias in performance metrics due to the well-known urban heat island (UHI) effect (Arnfield, 2003). To work around this bias, a modeler may collect weather data from an urban station if one is available. However, if one is not available, or if the planned urban site and context is not yet built, methods exist that facilitate the use of a rural reference station instead.

This chapter defines the thesis’s purpose, then further describes the UHI effect and its implications on whole-building simulation, which further establishes the purpose, and concludes with a brief outline of the topics to follow.

1.1 Purpose

To facilitate the use of more representative weather files during whole-building simulation, this thesis evaluates two recently developed techniques for generating urban weather files from a rural station. The two methods examined are computationally inexpensive. The first method is the urban weather generator (UWG) a model developed at MIT by Bueno *et al.* (2012). The second is a temperature alteration scheme developed by Crawley (2008).

To test these models, we use them to transform rural weather data from two sites outside of Cambridge, MA, USA into urban weather files. Observed urban weather data from central Cambridge are compared to the modeled data.

The main questions addressed are:

1. How much can differences between urban and rural weather data affect the energy use intensity (EUI) of a typical residential and small commercial building?
2. Can the UWG or Crawley methods reduce these discrepancies?

1.2 The Urban Heat Island Effect

Anthropogenic processes impact many aspects of society including human health, global economics and access to natural services (Patz *et al.*, 2005; Heal, 2008; Committee on Ecological Impacts of Climate Change, 2008).

A significant manifestation of these anthropogenic processes is climate change on both global and regional scales. At the regional scale, cities and associated urban areas have a documented effect on regional weather elements (Baklanov *et al.*, 2005). In particular, the central core of urban areas tends to have the greatest impact on weather

elements (Oke, 1982). Analyzing the spatial temperature distribution throughout a city in cross-section reveals behavior that can be described as a ‘heat island’ (Fig. 1-1). This phenomenon, named the urban heat island (UHI) effect, is well documented throughout the literature of atmospheric sciences and has been generally accepted as fact since the mid-1970s (Oke, 1973; Lowry, 1977).

The impact of cities on the regional environment entered the realm of atmospheric science with a series of books by Luke Howard in the 19th century, in which he analyzed the climate of London (as cited in Landsberg 1981). Howard made the first published observations that London’s urban center is warmer than the surrounding countryside. Yet the foundation for understanding the physical processes that govern the UHI effect is found in the body of work extending from the late 1960s to early 1980s (Oke, 1974; Landsberg, 1981; Oke, 1979). Establishing the energetic and physical basis of the UHI allowed the work of the late 20th and early 21st centuries to focus on novel methods of UHI quantification, mitigation techniques, and modeling of urban influences on regional climate (Bechtel, 2011; Hsieh *et al.*, 2007; Erell, 2008; Lun *et al.*, 2009).

A complete review of the UHI literature is beyond the scope of this thesis and the reader is directed to the thorough work of Arnfield 2003. However, to place this thesis into the proper context, necessary background on the UHI, its energetic basis and implications to architecture will now be discussed.

1.2.1 Energetic Basis & Analysis Methods

The UHI literature is primarily concerned with two manifestations of the impacts of urbanization on regional weather elements: air-temperature and surface-temperature heat islands. Throughout this thesis, use of UHI refers exclusively to air-temperature heat islands in cities as explained in the following sections.

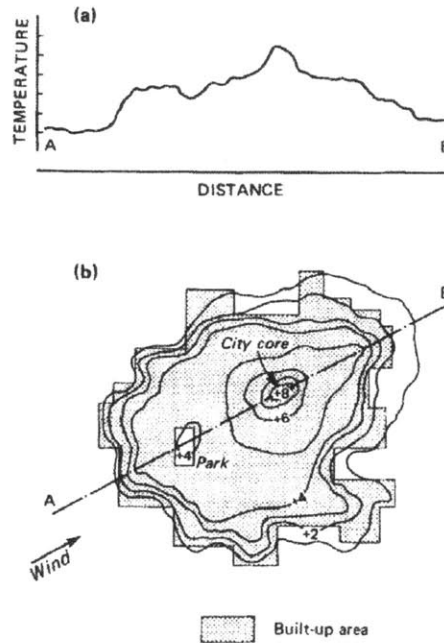


Figure 1-1: Spatial distribution of the air-temperature across a city in section (a) and plan (b) view. The peak air-temperature occurs at the center of the ‘island’ as wind traverses from the city edge at A to B.(Figure from Oke)

Surface-Temperature Heat Island

Due to the growth in available remote sensing technologies, there has been a recent emergence of research interested in documenting surface level variation in temperature throughout urban areas (Tomlinson *et al.*, 2011). By analyzing pixel data generated from overhead satellites, scientists have extensively mapped the temperatures of rural and urban surfaces (Weng, 2009). In their work, the assumption is that urban air temperatures are inherently linked to surface-temperatures, following similar diurnal patterns of spatial variation. This assumption is not generally true and it has been shown that in fact urban surface temperatures and air temperatures have distinctly different time scales (Arnfield, 2003; Weng, 2009). Additional complexity is introduced during the analysis of surface-temperature heat islands due to the method of sensing.

Sensing occurs at two distinct reference points: low-altitude and high-altitude (Arnfield, 2003; Weng, 2012). Low-altitude sensing is characterized by an ability to

determine the local geometry including streets, roofs and walls, while high-altitude sensing is generally unable to resolve urban surface details (Weng, 2012). Despite the unique characteristics of the surface urban heat island, advantages of studying this phenomenon are that data covering large areas is readily available and new processing algorithms allow better distinction of surface properties (Tomlinson *et al.*, 2011).

In modeling exterior longwave radiation incident on the building envelope, a common assumption in architectural thermal simulations is that the ground temperature is equivalent to the air temperature (Hensen, 2011). However, it is unclear what role observations of surface level heat islands may eventually play in architectural thermal simulation. Obstacles to using this information are a lack of synchronization with urban air-temperatures, the lack of a direct relationship between sensed surface-temperatures and ground-slab interface temperatures, and implementing exterior ground temperature data during simulations. As such the UHI, or air-temperature differences between urban and rural surroundings, is the focus of this thesis.

UHI

Urban buildings require additional treatment during the design phase due to the UHI effect, which is the increase in urban air-temperature versus a rural reference site. The UHI has two distinct modes that influence urban site weather conditions: the urban boundary layer (UBL) and urban canopy layer (UCL) (Oke, 1982). The UBL is a local affect that extends above the mean building height of a city to a prescribed maximum while the UCL is a microscale affect that defines the climate between buildings. A fundamental unit of the urban area used to define a building's local microclimate is the urban canyon (Oke, 2006b). This formulation has been offered to allow a more physical study of the UHI. A common method to evaluate a microclimate is to assess the energy balance of the urban canyon. Via urban canyon analysis, the spatial and temporal scale of the UHI effect can be discretized into manageable processes for advanced study (Masson, 2000).

Microclimates of urban areas vary within the UCL due to the myriad of energetic processes. Each process, which may be modeled from one or a combination of tech-

niques, is impacted by the geometric, surface, material, and anthropogenic attributes of a city. For instance, city form affects variables such as wind direction and speed around buildings, shading, urban albedo and surface sky view factors. The presence of anthropogenic heat sources including heating, ventilation, and air-conditioning (HVAC) equipment and vehicular traffic also affects microclimate variation. Additionally, each urban surface's intrinsic thermal, moisture and aerodynamic properties influences local surface moisture content, evaporation rates, etc. Accounting for these microclimate perturbations to determine the effect on local weather has traditionally required modeling techniques separated from detailed architectural thermal simulation. Therefore, despite research that has continually shown the impact of urban microclimate effects on building energy use, there has been little practical impact on thermal simulation at neither the individual building nor the urban scale (Taha *et al.*, 1988; Santamouris *et al.*, 2001; Mihalakakou *et al.*, 2002; Yang *et al.*, 2012).

1.2.2 Implications for Building Energy Use

Providing the requisite indoor air quality (IAQ) and thermal comfort to occupants of urban buildings while reducing the magnitude of building related emissions requires integrated design solutions that better incorporate local climates. In 2010, U.S. commercial and residential buildings consumed 41% of the nation's primary energy, of which 80% was fossil fuels (Department of Energy, 2009). Recognizing the need to reduce building energy consumption, the American Institute of Architects (AIA) and the federal government issued the Architecture 2030 challenge and the Energy Independence and Security Act (EISA) of 2007, respectively, each called for net-zero energy use in newly constructed buildings by the year 2030 (AIA, 2012; DOE, 2012). However, by 2030, nearly 60% of the earth's population will live in cities thus the majority of new construction will most likely occur in urban areas (United Nations, 2011). It seems apparent that integration of local urban climates into the determination of a building's operational energy use is necessary to deal with the increased demands for housing that such a population influx will generate.

In Chapter 2, the state of urban climatology applied to whole-building simulation

will be reviewed. Then we will describe our methods of evaluation in Chapter 3 with the results and discussion in Chapter 4. Finally, we will draw conclusions on the utility of these low-computation urban modeling techniques and propose future work in Chapter 5. A demonstration that replicates the weather files analyzed in this thesis is included as Appendix A. Complete descriptions of the building models used for analysis are included in Appendix B.

Chapter 2

Literature Review

Climate change and climate modeling are research subjects that have touched a diverse group of fields. Investigations into the UHI effect is a subset of this work and has followed a trend of increasing diversity. Therefore numerous analytic frameworks have been developed that allow researchers to explore problems important to their field.

A review of communication throughout the urban climate literature by Oke highlights the differentiation that exists among those that research the UHI effect (Oke, 2006b). In this thesis, we frame the UHI effect as an issue to be handled in the early stages of thermal simulation in architecture. Which defines the intended audience of this work as users of architectural thermal simulation and associated applications (i.e., thermal simulation of individual HVAC components, analytic urban design, etc.).

This chapter reviews several of the currently available tools in assessing urban climate from the simple to complex. We are most interested in tools that quantify the impact of urbanization on weather elements and produce either new weather data or building energy consumption data. The emergence of urban climate assessment tools with such output is discussed and we conclude with the current research needs of the intended audience.

2.1 Simple Modeling Tools in Urban Climate Assessment

2.1.1 Empirical Models

Early in the study of the UHI effect, research focused largely on empirical measurements of weather elements in various urban locations. This information was notably synthesized into empirical relationships between city population and UHI magnitude.

Oke analyzed the UHI effect on cloudless nights in ten Quebec settlements using a car mounted temperature sensor. His work sought to develop a functional form of the maximum UHI magnitude based solely on population. By eliminating consideration of nights with high winds and cloud cover, Oke was able to simplify previous analysis by Sundborg, Duckworth and Sandberg, and Chandler (Oke, 1973). Oke then sought out data from numerous UHI quantification studies in both North America and Europe. For North America he posited the equation:

$$\Delta T_{u-r(max)} = 2.96 * \log P - 6.41 \quad (2.1)$$

while for Europe the following was found to be a better fit:

$$\Delta T_{u-r(max)} = 2.01 * \log P - 4.06 \quad (2.2)$$

Where P is population and $T_{u-r(max)}$ is the maximum dry-bulb temperature difference between the urban and rural site. This regression suggests that for North America, 96% of UHI magnitude is predicted by population and for Europe this figure is 74%. Such strong correlation to a single predictor has garnered attention for better research into populations and population density. One such evaluation in Delhi was able to link increased land surface temperature to elevated construction of impervious surfaces due to rising population density (Mallick and Rahman, 2012).

However, it is clear that population cannot be the sole UHI indicator and often the assumptions necessary to support analysis with these regression techniques is ignored

(Lee, 2012). Beyond that, there is also the issue that quantifying a single value of the maximum UHI does not directly improve one’s ability to design urban buildings and settlements.

Modern tools of thermal design often require weather variables at a minimum of hourly frequency. Therefore, empirically based methods for altering weather files have emerged to facilitate the incorporation of the UHI effect in thermal simulations. In the United Kingdom, Kershaw *et al.* developed a sinusoidal representation of the UHI effect based on a month’s minimum temperature, average temperature, time of daily minimum temperature and time of daily temperature maximum (Kershaw *et al.*, 2010). The wavefunction is constructed via:

$$\delta T_{hourly} = \frac{\Delta T_{ave} - T_{min}}{2} \left[\frac{1 + \cos(\pi(t_i - t_{max}))}{t_{min} - t_{max}} \right] + T_{min}; t_{min} \leq t_i \leq t_{max} \quad (2.3)$$

and

$$\delta T_{hourly} = \frac{\Delta T_{ave} - T_{min}}{2} \left[\frac{1 - \cos(\pi(t_i - t_{max}))}{24 + t_{max} - t_{min}} \right] + T_{min}; t_{min} \leq t_i \leq t_{max} \quad (2.4)$$

where t_i is the hour of the day and t_{max} and t_{min} are the times of the maximum and minimum UHI. This function is offered with the explanation that it should be added to the hourly temperature data in either current weather files or those resulting from a weather generator.

The hourly UHI work of Kershaw *et al.* is related to an earlier algorithm developed by Chow and Levermore that produces hourly dry-bulb temperature values from a daily T_{ave} , T_{min} , and T_{max} (Chow and Levermore, 2007). Chow and Levermore recognized the need to downscale daily temperature values into hourly values in the form of Test Reference Years (TRYs) and Design Summer Years (DSY) for building thermal simulation. This need arose because several active UK weather stations and recently developed future climate change models provided only daily temperature values. Their solution was to utilize a quarter-sine wave approximation algorithm to generate the required hourly values. This work does not apply directly to UHI

studies, but is a further example of using empirical observations and wavefunctions to generate hourly dry-bulb temperature time series data. Kershaw *et al.* reference this methodology, but conclude that this level of detail is greater than required for architectural UHI investigations.

Crawley introduced a scheme to alter a city's diurnal dry-bulb temperature profile based on analysis done by Oke defining the energetic basis of the UHI effect (Crawley, 2008; Oke, 1982). This scheme is an algorithm that alters the dry-bulb temperature (DB) based on the time of day and then recalculates the relative humidity. There are two inputs to this scheme: hourly DB data from a reference site and the city's location. A defining characteristic of this scheme is the parameter ΔDB , which indicates how much the rural temperature increases for a given solar time. If the sun is up, the algorithm subtracts $0.1*\Delta\text{DB}$ from the reference signal; if the sun is down the algorithm adds ΔDB to the reference signal. Intermediate times just before sunset or just after sunrise add a prescribed fraction of ΔDB to the reference signal. Crawley applies two values of ΔDB to the reference weather data, with the goal of producing an upper and lower limit of the UHI effect on a building's microclimate. A city's location defines these two values of ΔDB . Cities in upper latitudes ($>48^\circ$) are assigned 1 and 3°C while remaining cities are assigned 1 and 5°C .

Building operators and designers seek to better incorporate current climate trends into the early stages of design. Doing so is an important aspect of high-performance and resilient design, but as with many engineering approaches the solutions to this complex issue tend to be empirically based. The building engineering community is most concerned with an adequate representation at the least expense from a time and capital perspective, which drives the framing of the solutions. In subsequent sections, this thesis reviews techniques that seek to incorporate local climate either qualitatively, from combined analytic solutions and correlations, or directly from the governing equations.

2.1.2 Physical Models

Physical models of cities have been used to study the UHI effect qualitatively and as tools to further understand fundamental physical processes. In such scenarios, similarity is maintained with a cluster of model ‘buildings’ to test hypotheses regarding either momentum or energy.

One of the first physical models developed to study the energy balance of the urban canopy layer was constructed by Oke (Oke, 1981). To that point there had been many observational UHI studies, resulting in multiple plausible hypotheses to describe the UHI effect. Yet few of these hypotheses had ever been proven. Oke determined that the simplest UHI ‘cause’ to test was the surface geometry hypothesis. This hypothesis states that the UHI reaches a maximum at night due to a reduced cooling rate versus the rural surface, which is the result of increased trapping of short-wave radiation in urban canyons, decreased loss of heat by turbulence, and reduced long-wave radiation exchange with the night sky. The model thus investigated the role of both geometry and thermal admittance in urban vs. rural temperature differences. Comparison to field data validated the model for the given conditions and helped to prove the importance of urban geometry on UHI (Oke, 1981).

More recently, Kanda *et al.* utilized data from the Comprehensive Outdoor Scale Model (COSMO) to estimate the roughness lengths for momentum and heat transfer over ‘urbanlike’ surfaces (Kanda *et al.*, 2007). This work is fundamental to the further development of urban canopy models (UCM) that predict urban heat fluxes. An UCM relies on simplifications of the surface layer heat transfer and local heat transfer correlations to reduce computational complexity. However, one of the more generally used simplifications, the Monin-Obukhov similarity theory (MOST), relies on momentum and heat transfer roughness lengths to determine the urban aerodynamic features (Kanda *et al.*, 2007). Two scale physical models of cubic concrete forms, situated outdoors, were instrumented in such a way that direct measurement of surface temperature and conductive heat flux at the roof, façade, and ground for each unit was collected. Kanda *et al.* used the resulting model data to derive a rela-

tionship between the desired length scales and a roughness Reynold's number, which they suggest should be used within the MOST framework to improve estimations of the bulk heat transfer coefficient in UCMs.

A common theme that emerges from these two studies is that investigation of energetic fluxes via physical modeling is of most use for furthering fundamental understanding of urban processes. In cities, the urban energy fluxes become too complex for physical models to provide direct insight. An architect or design team would never build a physical model that aims for energetic similitude with a proposed urban site. However, despite the lack of scale thermal models of urban areas in design, scaled aerodynamic models of urban areas have continued use in multiple fields. For the interested reader please refer to Ahmad *et al.* and Plate.

From this brief review of simplified modeling tools in urban climate assessment, we identify that the most pertinent models for building thermal simulation are those algorithmic and empirical methods that produce hourly data. The Kershaw algorithm was developed with empirical European data whereas the Crawley algorithm was developed more generally.

2.2 Advanced Modeling Tools in Urban Climate Assessment

In numerical climatology, researchers strive to accurately describe the impact of the earth's surface on atmospheric flow. Influences of the earth's surface are confined to a region of the atmosphere known as the troposphere (Oke, 1992). Within the troposphere, the characteristics of momentum and energy transfer are classified by a variety of turbulent regimes.

Due to the chaotic nature of turbulence, it is inherently difficult to resolve numerical solutions of atmospheric flow. Additionally, the complex interactions within cities that lie at the horizontal 'boundary' of atmospheric flows require great computational flexibility. Four generally accepted definitions of horizontal atmospheric

scale are (Oke, 1992):

1. micro-scale 10^{-2} to 10^3 m
2. local-scale 10^2 to 5×10^4 m
3. meso-scale 10^4 to 2×10^5 m
4. macro-scale 10^5 to 10^8 m

Each scale is inextricably linked within a complex system of thermal processes. Progress in numerical climate models has allowed an increasingly finer scale of atmospheric simulation in recent years, yet a key difficulty that the numerical weather prediction (NWP) community continues to address is the description of urban environments in mesoscale climate simulations (Baklanov *et al.*, 2005). Therefore, urban climatologists have emerged as a further subset of the numerical climatology community.

Urban climatologists apply knowledge of urban physical processes to better approximate the impacts of ‘urban surfaces’ (i.e., cities) on flow within the Troposphere. A city along the earth’s surface produces large transfer effects within the turbulent Troposphere. Approximate knowledge of these effects, which occur in a region known as the ‘atmospheric sublayer,’ is pivotal for accurate meso-scale atmospheric climate models. The urban canopy model (UCM) paradigm and many of the urban applied computational fluid dynamic (CFD) models are the direct result of this crucial need. It is important to note that NWP is not traditionally concerned with developing models of the urban environment that are tractable for all thermal simulation communities. Instead, there is a desire to develop numerical models of the atmosphere built up from numerous complementary modules built for specific time and length scales.

While work to model across scales may result in more accurate predictions of environmental variables, this level of computation is orders of magnitude more than that currently used in building thermal simulation. Engineers typically operate at the lower thermal scales, while climatologists are interested in either higher thermal scale phenomena or in combining information across scales. An evolving dynamic has

emerged, in which greater computational power has allowed scientists to push the perceived limits of model complexity, while engineers often emerge to ‘cherry-pick’ information from a desired thermal scale.

The following section aims to describe the landscape of advanced models used by urban climatologists. It will conclude with a description of the Urban Weather Generator (UWG) by Bueno *et al.*, which is the only known example of an environmental model of the urban climate scaled to the same order of computation as building thermal simulation.

2.2.1 Emergence of Tractable Urban Climate Models

Baklanov *et al.* and Lun *et al.* review the current state of models and schemes that exist to parameterize the ‘urban surface’ for application to meso-scale climate models (Baklanov *et al.*, 2005; Lun *et al.*, 2009). The UCM is a subset of these tools. UCMs are either ‘single-layer’ or ‘multi-layer’ in reference to the number of turbulent layers modeled for the flux of momentum and energy into the meso-scale atmospheric model. Multi-layer and single-layer models both rely on an averaged building geometric representation; however, multi-layer models involve discretization of the conservation equations and direct numerical solutions whereas single-layer models rely on dimensional correlations and empirical coefficients.

An alternative to the UCM method is the use of combined high (i.e., street level) and medium (i.e., meso-scale) resolution numerical solutions to the conservation equations. The literature contains examples of both existing and altered meso-scale atmospheric models with coarse horizontal resolutions coupled to higher resolution computational fluid dynamic (CFD) techniques. The uses of such a method include human outdoor comfort modeling, calculating wind fields around single or multiple buildings, dispersion of pollutants, and prediction of urban weather elements. Oxizidis *et al.* applied an existing meso-scale atmospheric model to a micro-scale CFD and statistical weather model to develop synthetic weather years for building thermal simulation (Oxizidis *et al.*, 2008). This level of computation is of much greater order and expense than building thermal simulation. We are interested in models of the

urban environment suitable for architectural design; therefore we focus on single-layer UCMs.

In particular, Masson introduced the Town Energy Balance (TEB) specifically to improve the physical representation of urban surfaces in meso-scale climate models. TEB and the building-averaged ‘urban-canyon’ representation are precursors to the UWG by Bueno *et al.* The TEB scheme applied numerical methods previously used in urban climatology to an atmospheric model. It was necessary to reconsider significant physical interactions between urban areas and the atmosphere such as shortwave radiation, urban heat fluxes and moisture. Since TEB was designed as a tool for urban surface parameterization, its output is confined to variables that describe the turbulent energy and momentum fluxes from surface grids into the atmosphere. TEB output consists of latent and sensible heat fluxes [W/m^2], upward radiative fluxes [W/m^2] and component momentum fluxes [m^2/s^2]. However, despite the advantages of low computational order, the TEB scheme neither considers the impact of dynamic building operation on urban environmental variables, nor was it designed explicitly for use outside of a meso-scale atmospheric model (Masson, 2000).

Kikegawa *et al.* were more explicitly interested in the ability to mitigate the UHI effect in urban areas. Therefore they developed a methodology that coupled a meso-scale atmospheric model, a UCM, and a building energy model to explore the impacts of various urban parameters on the cooling energy demand of Tokyo, Japan. This work represents a greater level of detail than the TEB scheme in that building cooling energy demand is calculated, but it also relies on an external meso-scale atmospheric model. Additionally, this work is limited in that the meso-scale atmospheric model domain is constrained to the Japanese context (Kikegawa *et al.*, 2003).

The urban weather generator (UWG) from Bueno *et al.* is an alteration to the TEB scheme for use in architectural thermal analysis. The UWG consists of four components: the rural station model (RSM), the vertical diffusion model (VDM), the urban boundary layer model (UBL) and the urban canopy building energy model (UCM). The RSM uses meteorological values from a rural site to calculate the rural sensible heat fluxes, which the VDM then processes into a vertical temperature

profile. The vertical temperature profile above the rural station is an input to the UBL model. The UBL then calculates the air temperatures above the urban canopy layer and couples with the UCM to solve for the dry-bulb temperature (DB) and relative humidity (RH) in the urban canyon for each hour of rural reference data.

The UWG is a streamlined meteorological model that combines UCM-based energy balance calculations with a building energy model and a reduced order atmospheric model. By examination of the available single-layer UCMs, the UWG is the only known use of this low-computational order scheme, with a complementary low-computational order urban boundary layer model, for direct application to thermal simulation of buildings in urban areas.

2.3 Needs & Current Limitations

In this literature review we have identified that two approaches have the greatest potential utility to the thermal simulation user group: semi-empirical models and numerical solutions to atmospheric conditions that result in hourly weather data. Despite the existence of these methods, our user group of interest still needs to know: ‘Which of these two methodologies is most appropriate for current practice in building thermal simulation?’

Currently, there is no answer to this question because the methodologies have not typically had appeal across user groups. That is to say, climatologists have little interest in semi-empirical, hourly weather models and engineers have little time to invest in NWP across an entire urban domain. A limitation in the research to this point has been the lack of methodological comparison. Without a quantification of the advantages or disadvantages of either methodology there is concern that less appropriate climate information will remain in use throughout the thermal building simulation user group.

Therefore, to address the thermal design community’s stated need and the current limitations of research into urban architectural analysis, this thesis compares two low-computational order schemes for defining weather elements in urban environments.

Chapter 3

Methodology

Section 3.1 first describes the study region and the conditions at each of the urban and rural weather data sites. Section 3.2 introduces the analysis of the UHI effect in central Cambridge, MA, our chosen urban site. Then a method to assess the impact of weather data source (i.e., rural versus urban data) on predicted energy use is defined in Section 3.3. The metric for comparing energy use across sites and across building types is energy use intensity (EUI), which is a normalized metric defined fully in Section 3.3. Next, Section 3.4 defines the method to generate urban weather data from a rural site using each of the models. Section 3.5 explains a method for quantifying the improvements that simulated urban weather can provide in predicting a building's EUI as well as a method for determining the most important weather elements for a given scenario. Finally, in Section 3.6 we define our method for quantifying the effect of urban morphology on the ability to predict urban weather.

3.1 Site Descriptions

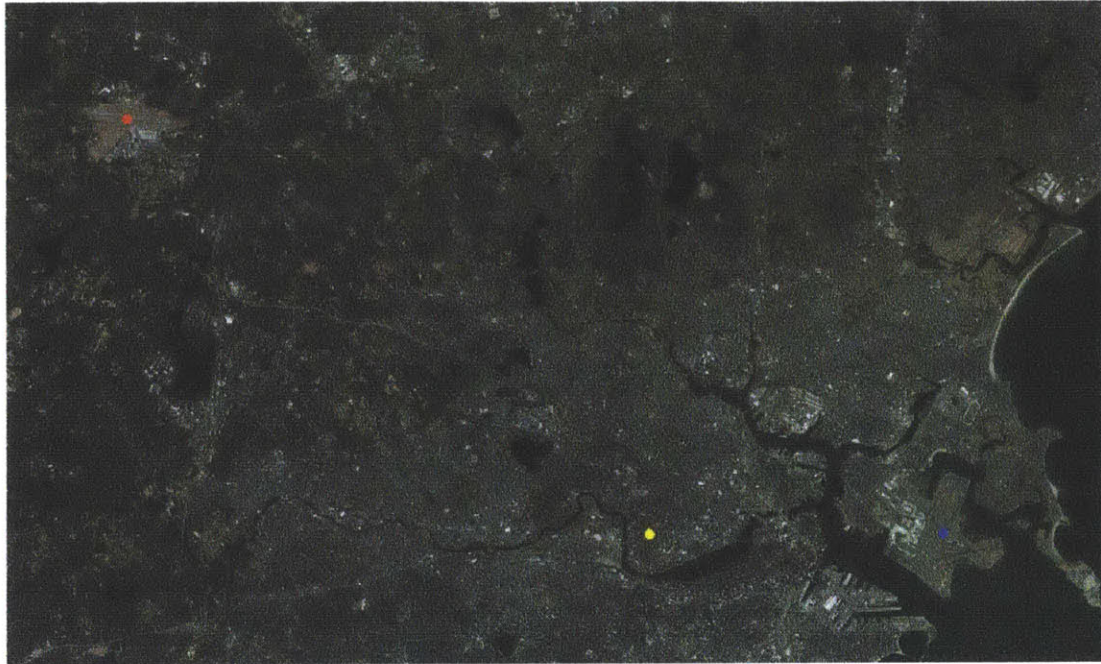
Boston, MA is located in the northeast United States and the regional climate is classified as cold and moist (Climate Zone 5A) by the International Energy Conservation Code (Council, 2009). However, the broader Koppen-Geiger climate classification defines the region as warm-temperate, fully humid with a warm summer (Kottek *et al.*, 2006).

Three sites were identified for data collection. Weather station data was accessed via an online repository of Automated Surface Observing System (ASOS) and Personal Weather Station (PWS) (Masters, 2012). Fig 3-1 shows the locations of each weather station. The weather station (KMACAMBR4) providing our urban signal is located in southwest Cambridge. The two sites examined as rural are the airport weather station located at Hanscom Air Force Base (KBED) and the station located at Boston-Logan International Airport (KBOS).

The urban location is composed mainly of residential buildings, with a mix of some small commercial buildings (Fig. 3-5). There is very little vegetated area and no major parks or water features exist within a 500 m radius of the station. The topography is flat with few variations and no major rises in elevation. Using urban patterns defined by Oke, this station is classified as urban climate zone two (Fig. 3-3) (Oke, 2006a). The KBED station is 19 km inland to the northwest of the urban station and situated on a flat patch of grass on the runway (Fig. 3-4). The KBOS station is located 8.3 km due east of the urban station, also on the airport runway, which is a peninsula that extends into a subsidiary of the Massachusetts Bay (Fig. 3-1 and Fig. 3-2).

A rural site is defined as a site within the study region, but outside the urban area and its affected environs with minimal influence from large geographic features (e.g., valleys, large bodies of water, etc.) (Lowry, 1977; Oke, 2006a). The two sites examined as rural were the airport weather station located at Hanscom Air Force Base (KBED) and the station located at Boston-Logan International Airport (KBOS). We note after this brief description that the KBOS station does not conform to the definition of rural; however, weather data from KBOS is the basis for the Boston TMY data and is therefore of particular interest to building modelers.

Observed weather data in the EnergyPlus Weather File (EPW) format was necessary to perform the desired building thermal simulations (Crawley *et al.*, 1999). The necessary variables were gathered from each of the stations shown in Fig. 3-1 and converted to EPW format following the methodology defined in Appendix A.



Weather Station ● Rural ● TMY ● Urban

Figure 3-1: Map of the Boston, MA metropolitan area and locations of each of the weather stations used to collect data. Each site’s local geography and proximity to the urban station may be seen. From left to right: Rural, Urban, TMY. Aerial photograph from Microsoft’s Bing Maps

3.2 Experiment 1: UHI Quantification

Our first objective is to determine the magnitude of the UHI effect at the urban site. To assess the UHI effect at the urban site, the observed urban temperature signal was compared to both airport temperature signals based on the framework developed by Lowry. Lowry’s framework models weather elements as the linear combination of three components: the background or reference climate C , the effects of the local landscape L , and the effects of local urbanization E . Thus,

$$M_{itx} = C_{itx} + L_{itx} + E_{itx} \tag{3.1}$$

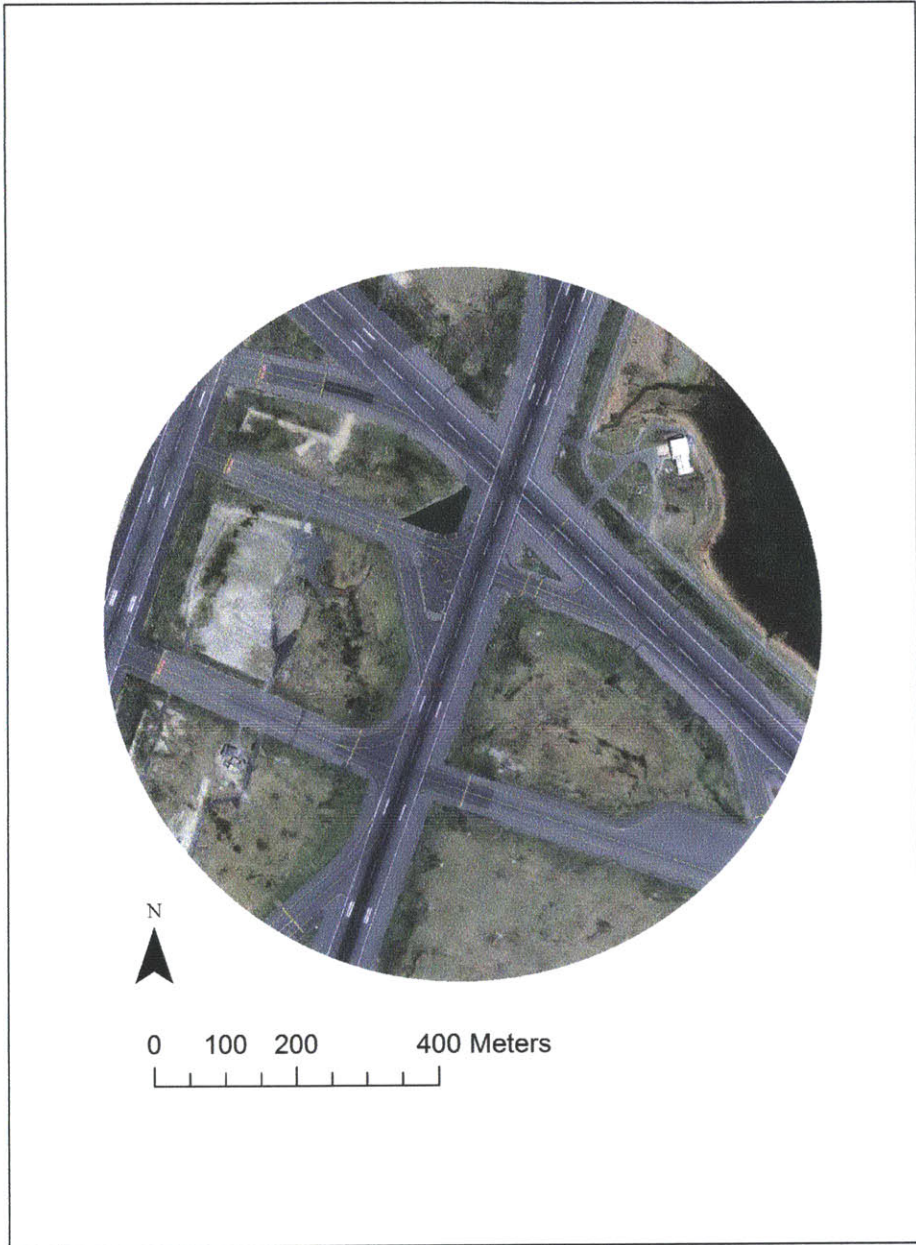


Figure 3-2: Boston Logan International Airport is shown. We see just to the right the coastline of the larger peninsula and a number of runways. Aerial photograph from MassGIS (Office of Geographic Information (MassGIS), 2011).

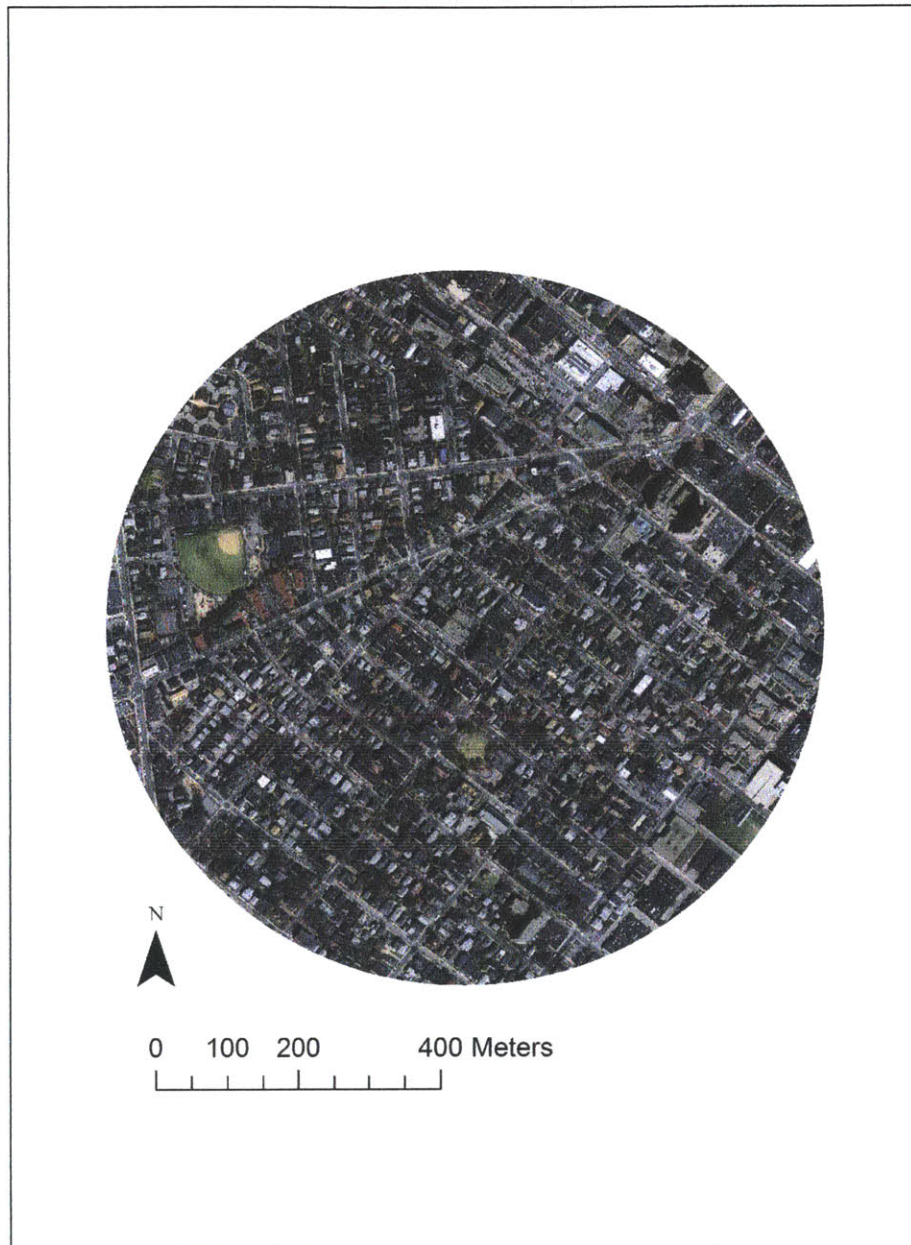


Figure 3-3: The urban context is shown. We see that there are not many tall buildings, but the overall density and urban fabric is much more built up than at either reference station. Aerial photograph from MassGIS (Office of Geographic Information (MassGIS), 2011).

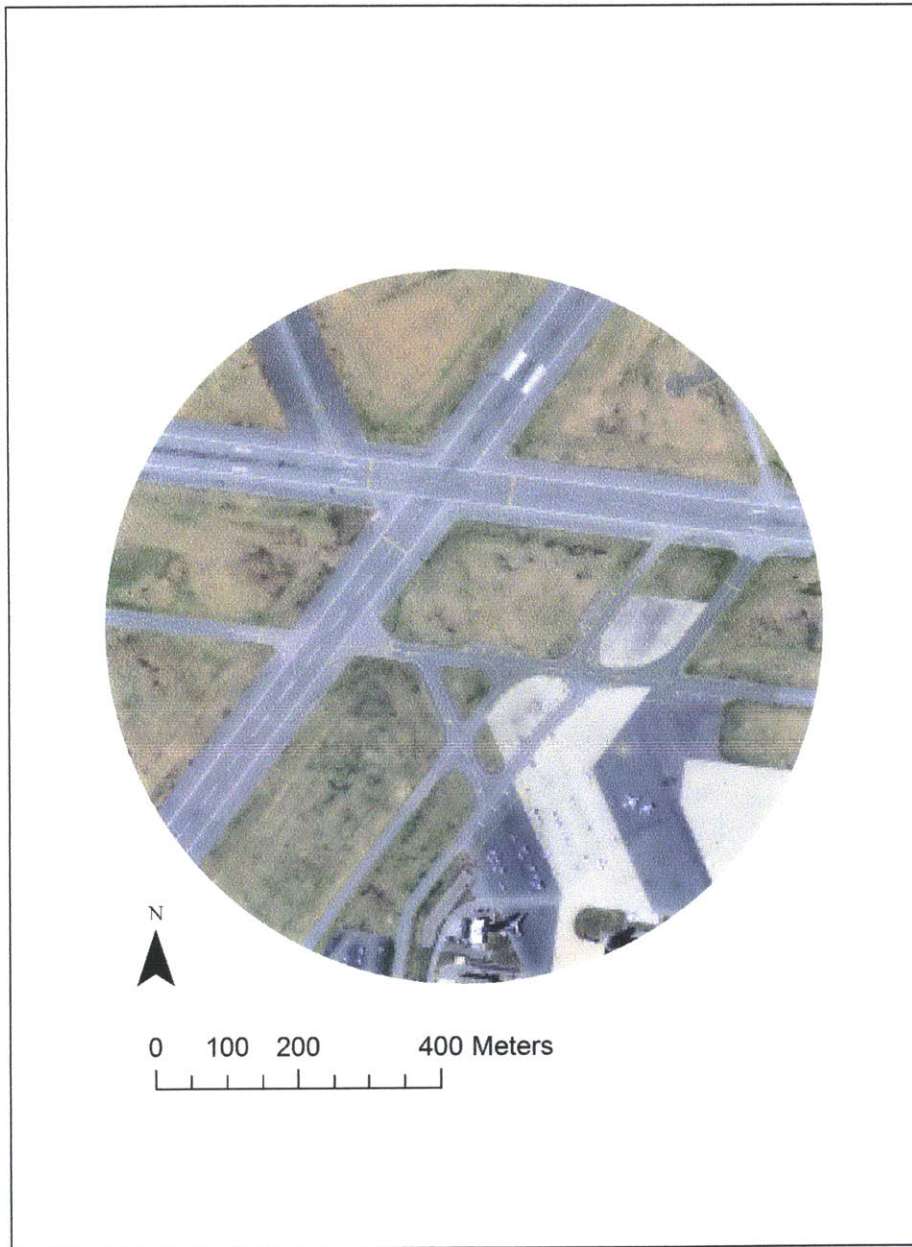


Figure 3-4: Hanscom Air Force base is shown. Again there are a number of runways that differ from a grassy rural area, but there are neither large geographic obstructions nor bodies of water. Aerial photograph from MassGIS (Office of Geographic Information (MassGIS), 2011).



Figure 3-5: The KMACAMBR4 PWS weather station is shown with instruments mounted above a residential building in central Cambridge, MA. Image by the author.

Where M is the measured value of a given weather element i during the time period t at station x . C is the value weather element i observed in the absence of landscape and urbanization effects. Lowry notes that weather stations divide into three subsets: u for stations within the urban area itself; e for stations within the surroundings of the urban area, but not immune from urbanization effects (i.e. $E \neq 0$, $L = 0$); r for stations outside of urbanization and geographic effects (i.e. $E = L = 0$). Boundaries separating the urban and rural sites are not explicit and can only be inferred from site analysis and initial comparison of measured weather elements. Once EPW files for each weather station were developed, hourly values were compared between stations for the maximum differences. Due to limitations in the generation of the EPW files the maximum urban versus rural temperature difference is selected without considering outliers. Outliers are calculated as:

$$Q_1 - 1.5 * IQR < x_{outlier} < Q_3 + 1.5 * IQR \quad (3.2)$$

where Q_1 is the first quantile of the data, Q_3 is the third quantile and IQR is the interquartile range (Fig. 4-2 through Fig. 4-5). Additionally, the maximum urban

versus rural temperature difference was calculated after selecting out only night hours with wind speed less than 1.8 [m/s] (Fig. 4-8 through Fig. 4-7).

3.3 Experiment 2: UHI Impact on Building EUI

The second objective is to quantify the impact that location has on building energy use intensity, which will further attest to the need for prediction of urban weather elements. This is accomplished by simulating each of the described whole-building thermal models for one year of operation. Specification of each model is defined in Appendix B. For building simulations, the EnergyPlus simulation engine is used. In this case, we apply the metric of annual cooling and heating energy use intensity. Energy use intensity (EUI) is defined as the amount of site energy consumed by the model per unit of floor area.

$$EUI = \frac{\sum_{i=1}^{8760} E_i}{A_{conditioned}} \quad (3.3)$$

where E_i is the site energy at hour i and $A_{conditioned}$ is the total conditioned area of the building. The simulation energy values are listed under the EnergyPlus meters 'Cooling:Electricity' and 'Heating:Gas'. Simulation weather conditions are evaluated with an EPW file from two airport stations and the urban station. A total of six annual simulations are analyzed (Fig. 4-10 and Fig. 4-11).

3.4 Experiment 3: Simulated vs. Actual Weather Elements

An urban weather file was first generated using the Crawley scheme. Based on the location of Cambridge, $\Delta DB = 1^\circ\text{C}$, 5°C was applied to each rural site. The sun's position relative to each reference weather station was calculated in the numerical program R version 2.14.2 using the package 'solaR' (Perpinan, 2012). The Crawley algorithm re-calculates relative humidity using the new DB temperature and the

unchanged wet-bulb temperature.

Next, the UWG was applied to our proposed building site. Utilizing the UWG to produce an EPW format weather file requires multiple input parameters. Cambridge was selected precisely because of the access to both an operational weather station and characteristic urban data (i.e., building height, building footprint, aerial imagery, etc.). Input values for the UWG are in Table 3.1. An initial sensitivity analysis by Bueno *et al.* indicates that factors governing the specific urban site’s morphology, vegetative features and reference weather station are of the greatest importance (Bueno *et al.*, 2012).

Cambridge, MA has amassed detailed information on the buildings within the site area (Office of Geographic Information (MassGIS), 2011). A 500 m radius circle centered at the KMACAMBR4 weather station defined the site area. A 500 m radius is the area assumed to influence urban weather station readings directly (Oke, 2006a). The average building height, horizontal building density and vertical-to-horizontal ratio of the buildings within this area were then calculated from the Cambridge buildings data layer furnished by MassGIS and the following equations:

$$h_{bld} = \frac{\sum_{i=1}^N h_i}{N} \quad (3.4)$$

$$\rho_{bld} = \frac{\sum_{i=1}^N B_i}{A_{urb}} \quad (3.5)$$

$$VH = \frac{\sum_{i=1}^N FA_i}{A_{urb}} \quad (3.6)$$

where h_i = height of building i , B_i = footprint area of building i , A_{urb} = area of circle defining the urban site, and FA_i = façade area of building i . To assess the urban area’s vegetated features, bounding curves were overlaid atop color (24 bit, 3 channel), 30 cm resolution, orthographic imagery of the urban area. By calculating the area of the closed curves and dividing by the size of the urban area, we arrived at a value for the horizontal vegetation density. Defining the building model parameters

Parameter	Central Square
Urban parameters	
<i>Location</i>	Cambridge, MA
<i>Latitude</i>	42.363°
<i>Longitude</i>	-71.108°
<i>City diameter</i>	5000 m
<i>Average building height</i>	9.7 m
<i>Latent anthropogenic heat</i>	0.0 W/m ²
<i>Sensible anthropogenic heat</i>	0.0 W/m ²
<i>Horizontal building density</i>	0.38
<i>Vertical-to-Horizontal urban area ratio</i>	1.3
<i>Horizontal vegetation density</i>	0.05
<i>Wall construction</i>	Brick - 0.2 m; Insulation - 0.03 m
<i>Wall albedo</i>	0.15
<i>Roof construction</i>	Tile - 0.06 m; Wood - 0.2m; Insulation - 0.03m
<i>Roof albedo</i>	0.25
<i>Building floor construction</i>	Concrete - 0.2 m
<i>Road construction</i>	Concrete - 0.2 m; Asphalt - 0.05 m; Stones - 0.2 m; Gravel and soil
<i>Road albedo</i>	0.08
Building parameters	
<i>Glazing ratio</i>	0.3
<i>Window construction</i>	Double-pane clear glass
<i>Internal heat gains</i>	6.25 W/m ²
<i>Infiltration/ventilation</i>	0.5 ACH
<i>Cooling system</i>	Off
<i>Heating system</i>	Furnace
Weather station parameters	
<i>Construction</i>	Soil
<i>Non-vegetated surface albedo</i>	0.15
<i>Vegetated fraction</i>	0.8

Table 3.1: Inputs to the UWG with Cambridge specific urban geometric parameters. Other parameters from UWG validation in Toulouse, France.

and canyon materials is a subjective problem. These inputs are the most uncertain parameters. Lacking site-specific data, we used thermal, radiative, anthropogenic flux and building parameters from a UWG validation for Toulouse, France.

Simulated EPW data from each model was compared to the observed urban data via the root mean square error (RMSE) and mean bias error (MBE) statistics:

$$RMSE = \sqrt{\frac{\sum_{i=1}^N (x_{i,1} - x_{i,2})^2}{N}} \quad (3.7)$$

$$MBE = \frac{\sum_{i=1}^N (x_{i,1} - x_{i,2})}{N} \quad (3.8)$$

where $N = 8760$ is the number of hours in an EPW file, $x_{i,1}$ is the estimated weather element and $x_{i,2}$ is the observed weather element.

3.5 Experiment 4: Building EUI & Simulated Weather

After statistically analyzing the simulated EPW files, the fourth objective is to determine:

1. **What are the most influential weather elements on each building model's EUI?**

If the dry-bulb temperature and relative humidity are not the most influential variables on each building's EUI then these urban environment models are less useful. Bhandari *et al.* show the influence of individual weather elements on building heating and cooling loads (Bhandari *et al.*, 2012). Four experimental EPW files were developed from observed data for each airport station. The experimental EPW files are developed by inputting a combination of urban weather elements into each airport EPW file. A summary of the data replacement is shown in Table 3.2 (Fig. 4-16 through Fig. 4-19).

2. **How well does the EPW file generated by the UWG mimic the EUI prediction produced by the urban observed EPW file?**

Observed Urban Element	DB	RH	DB + RH	Local Wind
Dry-Bulb Temperature	X		X	
Relative Humidity		X	X	
Wind Direction				X
Wind Speed				X

Table 3.2: An ‘x’ indicates, which urban variables are placed into each airport EPW to create the experimental weather files.

Each building is simulated for one year of operation using the EPW file generated by the UWG. The predicted EUI is then compared to that predicted by the observed urban EPW file. Four simulations are analyzed (Fig. 4-20 through Fig. 4-23).

3. Do the EPW files created from the Crawley method’s ‘upper’ and ‘lower’ bounds for Δ DB bracket the EUI prediction produced by the urban observed EPW file?

Each building is simulated for one year of operation using the EPW file generated by the Crawley algorithm for Δ DB = 1°C and Δ DB = 5°C. The predicted EUI is then compared to that predicted by the observed urban EPW file. Eight simulations are analyzed (Fig. 4-20 through Fig. 4-23).

3.6 Experiment 5: Parametric Analysis of UWG

The urban morphology UWG input parameters may vary distinctly based on the radius of influence that one chooses to define the urban site. To quantify this influence the urban area is varied with five separate radii: 100 m, 250 m, 500 m, 1000 m, and 2000 m. Each value of the urban radius produced a new set of values defining the horizontal building density, vertical-to-horizontal area ratio, and average building height (Table 4.9). These new values were used to generate EPW files with the UWG. Five additional annual whole-building simulations were analyzed to calculate the impact of urban radius on annual EUI (Fig. 4-24 through Fig. 4-27).

3.7 Summary

In this chapter we re-iterated the purpose of this thesis and described the methods preceding the results in Chapter 4. Section 3.1 initialized our problem by defining the locations of interest and provided associated imagery. Section 3.2 defined the analysis of the UHI effect present at central Cambridge, MA, the urban site. Section 3.3 defined both a method to assess the impact of weather data source on predicted energy use and the normalized energy metric of EUI. Section 3.4 provided a detailed description of the inputs to the UWG and Crawley algorithm and defined how each input was selected. Section 3.5 explained a method for quantifying the improvements that simulated urban weather can provide in predicting a building's EUI as well as a method for determining the most important weather elements for a given scenario. Finally, Section 3.6 defined a parametric methodology for separately quantifying the effect of urban morphology on the generation of urban weather with the UWG. Note that descriptions of the thermal building models are in Appendix B and a demonstration of re-producing the weather data is in Appendix A.

Chapter 4

Results & Discussion

In this chapter we present the results of each experiment described in Chapter 3. Section 4.1 quantifies the UHI effect at the urban site. Once the magnitude of the UHI is established, Section 4.2 quantifies the impact of the UHI on the predicted energy use of typical urban buildings. Section 4.3 presents the results of each urban weather generator and calculates statistical measures of how well each simulated signal replicates the urban signal. Simulation results of the typical buildings with actual and experimental weather data is presented in Section 4.4. Section 4.5 contains the sensitivity analysis of the UWG to urban morphology and anthropogenic heat parameters. Finally, a summary of results is compiled in Section 4.6.

4.1 Experiment 1: UHI Quantification

We hypothesized that there exists a systematic dry-bulb temperature difference between the defined urban site in central Cambridge, MA and both reference sites.

To examine this hypothesis, a year of dry-bulb temperature residuals between the urban site and each of the rural sites were calculated. Dry-bulb temperature differences between Hanscom Air Force Base and the urban site are in Fig. 4-2 and Fig. 4-3. From Fig. 4-2 note that $T_{u-r(max)}$ is reached twice during the summer and the histogram in Fig. 4-3 shows that there is large variance in the sample of residual dry-bulb temperature values. The same analysis applied to the dry-bulb temperature

residuals between Boston-Logan International Airport and the urban site show that 3.1°C occurs with more frequency (Fig. 4-4), but the sample variation is reduced and the annual mean of the residuals peaks sharply around 0°C (Fig. 4-5).

A result of classic heat island theory is that the maximum dry-bulb temperature difference between an urban and rural site should occur at night during times of very calm winds (Chapter 2). To test this classic behavior, data was selected from times when the sun was down and the wind speed was less than 2 m/s . Fig. 4-8 and Fig. 4-6 show that $T_{u-r(max)}$ does increase. The variance of the Boston-Logan sample decreases (Fig. 4-7), while the mean stays approximately the same. However, the Hanscom Air Force Base sample variance increases and the mean is shifted higher (Fig. 4-9).

Finally, to test the significance of observed dry-bulb temperature differences between the urban and the rural sites we apply a t-test. The null hypothesis to test is: H_0 : *The mean of the peak, night-time, dry-bulb temperature for each month is the same at the urban and rural sites.* The alternative hypothesis is: H_1 : *The mean of the peak, night-time, dry-bulb temperatures are different between the urban and rural sites.*

After calculating the peak, night-time temperature for each day of a month, the mean of these values was calculated (Table 4.1). Taking the urban site mean as the population mean for a given month and the calculated rural site mean as the sample mean, a t-statistic was calculated. Fig. 4-1 plots the p-values for each test. None of the monthly peak, night-time, dry-bulb temperatures observed at Boston-Logan International Airport lie within the 95% confidence interval, while 7 months from Hanscom Air Force Base meet this level of significance.

A typical UHI effect will be relatively non-existent during the day and a maximum at night, but temperature differences between the urban site and Boston-Logan International Airport show no statistically significant difference during night-time hours. Conversely, Hanscom Air Force Base appears to exhibit a strong reference signal with a statistically significant ($p < 0.05$) night peak for 7 months of the year. These results confirm that the rejection of KBOS as a rural site is well founded.

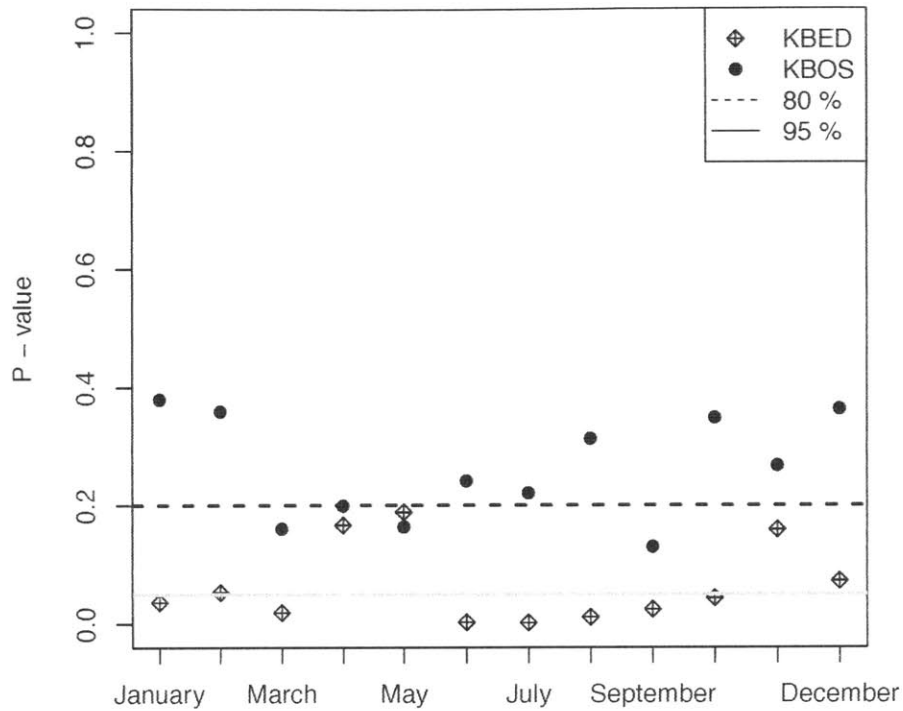


Figure 4-1: T-test results for the urban versus rural comparison of mean peak, night-time temperature for each month of the year 2011. The 80% confidence interval is the dashed line. Only months from KBED fall within the 95% confidence interval.

	[°C]		KBED		KBOS		Urban	
	μ	σ	μ	σ	μ	σ	μ	σ
January	-2.1	0.8	-0.5	0.7	-0.3	0.8		
February	0.6	0.9	2	0.8	2.4	0.9		
March	3.7	0.8	4.9	0.7	5.9	0.8		
April	10.8	0.9	11	0.8	11.9	0.8		
May	15.1	0.8	15	0.8	16	0.8		
June	18.2	0.6	19.9	0.7	20.6	0.7		
July	23.4	0.5	25.1	0.5	25.6	0.5		
August	21.9	0.5	23.2	0.3	23.4	0.3		
September	19	0.7	20	0.5	20.8	0.6		
October	12.7	0.9	14.9	0.8	14.5	0.9		
November	11.7	0.8	12.2	0.6	12.8	0.7		
December	5.8	1	7.4	0.8	7.7	0.9		

Table 4.1: Average peak, night-time dry-bulb temperature for each month of 2011 at each weather data site. The statistical significance of urban versus rural temperature differences is plotted in Fig. 4-1.

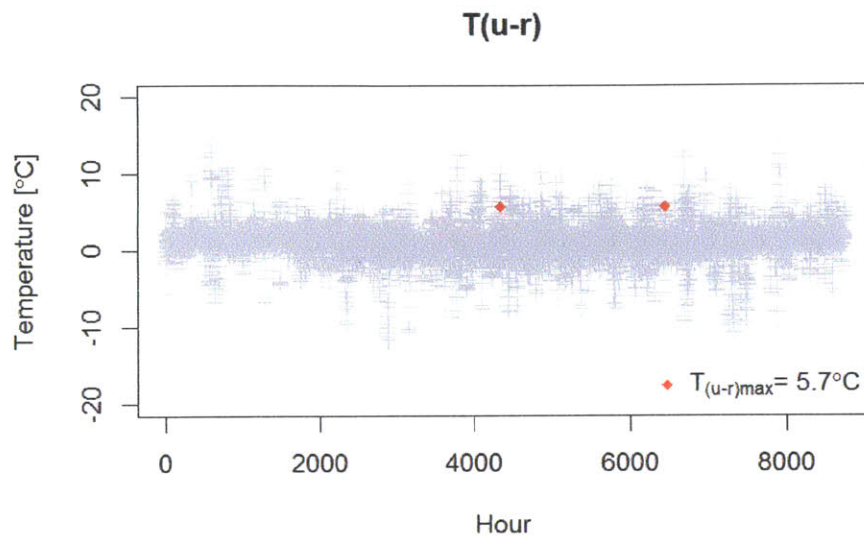


Figure 4-2: Dry-bulb temperature residuals between KBED and KMACAMBR4. The maximum urban-rural temperature difference is 5.7°C when all 8760 hours of the EPW file are considered. Outliers are excluded from selection of the maximum temperature difference

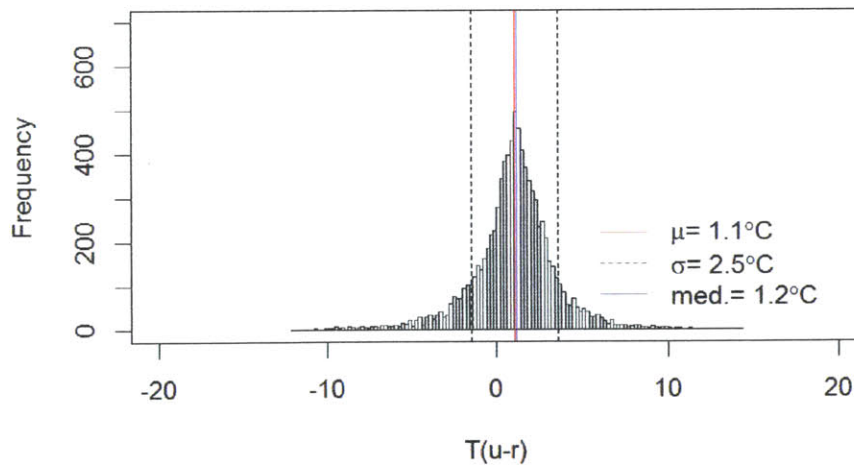


Figure 4-3: Distribution of dry-bulb temperature residuals between KBED and KMACAMBR4. All 8760 hours of the EPW file are considered for calculation of mean and standard deviation. For improved robustness the median is also calculated.

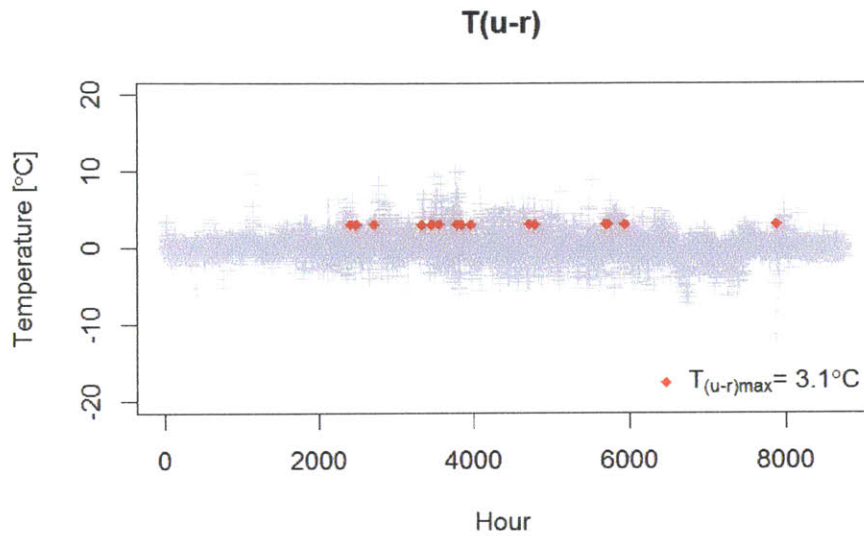


Figure 4-4: Dry-bulb temperature residuals between KBOS and KMACAMBR4. The maximum urban-rural temperature difference is 3.1°C when all 8760 hours of the EPW file are considered. Outliers are excluded from selection of the maximum temperature difference

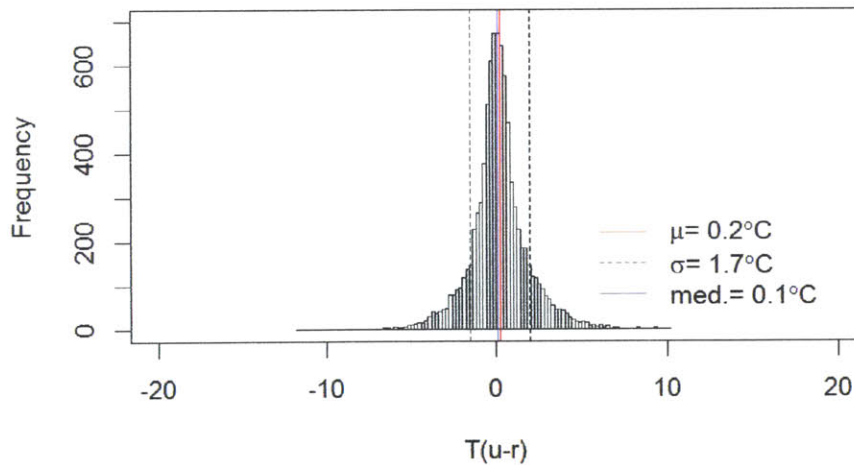


Figure 4-5: Distribution of dry-bulb temperature residuals between KBOS and KMACAMBR4. All 8760 hours of the EPW file are considered for calculation of mean and standard deviation. For improved robustness the median is also calculated.

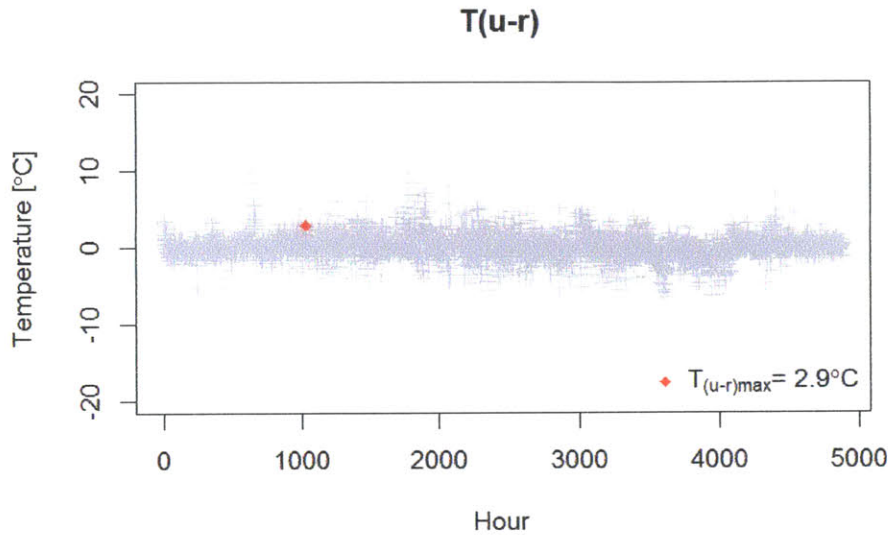


Figure 4-6: Dry-bulb temperature residuals between KBOS and KMACAMBR4. The maximum urban-rural temperature difference is 2.9°C when only night and low-wind speed hours of the EPW file are considered. Outliers are excluded from selection of the maximum temperature difference

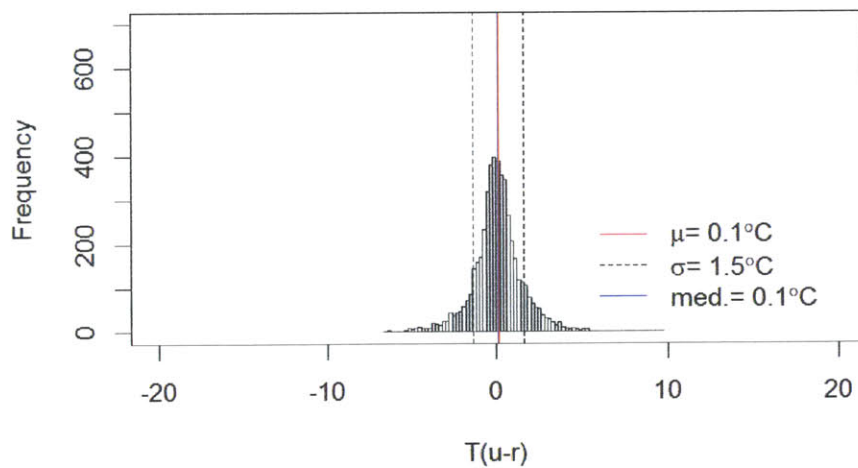


Figure 4-7: Distribution of dry-bulb temperature residuals between KBOS and KMACAMBR4. Only night and low-wind speed of the EPW file are considered for calculation of mean and standard deviation. For improved robustness the median is also calculated.

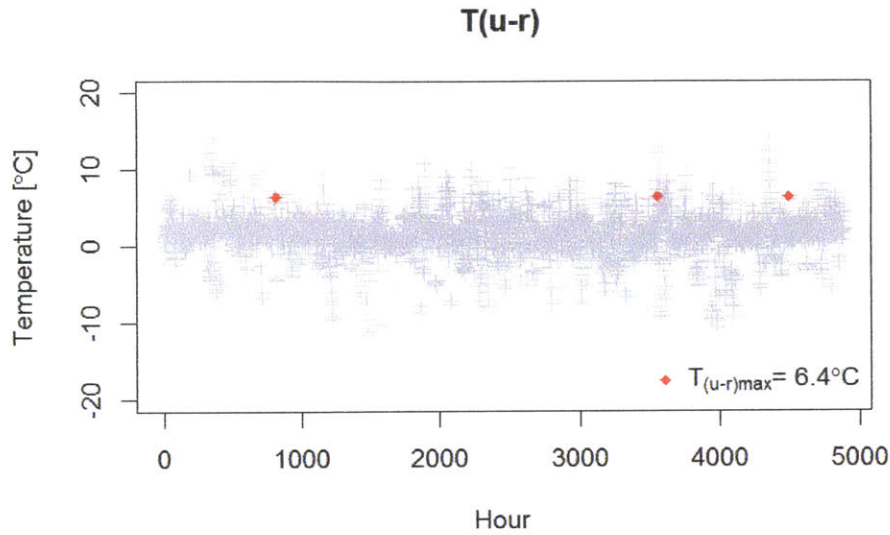


Figure 4-8: Dry-bulb temperature residuals between KBOS and KMACAMBR4. The maximum urban-rural temperature difference is 2.9°C when only night and low-wind speed hours of the EPW file are considered. Outliers are excluded from selection of the maximum temperature difference

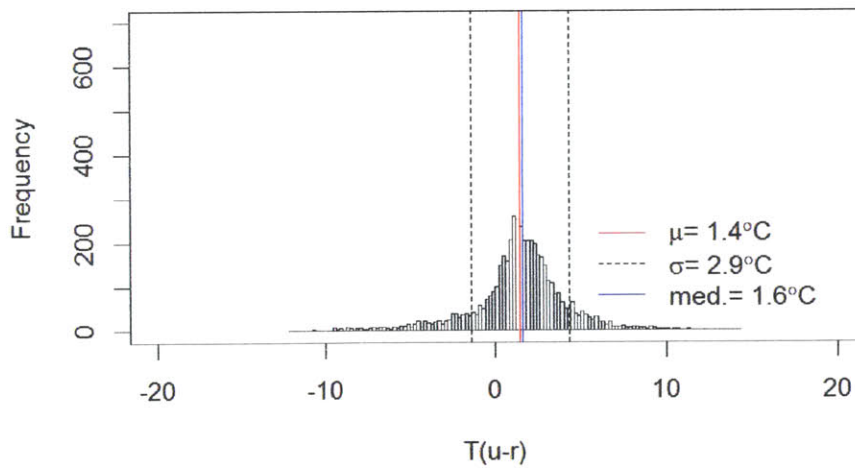


Figure 4-9: Distribution of dry-bulb temperature residuals between KBOS and KMACAMBR4. Only night and low-wind speed of the EPW file are considered for calculation of mean and standard deviation. For improved robustness the median is also calculated.

4.2 Experiment 2: UHI Impact on Building EUI

Section 4.1 has shown that there is a significant difference in dry-bulb temperature between Hanscom Air Force Base and the urban site. Recognizing these significant anomalies in the dry-bulb temperature signal, the next step is to quantify the impact this variation has on building thermal simulation and prediction of an urban building's energy use. We will employ a normalized energy metric, energy use intensity (EUI), which is the sum of either cooling or heating energy required for operation normalized by the building's conditioned area.

Although the weather station signal at Boston-Logan International Airport does not vary significantly from the urban weather signal, we will also quantify the micro-climate variation between these two sites through building thermal simulation and the EUI. We carry this on because the Boston, MA typical meteorological year (TMY) weather file is derived from this signal. Users of building thermal simulation often employ TMY files to determine average performance and these simulations will aid in determining the degree of bias that is introduced into EUI predictions by using weather data from outside the urban site. Therefore, we analyze annual EUI of each building type for each airport station.

Table 4.2 and Table 4.3 quantify the simulation results. From Table 4.2 we see that the energy use of the single-family building is dominated by heating. This table represents three possible simulation outcomes depending on which weather data is used to predict the building's annual EUI. If KBOS input weather data is used for simulation then, the results would predict 16% higher total EUI than the urban results. If KBED weather data is used for simulation, then the prediction would be 20% higher than actual performance in the urban area. The single-family building demonstrates that it is quite sensitive to the choice of environmental variables during simulation. This shows that using rural (KBED) or typical (KBOS) weather stations to predict the total EUI of a typical urban single-family building will introduce a variation in EUI prediction from $+ 19 \text{ kWh/m}^2$ (+ 20%) to $+ 15 \text{ kWh/m}^2$ (+ 16%), respectively.

Table 4.3 shows that a small office building located near Hanscom Air Force Base would use $8 \text{ kWh}/\text{m}^2$ (+ 19%) more energy for heating per square meter than an urban small office building, while a small office building located near Boston-Logan International Airport would use only $2 \text{ kWh}/\text{m}^2$ (+ 5%) more energy for heating per square meter than an urban small office building. The comparative magnitudes of heating and cooling negate the negative impact of increased cooling energy consumption. The small office is slightly less sensitive to the environmental conditions during simulation, which is seen in the flattening of the EUI curve between KBOS and Urban (Fig. 4-11). Results in Table 4.2 and Table 4.3 confirm that using rural (KBED) or typical (KBOS) weather stations to predict the total EUI of a typical urban small office building will introduce a variation in EUI prediction from $+ 7 \text{ kWh}/\text{m}^2$ (+ 15%) to $+ 1 \text{ kWh}/\text{m}^2$ (+ 2%), respectively.

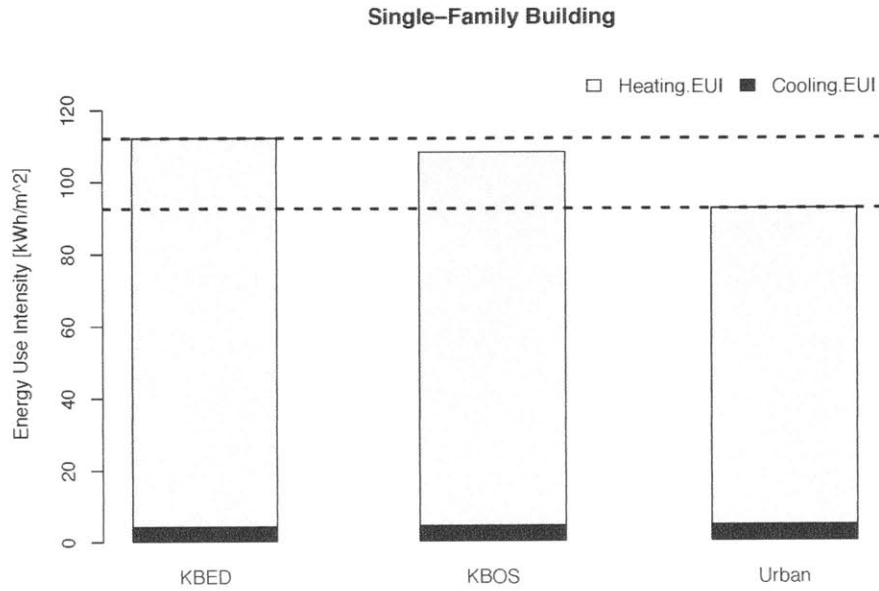


Figure 4-10: Variation in a single-family building’s simulated total EUI, heating EUI, and cooling EUI based on the source of weather data for simulation. The goal is to predict EUI at the Urban site, but typically only data from rural sites is available. Cooling EUI is two orders of magnitude less than heating EUI for this cold, moist climate.

[kWh/m ²]	single-family		
	Cooling	Heating	Total
KBED	4	108	112
KBOS	4	104	108
Urban	5	88	93

Table 4.2: Normalized energy metrics for the single-family building under three separate simulation cases. The target values are those predicted from observed Urban weather data.

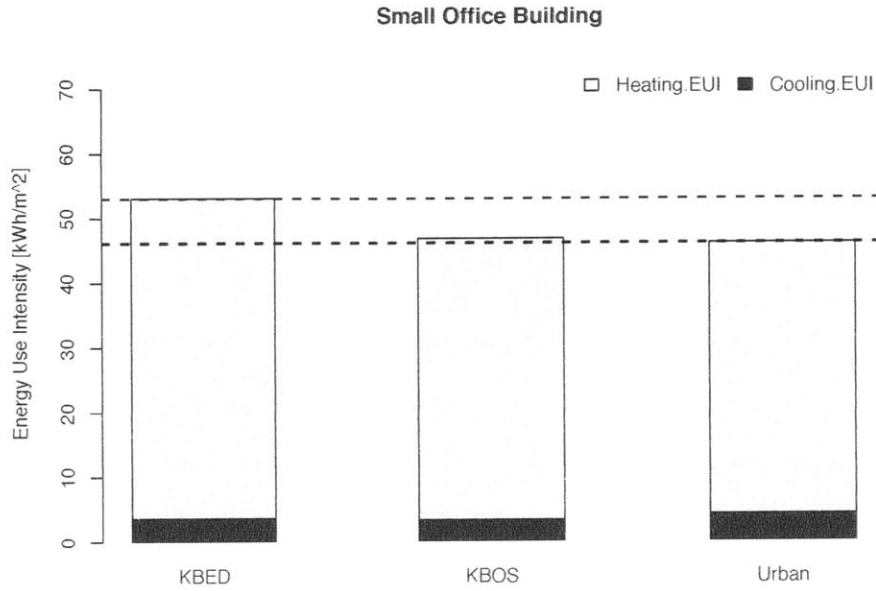


Figure 4-11: Variation in a small office building’s simulated total EUI, heating EUI, and cooling EUI based on the source of weather data for simulation. The goal is to predict EUI at the Urban site, but typically only data from rural sites is available.

	Small Office		
[kWh/m ²]	Cooling	Heating	Total
KBED	4	50	54
KBOS	3	44	47
Urban	4	42	46

Table 4.3: Normalized metrics of the small office building under three separate simulation cases. The small office building responds weakly to climatic variables when compared to the single-family building. KBOS and Urban weather data predict nearly identical values of the EUI.

4.3 Experiment 3: Simulated vs. Actual Weather Elements

Section 4.1 showed that there exist significant variation in dry-bulb temperature between the rural and urban building sites examined in the Boston, MA metropolitan area. Section 4.2 quantified these differences with normalized energy metrics. Now that we know there are errors introduced to building thermal simulation due to using either rural (KBED) or typical (KBOS) weather data to model an urban building, we move to the step of generating more representative urban weather data.

An unknown combination of local urbanization and local geographic effects alters rural weather data into the urban weather data finally observed. Using the Crawley algorithm and the Urban Weather Generator (UWG) we will generate urban weather data from the rural data sets following the methodology described in Chapter 3.

The results of microclimate prediction schemes were analyzed with the root mean square error (RMSE) and mean bias error (MBE) statistics. There are three periods of interest: annual, summer design week and winter design week. For each period of interest, the target signal to replicate is the urban dry-bulb temperature measured at KMACAMBR4.

Each of the microclimate prediction schemes attempts to reduce both the RMSE and MBE with respect to the urban air temperature signal. A RMSE of zero indicates that the urban signal was predicted with no error. Comparing the observed rural weather data to the observed urban data, KBED has an annual RMSE of 2.8°C and KBOS has an annual RMSE of 1.8°C . The corresponding MBE is -1.1°C and -0.2°C , respectively. If the Crawley algorithm or UWG are successful then we will have a reduction in the RMSE for rural sites and the MBE will be closer to zero.

Each weather generator is applied with either the Hanscom Air Force Base or Boston-Logan International Airport weather data as the input data. Results from the weather simulations are tabulated in Table 4.4. The UWG reduces the RMSE at an annual time scale and for both winter and summer design weeks for both stations as input. UWG either reduces the magnitude of the MBE or causes no change in

magnitude for all time periods and with both input stations.

Dry-bulb temperature statistics on the Crawley algorithm are varied. For most cases, the Crawley algorithm produces a worse RMSE than the unadjusted signal (Table 4.4), except for $\Delta\text{DB} = 1^\circ\text{C}$. This is most likely attributed to the mismatch between the observed UHI effect and that prescribed by the Crawley algorithm for $\Delta\text{DB} = 5^\circ\text{C}$. Viewing the design week figures demonstrates the characteristic features of the Crawley algorithm (Fig. 4-12 to Fig. 4-15). Observing the summer and winter design week hourly data we can see that neither model captures large swings in the temperature signal. We conclude by noting that, as measured by the RMSE, the UWG reproduces the urban dry-bulb temperature signal better than the Crawley algorithm for all time and data input combinations, except for the winter design week with KBOS data as input (Table 4.4).

	[°C]	Reference Station			
		KBED		KBOS	
		RMSE	MBE	RMSE	MBE
Base		2.8	-1.1	1.8	-0.2
U		1.7	-0.1	1.5	0.2
A	1	2.5	-0.5	1.9	0.3
	5	3.5	1.6	3.9	2.5
	U	1.8	0.2	1.7	0.6
S	1	2.9	-0.7	2.1	0.3
	5	3.5	0.9	3.6	2
	U	1.2	-0.5	0.8	0.4
W	1	1.5	-0.6	1.1	0.7
	5	3.3	2.2	4.1	3.4

Table 4.4: Annual (*A*), summer (*S*) and winter (*W*) statistical analysis of modeled weather files: UWG (*U*), $\Delta\text{DB}=1^\circ\text{C}$ (1) and $\Delta\text{DB}=5^\circ\text{C}$ (5).

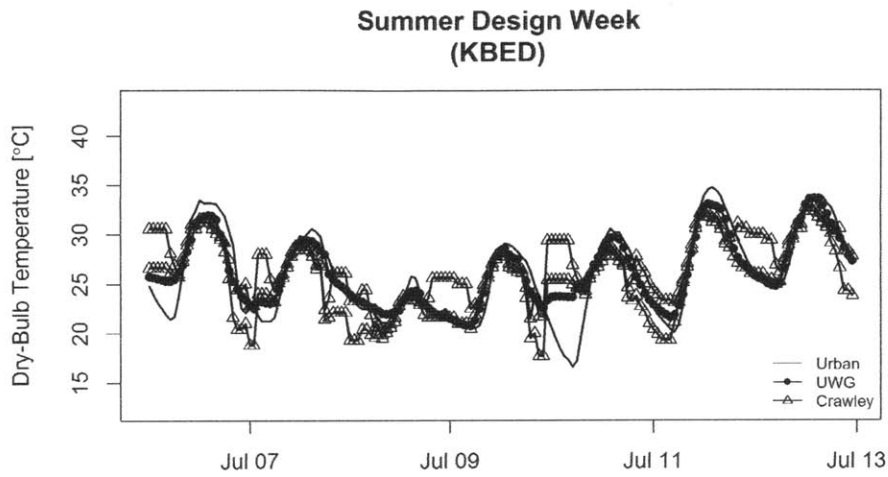


Figure 4-12: A summer design week comparison between the urban station and two modeled stations with KBED as the input rural station.

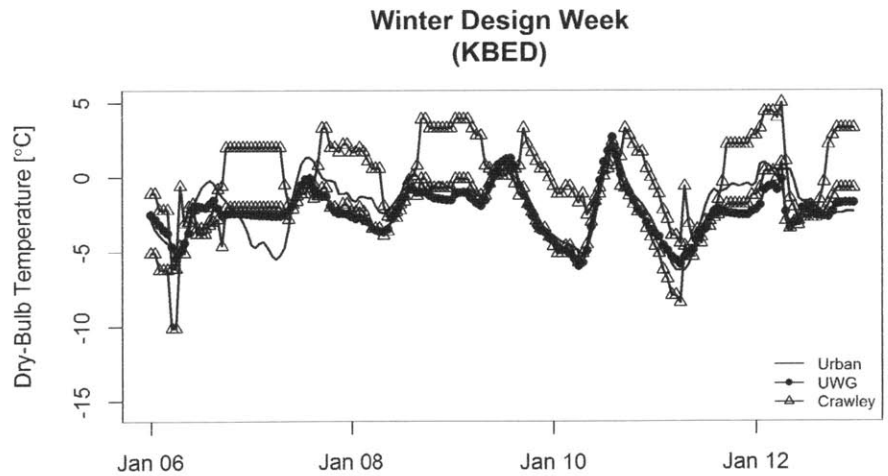


Figure 4-13: A winter design week comparison between the urban station and two modeled stations with KBED as the input rural station.

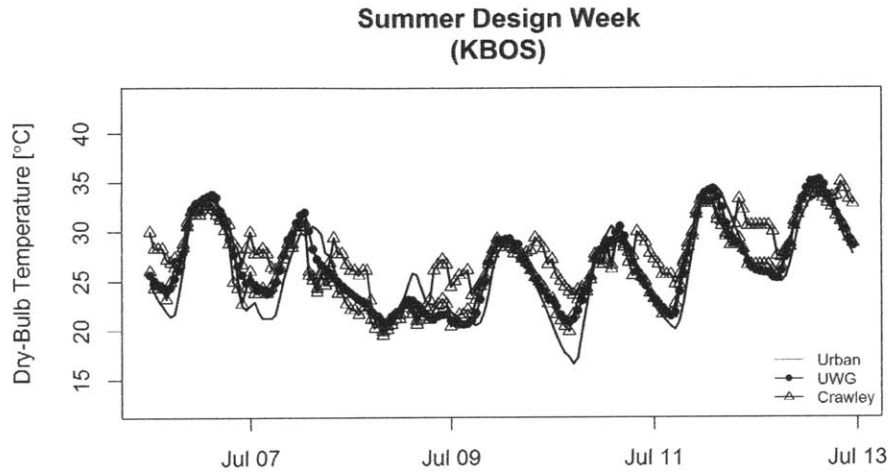


Figure 4-14: A summer design week comparison between the urban station and two modeled stations with KBOS as the input rural station.

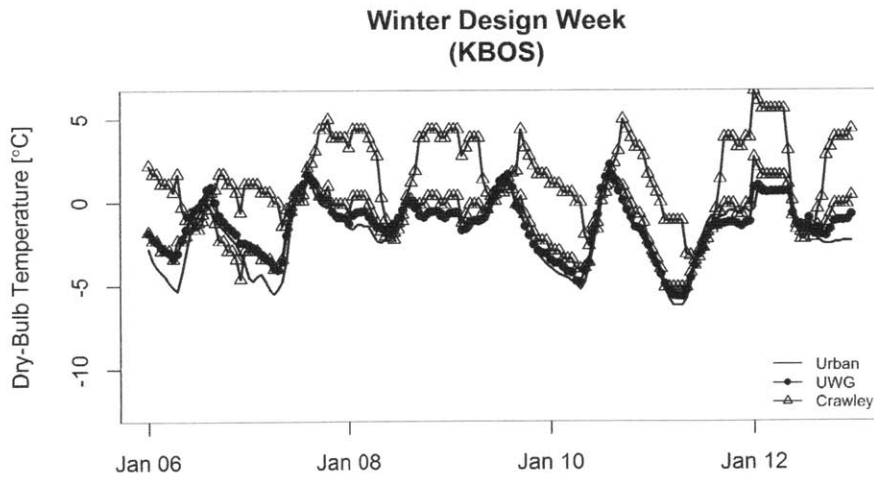


Figure 4-15: A winter design week comparison between the urban station and two modeled stations with KBOS as the input rural station.

4.4 Experiment 4: Building EUI & Simulated Weather

After statistically comparing the results of each model we turn to evaluate the impact of individual weather elements and specific combinations of these elements on each building's energy use intensity. Four experimental EPW files were created by inserting values from the urban EPW into the corresponding column of each airport EPW. Simulation results with KBED as the base airport station are plotted for the single-family building in Fig. 4-16 and for the small office building in Fig. 4-17.

Examining the single-family building simulation results in Fig. 4-16 from left to right in these figures we can see the decrease in both total EUI and heating EUI from the rural to the urban EPW file. Intermediate values of the EUI occur for each of the experimental EPW files. Inserting either the urban dry-bulb temperature ('DB'), the wind speed and wind direction ('Local Wind') or the dry-bulb temperature and relative humidity ('DB + RH') values into the rural EPW accounts for nearly half of the difference in EUI between rural and urban sites (Fig. 4-16).

However, with the small office building the influence of the wind speed and wind direction is negligible (Fig. 4-17). The largest reduction in total EUI difference for the small office building is with the urban dry-bulb temperature ('DB') and the combined dry-bulb temperature and relative humidity ('DB + RH') EPW files (Fig. 4-17). We may conclude that for KBED as the rural airport station the most influential variables for reducing the difference between rural and urban EUI are the dry-bulb temperature and relative humidity. The results also suggest that improved prediction of dry-bulb temperature itself is as good as predicting both DB and RH together.

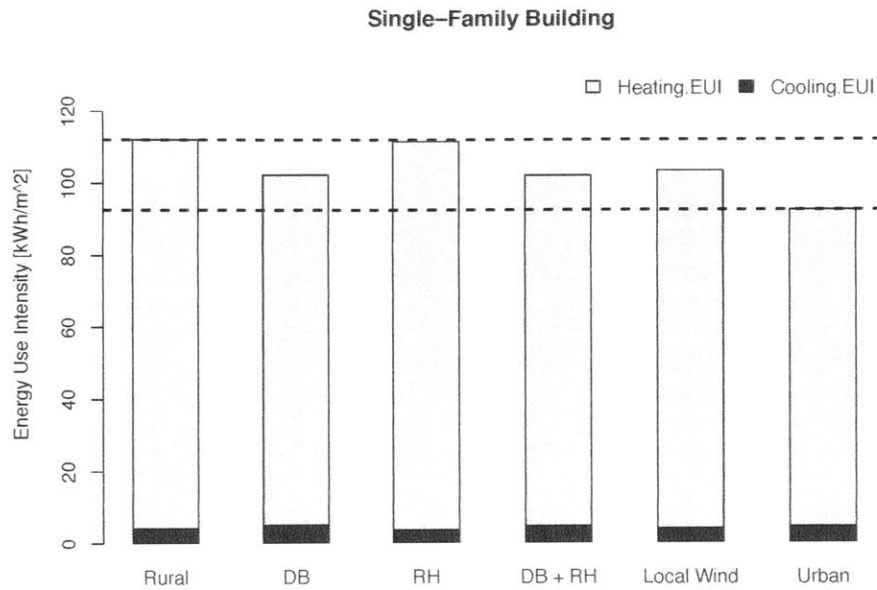


Figure 4-16: Changes in the simulated total EUI for a single-family building with variation of EPW values. KBED as the rural base.

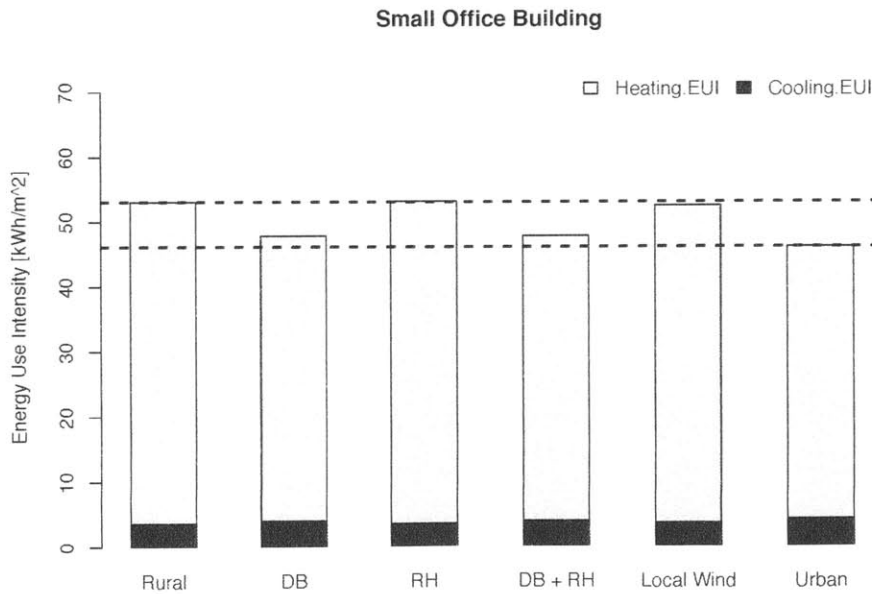


Figure 4-17: Changes in the simulated total EUI for a small office building with variation of EPW values. KBED as the rural base.

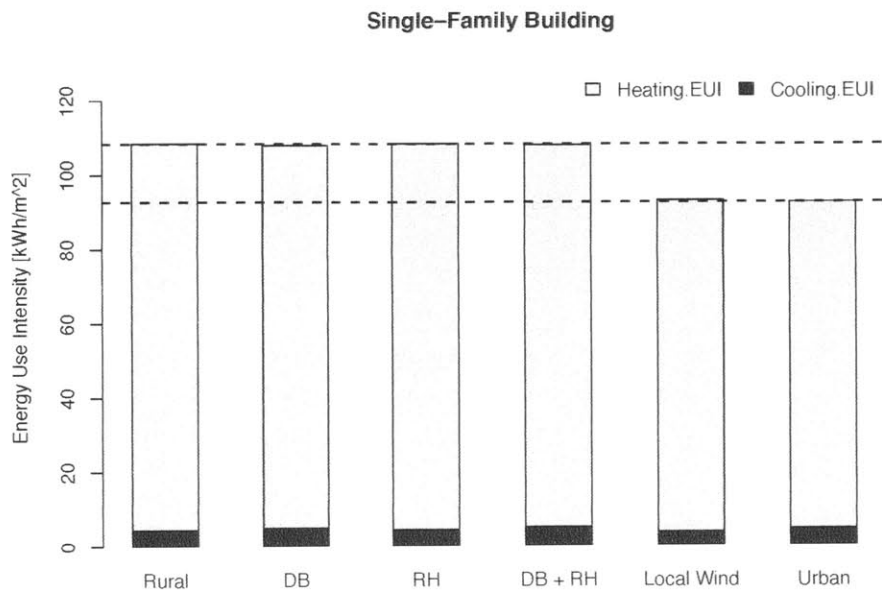


Figure 4-18: Changes in the simulated total EUI for a single-family building with variation of EPW values. KBOS as the rural base.

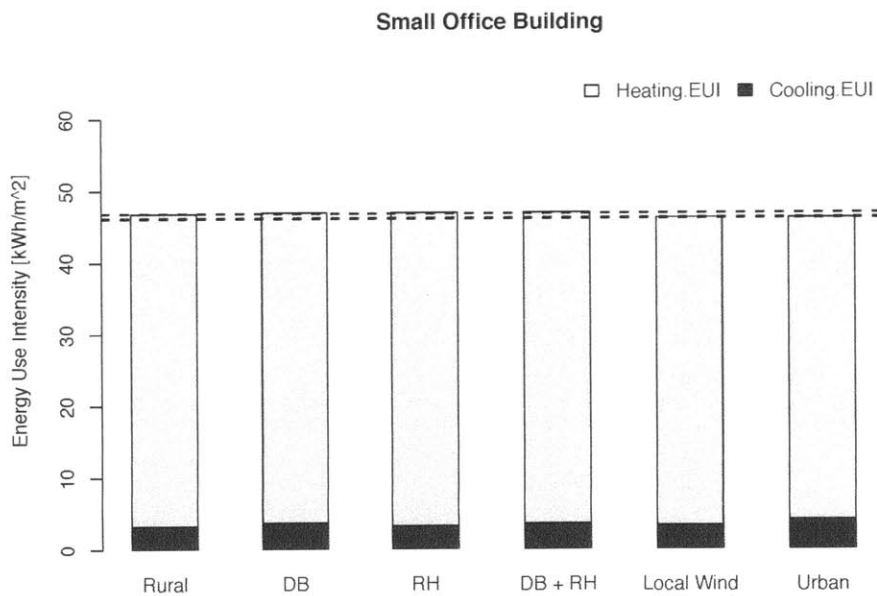


Figure 4-19: Changes in the simulated total EUI for a small office building with variation of EPW values. KBOS as the rural base.

The results from the same experimental variation with KBOS as the rural base EPW file are very different. Examining the single-family building results we see that exchanging urban values for either relative humidity, dry-bulb temperature or both has negligible impact on reducing the EUI difference between the urban and rural site. The most influential variables in this situation now become the wind speed and wind direction, which accounts for nearly all of the EUI difference under the experimental conditions (Fig. 4-18).

The importance of dry-bulb temperature and relative humidity between KBOS and the urban station is de-valued in terms of EUI reduction because KBOS is not a rural station. KBOS is within the urban regime as we discovered by both aerial site analysis and comparison of weather elements. The proximity of KBOS to the urban site implies that the dry-bulb temperature and relative humidity signals already share many similar characteristics, therefore for the single-family home the differences in local wind speed and wind direction dominate the building's thermal load and thus greatly influence the predicted EUI. For the small office building, which is less sensitive to external loads than the single-family building, there is a negligible impact of altering weather elements (Fig. 4-19).

After quantifying the statistical improvements to the DB temperature signal, we now present the results for building simulations with the modeled EPWs (Fig. 4-20 through Fig. 4-23). Each table accompanying the Fig. 4-20 through Fig. 4-23 details the difference in EUI results between modeled EPWs and the urban EPW.

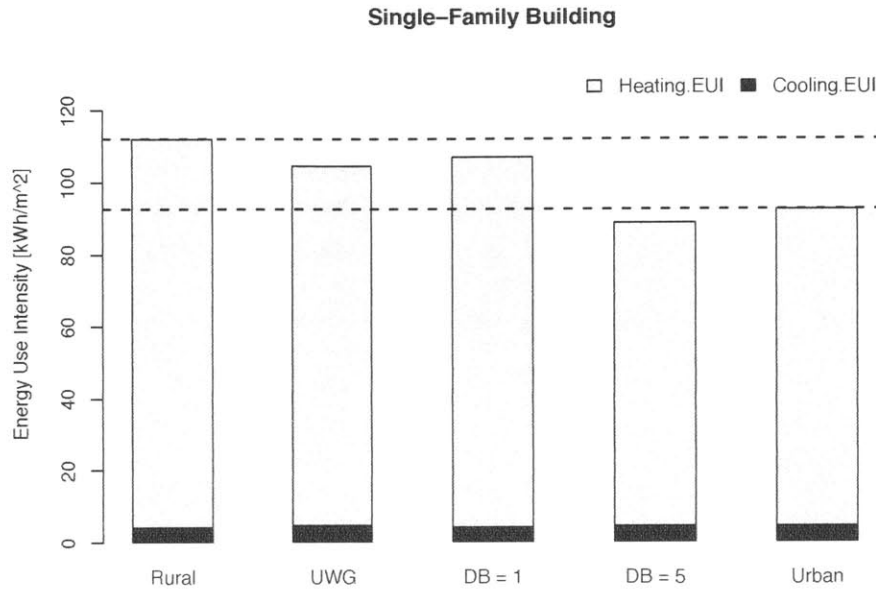


Figure 4-20: Changes in the total EUI for a single-family building. The rural station is KBED and the dashed lines are the limits imposed by the rural and urban values.

$[kWh/m^2]$	Cooling	Heating	TotalEUI
Rural	4	108	112
Crawley_1	4	103	107
UWG	5	100	105
Urban	5	88	93
Crawley_5	5	84	89

Table 4.5: Normalized energy metrics for the single-family building with both urban weather schemes and KBED as the rural station.

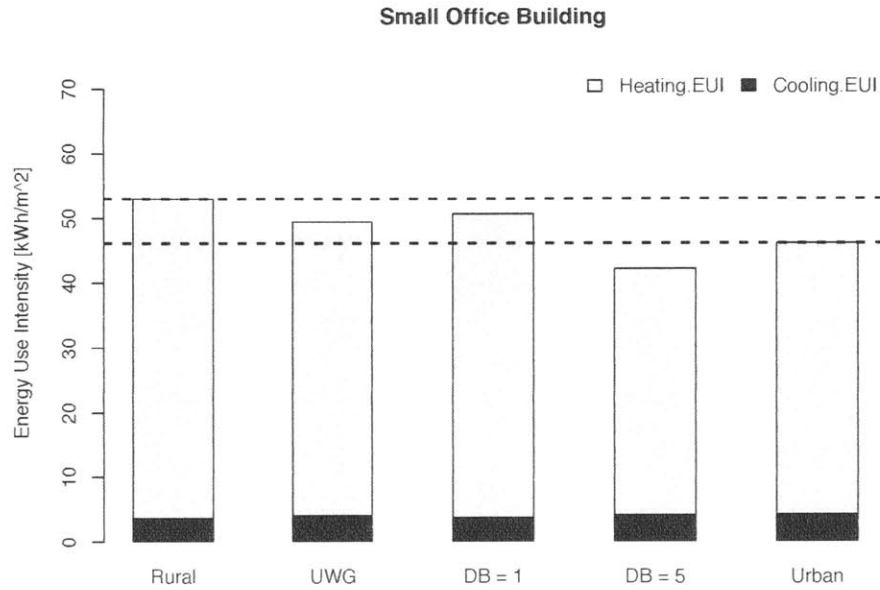


Figure 4-21: Changes in the total EUI for a small office building. The rural station is KBED and the dashed lines are the limits imposed by the rural and urban values.

$[kWh/m^2]$	Cooling	Heating	TotalEUI
Rural	4	50	54
Crawley_1	4	47	51
UWG	4	46	50
Urban	4	42	46
Crawley_5	4	38	42

Table 4.6: Normalized energy metrics for the small office building with both urban weather schemes and KBED as the rural station.

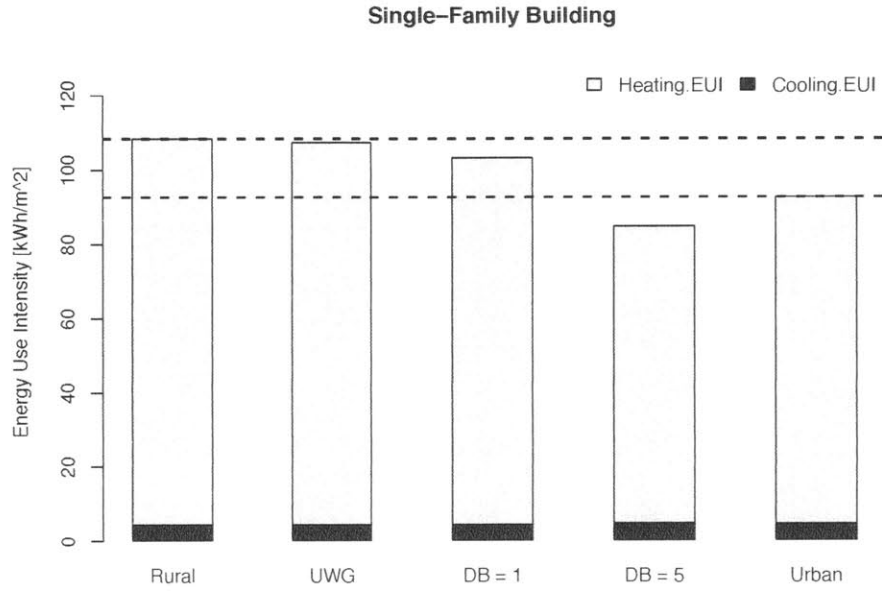


Figure 4-22: Changes in the total EUI for a single-family building.

[kWh/m ²]	Cooling	Heating	TotalEUI
Rural	4	104	108
UWG	4	103	107
Crawley_1	4	99	103
Urban	5	88	93
Crawley_5	5	80	85

Table 4.7: Normalized energy metrics for the single-family building with both urban weather schemes and KBOS as the rural station.

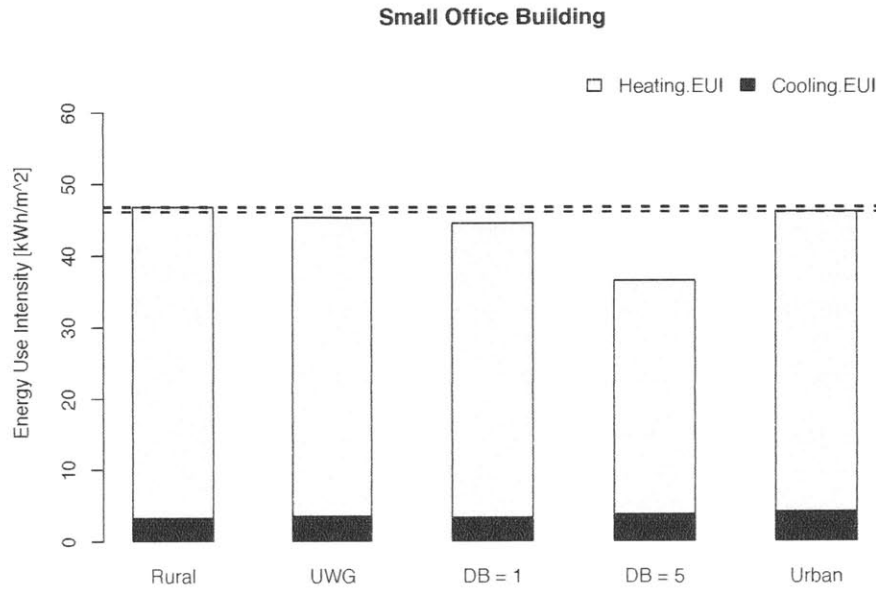


Figure 4-23: Changes in the total EUI for a small office building.

<i>[kWh/m²]</i>	Cooling	Heating	TotalEUI
Rural	3	44	47
UWG	4	42	46
Urban	4.1	42	46
Crawley_1	3	41	45
Crawley_5	4	33	37

Table 4.8: Normalized energy metrics for the small office building with both urban weather schemes and KBOS as the rural station.

Fig. 4-20 - Fig. 4-23 summarize the findings of the thesis as they display simulated EUI results for both models as well as for all observed data. In each figure the ‘Urban’ simulation result for each building type is a constant. The ‘Rural’ value is dependent on, which rural weather station was used to define the simulation conditions (i.e., either Boston-Logan International Airport or Hanscom Air Force Base). Thus, the difference in simulated EUI between the ‘Urban’ and ‘Rural’ value is the error to be expected if no urban weather data is available during simulation.

Table 4.8 and Table 4.7 highlight that KBOS has a temperature profile very similar to the urban area and is much warmer than KBED. In general, methods to modify rural weather data to form urban data will increase the temperature of the input signal. Since the urban area and KBOS experience similar climate effects due to geography and urbanization, applying microclimate prediction models to this data results in EPW files that greatly under predict the heating EUI. In particular, applying the UWG to weather data from a station that does not meet the definition of rural, produces EPW files for simulation that will result in worse predictions of the urban building’s EUI (Fig. 4-22 and Fig. 4-23). The Crawley algorithm is still capable of producing upper and lower limits to the urban single-family building EUI even with KBOS as input data; however, for the small office building this is no longer the case. For both building types and for both sets of input weather data, the Crawley algorithm with $\Delta DB = 5^{\circ}C$ produces EPW files whose simulations result in extreme under prediction of the urban EUI.

4.5 Experiment 5: Parametric Analysis of UWG

Several key inputs to the UWG are the urban morphology parameters, which vary distinctly based on the radius considered to define the urban site. We varied the defining urban area with five separate radii: 100 m, 250 m, 500 m, 1000 m, and 2000 m (Table 4.9). However, due to the rather homogeneous nature of Cambridge, MA the greatest variation is in the vertical-to-horizontal area ratio ($0.55 \leq VH \leq 1.54$) and horizontal building density ($0.17 \leq H_{bd} \leq 0.42$).

In Fig. 4-24 and Fig. 4-25 the EUI prediction gets better as the radius decreases and approaches the rural station EUI prediction for large values. This result is expected for a relatively homogeneous urban area because as the geometry defined in the UWG becomes less dense, fewer buildings contribute to the energy balance, which implies less modification to the input rural data. Fig. 4-26 and Fig. 4-27 illustrate the results when KBOS is the input rural station. For a very small radius the EUI prediction dips below that of the 'DB/RH' prediction, but then increases with increasing radius. The negligible change in EUI prediction with radius with KBOS as the rural base is to be expected from the analysis in Section 4.4. Dry-bulb temperature and relative humidity have negligible bearing on the EUI difference between KBOS and the urban site due to their similar weather patterns. In general, the 500 m radius works well, but users must individually determine the dominant morphology surrounding an intended site and alter the area of influence accordingly. The range of EUI prediction that manifests due to variable radius of influence is negligible for the small office building and all cases with KBOS as the input weather.

Radius [m]	Avg. Height [m]	Hbld	VH
100	9.65	0.42	1.54
250	9.23	0.35	1.31
500	9.7	0.38	1.3
1000	10.2	0.3	0.96
2000	10.1	0.17	0.55

Table 4.9: Change in urban parameters with increasing radius.

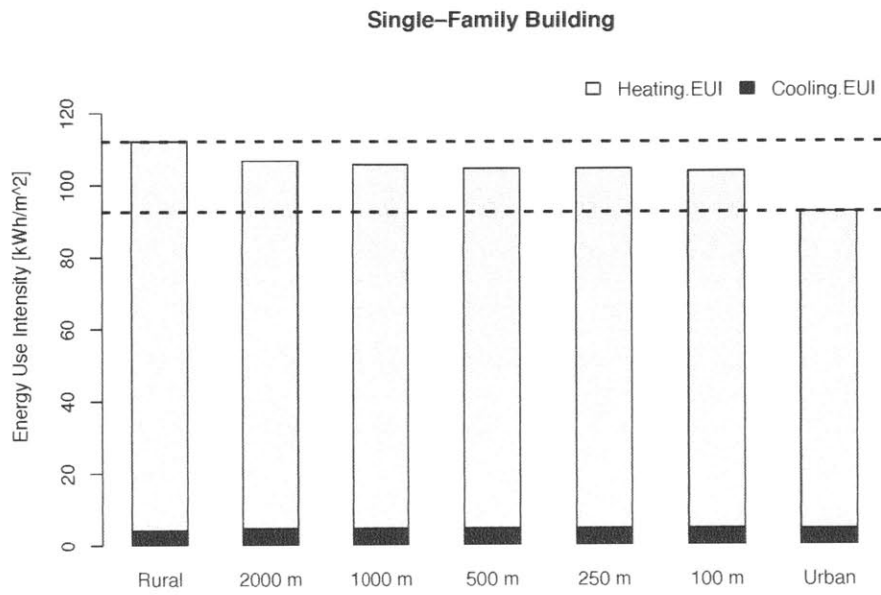


Figure 4-24: Evolution of the EUI for a single-family building for various iterations of the UWG. KBED as the rural base.

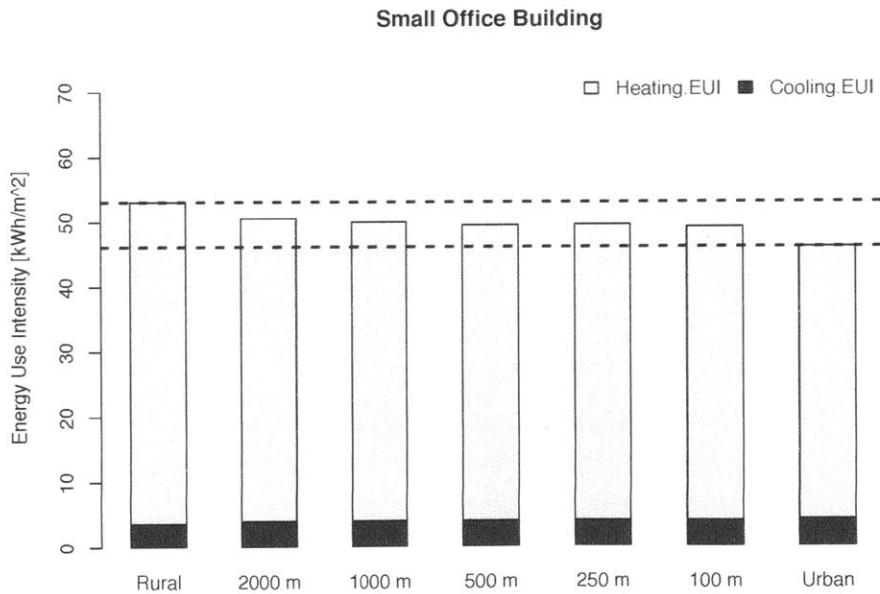


Figure 4-25: Evolution of the EUI for a small office building for various iterations of the UWG. KBED as the rural base.

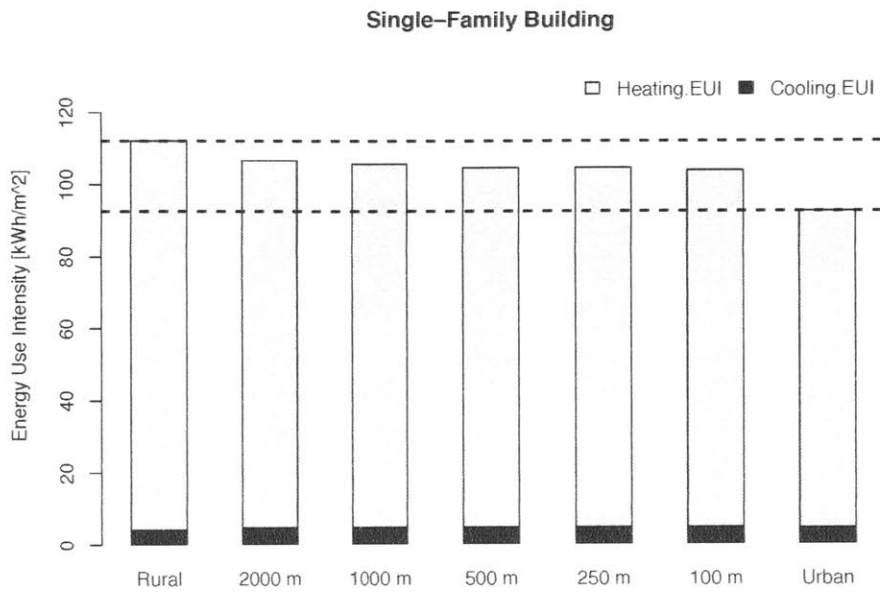


Figure 4-26: Evolution of the EUI for a single-family building for various iterations of the UWG. KBOS as the rural base.

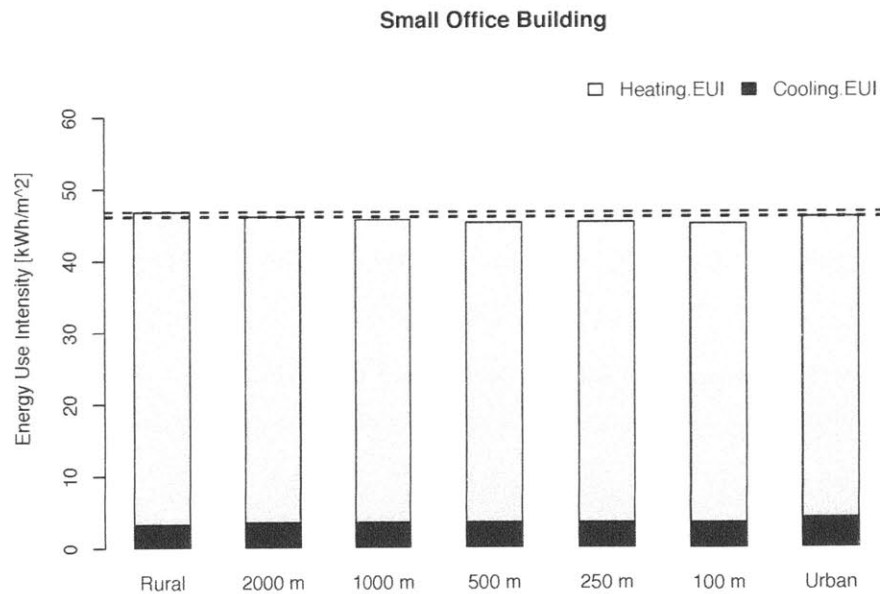


Figure 4-27: Evolution of the EUI for a small office building for various iterations of the UWG. KBOS as the rural base.

4.6 Summary

Observing the actual $T_{u-r(max)}$ between Cambridge, MA (KMACAMBR4) and Hanscom Air Force Base (KBED) for 2011, with all hours considered, showed $T_{u-r(max)} = 5.7^{\circ}\text{C}$. Observing the actual $T_{u-r(max)}$ between Cambridge, MA and Boston-Logan International Airport (KBOS) for 2011, with all hours considered, showed $T_{u-r(max)} = 3.1^{\circ}\text{C}$. When only night hours with calm winds are observed $T_{u-r(max)} = 6.4^{\circ}\text{C}$ between Cambridge, MA and Hanscom Air Force Base for 2011. Alternatively, for 2011 night hours with calm winds, $T_{u-r(max)} = 2.9^{\circ}\text{C}$ between Cambridge, MA and Boston-Logan International Airport .

In addition, seven values of the monthly average night-time dry-bulb temperature peak of 2011 at Hanscom Air Force Base are significantly different than the urban elements at Cambridge, MA ($p < 0.05$). Zero of these 2011 values recorded at Boston-Logan International Airport are significantly different than the urban elements at Cambridge, MA ($p > 0.2$). We reject the hypothesis that Boston-Logan International Airport is a rural weather site. We accept the hypothesis that Hanscom Air Force Base is a suitable rural site in comparison to the urban site at Cambridge, MA.

Section 4.2 simulated a typical single-family building and small office building with three separate definitions of the simulation weather file. The total EUI predicted by using an urban weather definition is the minimum value for both building types. This is due to the beneficial effect of the UHI in a heating dominated climate. Using rural weather data from KBED results in $19 \text{ kWh}/\text{m}^2$ (20%) and $7 \text{ kWh}/\text{m}^2$ (15%) over prediction of the EUI in a single-family and small office building, respectively. Using rural weather data from KBOS results in $15 \text{ kWh}/\text{m}^2$ (16%) and $1 \text{ kWh}/\text{m}^2$ (2%) over prediction of the EUI in a single-family and small office building, respectively.

Section 4.3 utilized both Crawley's algorithm and the Urban Weather Generator to produce artificial urban weather data sets from each of the rural sites. The annual baseline error statistics for Hanscom Air Force Base versus the urban site are: RMSE = 2.8°C , MBE = -1.1°C . The annual baseline error statistics for Boston-Logan International Airport versus the urban site are: RMSE = 1.8°C , MBE = -0.2°C . Ap-

plying the UWG with inputs from Table 3.1 to KBED input data produces: $RMSE = 1.7^{\circ}C$, $MBE = -0.1^{\circ}C$. Applying the UWG with inputs from Table 3.1 to KBOS input data produces: $RMSE = 1.5^{\circ}C$, $MBE = 0.2^{\circ}C$. Applying the Crawley's algorithm with $\Delta DB = 1^{\circ}C$ and $5^{\circ}C$ to KBED input data produces: $RMSE_{\Delta DB=1^{\circ}C} = 2.5^{\circ}C$, $MBE_{\Delta DB=1^{\circ}C} = -0.5^{\circ}C$, $RMSE_{\Delta DB=5^{\circ}C} = 3.5^{\circ}C$, $MBE_{\Delta DB=5^{\circ}C} = 1.6^{\circ}C$. Applying the Crawley's algorithm with $\Delta DB = 1^{\circ}C$ and $5^{\circ}C$ to KBOS input data produces: $RMSE_{\Delta DB=1^{\circ}C} = 1.9^{\circ}C$, $MBE_{\Delta DB=1^{\circ}C} = 0.3^{\circ}C$, $RMSE_{\Delta DB=5^{\circ}C} = 3.9^{\circ}C$, $MBE_{\Delta DB=5^{\circ}C} = 2.5^{\circ}C$.

Crawley's algorithm alters the input dry-bulb temperature signal into one that fits the observed urban signal, based on the annual RMSE and MBE, worse for all cases, except for $\Delta DB = 1^{\circ}C$ applied to KBED. The UWG improves the input dry-bulb temperature signal fit to the observed urban signal for all cases. However, the UWG does not ideally capture large disturbances in the urban dry-bulb temperature signal.

Section 4.4 details the impact of specific weather elements on EUI prediction as well as the EUI prediction based on simulated weather data. A single-family building simulated with the urban weather data has a predicted EUI of $93 kWh/m^2$ and a small office building simulated with the urban weather data has a predicted EUI of $46 kWh/m^2$. When KBED is the input rural station, the most influential weather element on EUI prediction for both building types is the dry-bulb temperature (Fig. 4-16 and Fig. 4-17). Having the exact urban dry-bulb temperature signal with the remaining data from the rural station ('DB' in Table 3.2) results in $103 kWh/m^2$ (+ 11%) for the single-family building and $48 kWh/m^2$ (+ 4%) for the small office building. However, with KBOS as the input rural station, the most influential weather elements for predicting EUI of a single-family building are the combination of wind speed and wind direction (Fig. 4-18, but for the small office building altering weather elements has negligible impact on simulation results Fig. 4-19).

If Hanscom Air Force Base is used as the input weather data for the Crawley algorithm and UWG, then the UWG reduces the error between single-family building urban and rural energy predictions by nearly half. For a small office building the error is reduced from 15% to 9%. The Crawley algorithm with $\Delta DB = 1^{\circ}C$ does

provide an upper limit of the simulated EUI and $\Delta DB = 5^{\circ}\text{C}$ is a lower limit to the simulated EUI. However, if Boston-Logan International Airport is used as the input weather data for each model, then the simulated EUI resulting from the use of UWG output is not improved over the simulated EUI from observed rural data. Additionally, the Crawley algorithm now only forms upper and lower limits to the actual urban simulation results for the single-family building.

Section 4.5 quantified the the impact of radius of influence on generation of urban weather files with the UWG. With weather data from KBOS as the input data for the UWG, the variation in EUI with radius is negligible for both buildings (Fig. 4-26 and Fig. 4-27). With weather data from KBED as the input data for the UWG, the variation in EUI with radius is negligible for the small office building (Fig. 4-25) and for the single-family building, the EUI varies by 3% from radius = 100 m to radius = 2000 m (Fig. 4-24).

Each of the microclimate prediction methods has advantages and limitations, which are summarized in Table 4.10.

UWG		Crawley	
Advantages	Limitations	Advantages	Limitations
Analytic model of urban microclimates built from the bottom-up that incorporates urban morphological parameters and detailed building energy simulations.	Detailed information about the urban morphology is a prerequisite, which may not be available in various locales.	A variety of numerical platforms can implement this extremely simple methodology.	Only latitude and city population determine ΔDB , which greatly reduces the site specificity available to designers.
The UWG builds upon several important physical representations of the urban environment, in particular the average oriented urban canyon and Town Energy Balance (TEB).	The RSM defines the heat transfer phenomena at the reference site in a very strict manner, which can lead to poor results if the user does not understand these assumptions and inputs an improper reference weather station.		The algorithm's simplified structure leads to over-prediction of DB temperatures in the early morning and after sunset.
Extremely flexible in its ability to describe an urban area and the physical process that occur.	To reduce the model's computational structure the UWG does not solve for wind speed or wind direction. This increased model simplicity requires analytic correlations to compute the mixing of temperature in the UBL model, which becomes less effective as the height of the urban canopy increases.		The algorithm does not define suitable reference weather sites.

Table 4.10: Each model's advantages and limitations is summarized above. A core limitation of the UWG is the inability to handle input weather data that is not strictly rural.

Chapter 5

Conclusions

5.1 Key Findings

Currently, the design of urban buildings does not account for site-specific microclimates due to a lack of observable data from operational weather stations or the inability to model potential microclimates. Additionally, calibrating energy models of urban buildings is potentially limited due to a lack of urban site-specific weather data. While computational power is increasing and more advanced methods of urban analysis continue to emerge, finding low-order computational models, with relevance to design teams remains a great challenge. This thesis compared two low-computational order models of the urban climate that may be applied to address these issues.

Based on observed weather data for the year 2011 we predict the typical single family building to have an EUI of 93 kWh/m^2 and a small office building to have an EUI of 46 kWh/m^2 . If no urban weather data is available and data from a regional airport, Hanscom Air Force Base, is used instead, then we find an over prediction of the urban EUI by 20%, in the case of the single family building, and over prediction of the urban EUI by 15% for the small office building. If weather data from the nearest weather station reporting typical meteorological year (TMY) data, Boston-Logan International Airport, is used instead of urban data, then we find an over prediction of the urban EUI by 16% and 2% for the single family building and small office, respectively.

Analyzing the dry-bulb temperature signal from Boston-Logan International airport we reject the hypothesis that it is a rural station with a significant temperature difference from the urban site. Therefore, applying the Urban Weather Generator of Bueno *et al.* to the weather elements of Hanscom Air Force Base we improve our simulated predictions of the urban EUI for both single family and small office buildings. The over prediction is reduced from 21% to 13% for the single family building and from 15% to 9% for the small office building. Alternatively, if the Crawley algorithm is applied to Hanscom Air Force Base data in order to create upper and lower limits of the urban single family building's EUI, then the lower bound gives an 8% under prediction of the urban EUI and the upper bound gives an 11% over prediction of the urban EUI. For the small office building the lower bound gives 8% under prediction and a 10% over prediction.

In conclusion, we state that the critical first step to assessing the impact of UHI on early design simulations is to characterize the the weather site that is the source of data. If this site fails to meet the rural assumptions, then applying either of these models will not assist in annual EUI prediction. Once the weather source is properly identified as rural then the application of interest should be identified. For applications that either require feedback with the urban design or have extensive data on the urban morphology we recommend the use of the UWG. For applications that lack urban site data and are order of magnitude estimations, the Crawley algorithm generally is able to provide extremes of the predicted EUI. However, unlike the UWG, the Crawley algorithm does not allow parametric exploration of an urban design problem. If users of thermal simulation seek to answer questions about the coupled effects of their buildings and existing buildings, then the Crawley algorithm may not be appropriate. When modeling urban microclimates adhere to the following guidelines:

1. Ensure that the reference station used as input adheres to a rural definition: site within the study region but outside the urban area and its affected environs with minimal influence from large geographic features i.e. valleys, large bodies of water, etc.

2. If the station that collects TMY or AMY data does not fit the rural definition and there is no suitable rural site, do not apply either of these simple models to the data; this will likely result in a worse statistical fit to the actual urban DB signal.
3. If there is insufficient data to calculate urban morphological parameters, applying Crawley's scheme to a rural site can bracket the urban DB signal.

5.2 Future Work

Recommending tools that improve thermal simulation of buildings in urban climates should focus on the following areas of future research:

1. **Simple models that better account for weather sites that are not strictly rural** The KBOS weather station is at an airport and provides TMY data for thermal simulation of buildings. However, it is very near to the urbanized area and is on a peninsula. Each of these factors contributes to the observed weather elements from this station. Research should focus on a more robust urban weather generator that may have parameters that allow some greater flexibility in the definition of the input weather station.
2. **Advanced techniques for constructing EPW files for simulation** Incomplete environmental data is a common issue in the environmental sciences (Schneider, 2001). Techniques for managing statistical data with missing or incomplete data are varied in their complexity and applicability (Schneider, 2001; Junninen *et al.*, 2004). Deciding which methods are appropriate depend on the final use of the data. In the case of annual whole-building simulation there is a lack of research comparing the impacts of environmental data imputation methods on predicted building performance metrics.
3. **Comparing the impact of ground-slab interactions on EUI to UHI impacts on EUI**

Buildings with energy use tied to the envelope may have significant changes in energy use due to environmental interactions. The choice of which weather conditions to use for simulating urban buildings was discussed in this thesis. An additional concern is the effect of heat transfer at the building foundation. The single-family building modeled in this thesis utilized the Winkelmann model to estimate the ground-slab interface temperature while the small office building ground-slab interface was prescribed as a constant 18°C (Winkelmann, 2002). These parameters were not altered simply to adhere to the general standard that defines each building model. Andolsun et al. discuss the differences in EUI encountered for a selection of foundation conditions and models of the heat transfer (Andolsun *et al.*, 2010). Additional work may be done to compare the trade-off in thermal building simulation between more representative urban weather data and better data regarding foundation heat losses.

4. Generalizing model findings across more climate zones

The variation of climate between regions is an important factor when drawing conclusions about these low-order models. An advantage of the UWG is that it requires input from a rural weather station within the climate region. Therefore the deterministic momentum and heat transfer calculations that result in urban weather data are more readily generalized. As long as the user has adequate knowledge of the building site's urban area there is reason to believe that the UWG will result in similar performance across climate zones. However, for semi-empirical models and correlations such as the Crawley algorithm it may be more necessary to repeat comparisons across climate zones. The assumption that the urban heat island intensity for any city varies between 1 and 5°C, as is assumed by the Crawley algorithm, may of course have specific outliers, but as is noted by the EPA and referenced by Crawley there is reasonable data to support this assumption (USEPA, 2012).

5. Compare the Kershaw model to the UWG and Crawley schemes

An algorithm by Kershaw was introduced in Section 2.1.1. This semi-empirical

model uses constants developed by a regional analysis of UK weather stations to predict urban air-temperature anomalies. This method is comparable to the Crawley algorithm and may represent an additional viable alternative for estimating EUI variations in buildings due to the UHI.

Appendix A

EPW Tutorial

A.1 Weather Elements

The UWG and Crawley's algorithm are each designed to alter data in an EnergyPlus Weather (EPW) file format. The full specification for this format is found in the EnergyPlus Auxiliary Programs documentation and the paper by Crawley et al (DOE, 2010; Crawley *et al.*, 1999). Simulation weather data for an EnergyPlus thermal simulation must contain the following weather elements: Dry Bulb Temperature [$^{\circ}C$], Dew Point Temperature [$^{\circ}C$], Relative Humidity [], Atmospheric Station Pressure [Pa], Horizontal Infrared Radiation Intensity [Wh/m^2], Direct Normal Radiation [Wh/m^2], Diffuse Horizontal Radiation [Wh/m^2], Wind Direction[$^{\circ}$], Wind Speed [m/s], Opaque Sky Cover, Present Weather Observation, Present Weather Codes, Liquid Precipitation Depth [mm].

Each of these variables was downloaded from *www.weatherunderground.com* and the corresponding ASOS or PWS station. Solar radiation data for the year 2011 could not be accessed from *www.weatherunderground.com* for the urban weather station. Therefore this data was downloaded directly from <http://weather.keneli.org/>.

A.1.1 Mining & Processing

The principal tool for accessing online weather data used in this thesis is the statistical software package ‘R’ (R-2.142) (R Development Core Team, 2012) (Fig. A-1). Processing of data was done identically for each weather element type (Fig. A-2). Solar radiation was processed further from total solar radiation into its diffuse and direct components using the Reindl method (Reindl *et al.*, 1990). Neither of the two methods examined in this paper provides updated values of the urban solar radiation, therefore we controlled for radiation data in simulations by using data from the urban site in each EPW file. However, horizontal infrared radiation intensity was recalculated for each site based on observed dry-bulb and wet-bulb temperature according to the EnergyPlus documentation (DOE, 2010).

$$H_{IR} = \epsilon_{sky} * \sigma * T_{dry-bulb}^4 \quad (A.1)$$

where H_{IR} = horizontal infrared radiation intensity [Wh/m^2], σ = Stefan-Boltzmann constant = $5.67e^{-8}$ [W/m^2K^4], ϵ_{sky} = sky emissivity, and $T_{dry-bulb}$ = dry-bulb temperature [K]. To calculate the sky emissivity the following equation was used:

$$\epsilon_{sky} = (.787 + .764 * \ln(\frac{T_{dewpoint}}{273})) * (1 + .0224N - .0035N^2 + .00028N^3) \quad (A.2)$$

where $T_{dewpoint}$ = dew-point temperature [K], N = opaque sky cover [tenths]. Cloud cover observations were set to zero and were not included in calculations of horizontal infrared radiation intensity.

A.1.2 Data Sources

Observed values of urban and non-urban weather elements were taken from two types of weather stations: Automated Surface Observing System (ASOS) and Personal Weather Station (PWS). Each of the non-urban weather stations, Boston-Logan International Airport and Hanscom Air Force Base are serviced by weather stations that are a part of the ASOS. The urban station, KMACAMBR4, is a PWS.

The ASOS is the result of a collaboration between three U.S. governmental agencies: the National Weather Service (NWS), the Federal Aviation Administration (FAA), and the Department of Defense (DOD) (Oceanic and Administration, 1992). The primary goal of the ASOS is to provide the detailed minute-by-minute observational weather data necessary to safely operate an aviation facility. Data collected through the ASOS is also designed for use in climatologic and meteorologic research. Each ASOS station is composed of three components: sensor group, acquisition control unit (ACU), and operator interface device (OID). The standard sensor group instrumentation includes: cloud height indicator, visibility sensor, precipitation identification sensor, freezing rain sensor, pressure sensors, ambient/dew point temperature sensor, anemometer, and precipitation accumulation sensor. Select ASOS sites will also include a lightning sensor. Siting of the sensor group follows the Federal Standard for Siting Meteorological Sensors at Airports (for Meteorological Services and Research, 1994).

Location of ambient/dew point temperature sensors is important to the data and models described in this thesis. Per the ASOS siting standard:

Five feet above ground is the preferred height. The sensors will be protected from radiation from the sun, sky, earth, and any other surrounding objects but at the same time be adequately ventilated. The sensors will be installed in such a position as to ensure that measurements are representative of the free air circulating in the locality and not influenced by artificial conditions, such as large buildings, cooling towers, and expanses of concrete and tarmac. (for Meteorological Services and Research, 1994)

In general, a PWS does not conform to a specified standard. However, PWS's have integrated themselves into U.S. climatology due to the availability of quality instrumentation and network access. For example, PWS data providers that participate in the Cooperative Observer Program (COOP) must adhere to the same siting standards as ASOS along with a base level of instrumentation (for Meteorological Services and Research, 2010). Again, this is not the norm for a PWS. It is the combined

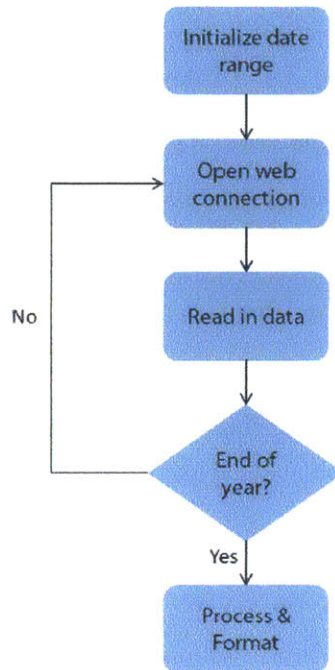


Figure A-1: Websites that store PWS information facilitate direct access of weather data through web addresses that house comma separated value files. Each address is defined by a station and date string.

sensing ability of the large PWS network that creates the value for these readings. Current online weather services collect and distribute data from across the U.S. See Fig. 3-5 for images of KMACAMBR4.

This methodology has limitations as the percentage of missing or invalid data increases. To allow re-production of the results a demonstration of the code is provided in the following sections. As stated in the future works, it is important to determine what degree of accuracy is needed when using actual weather data.

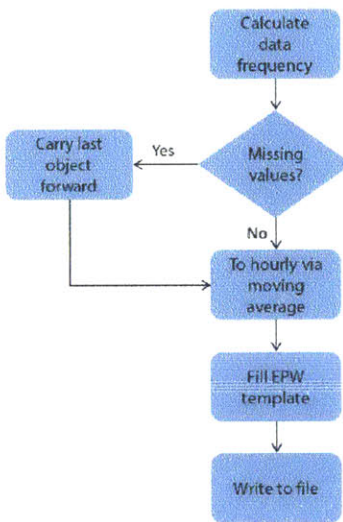


Figure A-2: All weather elements were processed via the same algorithm, in which the data frequency was determined and then missing elements were filled with the previous element carried forward. Sub-hourly data was first filled and an hourly average was then applied to produce the EPW.

A.1.3 User Functions

This section contains the functions that will be used throughout the demo in Section A.1.4.

```
> wunder_daily <- function(station = 'KBOS', date){
+   # Reads the daily information of an airport weather station
+   #   from weather underground.
+   # Data is formatted and transformed into a data frame.
+   #
+   # Args:
+   #   station: A string representing the naming convention of an airport on
+   #             weather underground.
+   #   date: A date in standard unambiguous format i.e. "2011-08-07"
+   #
+   # Returns:
+   #   The data frame of online information from the assigned day.
+   require(httr)
+   require(RCurl)
+   if(!is.POSIXct(date) & !is.Date(date)){
+     stop('Date must be of the type POSIXct.')
+   }
+
+   base <- 'http://www.wunderground.com/history/airport/'
+   end <- 'DailyHistory.html?format=1'
+   # parse date
+   m <- as.integer(format(date, '%m'))
+   d <- as.integer(format(date, '%d'))
+   y <- format(date, '%Y')
+
+   # compose final url
```

```

+   finalUrl <- paste(base,
+
+                       station,
+
+                       '/', y,
+
+                       '/', m,
+
+                       '/', d,
+
+                       '/', end, sep='')
+   tf <- 'tf.csv'
+
+   # reading in as raw lines from the web server
+   # contains <br> tags on every other line
+   flag <- try(
+
+       {
+
+           resp <- GET( finalUrl )
+
+
+           writeBin( content(resp, 'raw'), tf)
+
+       },
+
+       silent = T
+
+   )
+   if(
+
+       class( flag ) == 'try-error' |
+
+       ( resp$status_code == 404 )
+
+   ){
+
+       download.file( finalUrl,
+
+                       tf,
+
+                       mode = 'wb',
+
+                       method = 'curl')
+
+   }
+
+

```

```

+ data <- read.csv( tf,
+                   skip=1,
+                   header=T )
+ file.remove( tf )
+
+ # only keep records with more than 5 rows of data
+ if(nrow(data) > 5 )
+ {
+   colnames(data)[1]<-'TimeLocal'
+   flag <- grep('DateUTC', colnames(data), invert = T)
+   # Remove DateUTC column
+   data <- data[,flag]
+
+   # convert Time column into properly encoded string
+   data[[1]] <- strptime(data[[1]], format='%I:%M %p')
+   data[[1]] <- substr(data[[1]], 11, 19)
+   date <- format(date, '%Y-%m-%d')
+   data[[1]] <- str_c(date,data[[1]])
+
+   # remove all times that didn't occur on the hour and convert
+   # time to proper format
+   if (station == 'KBOS'){
+     data<-data[grep(':',54', data[[1]]),]
+   } else if(station == 'KBED'){
+     data <- data[grep(':',56', data[[1]]),]
+   }
+
+   data[[1]]<-ymd_hms(data[[1]], quiet=T)
+
+   # sort and fix rownames

```



```

+   data <- data[order(data[[1]]), ]
+   row.names(data) <- 1:nrow(data)
+
+
+   # Done
+   return(data)
+ }
+ }

> DegConverter <- function(data, base = 'celsius'){
+   # Converts degrees from Celsius to Fahrenheit and vice versa.
+   #
+   # Args:
+   #   data: A vector of temperatures that is to be converted
+   #   base: A character string defining the original temperature scale
+   #         Default is celsius.
+   # Returns:
+   #   The vector of converted temperatures.
+   n <- length (data)
+   # Error handling
+   if (n < 1){
+     stop ("Argument 'data' is of zero length.")
+   }
+   if (TRUE %in% is.na(data)){
+     stop ("Argument 'data' must not have missing values.")
+   }
+   if (base == 'celsius'){
+     data <- data*(9/5)+32
+   }
+   else
+     data <- (data - 32)*(5/9)

```

```

+
+   return (data)
+ }

> AddIndexColumns<-function(df){
+   # Function to add columns to an input data frame.
+   # The added columns are taken from the POSIXct class
+   # column of the data frame.
+   # Args: df: A data frame object whose first column is
+   #       assumed to be of the class POSIXct
+   # Returns: df: The input df with five additional columns
+   #         Hour, Day, Week, Month, Season
+   # Note: Requires the lubridate package.
+
+   if (is.POSIXct(df[[1]]) || is.Date(df[[1]))){
+     library(lubridate)
+     df$Hour <- hour(df[[1]])
+     df$Day <- day(df[[1]])
+     df$Week <- week(df[[1]])
+     df$Month <- month(df[[1]])
+     df$Season <- ifelse(
+       (df$Month == 1|
+        df$Month == 2|
+        df$Month == 12),
+       "DJF",
+       ifelse(
+         (df$Month == 3|
+          df$Month == 4|
+          df$Month == 5),
+         "MAM",
+         ifelse(

```

```

+         (df$Month == 6|
+           df$Month == 7|
+           df$Month ==8),
+         "JJA",
+         ifelse(
+           (df$Month == 9|
+             df$Month == 10|
+             df$Month == 11),
+           "SON", NA))))
+   return(df)
+ }
+ else{
+   stop('The first column must be of the class POSIXct.')
```

```

+ }
+ }

> SkyInfraredRadiation <- function(DB_temps, DP_temps, base = 'celsius'){
+   # Approximates horizontal infrared radiation from dry and wet bulb temps.
+   #
+   # Args:
+   #   DB_temps: A vector of dry bulb temperatures in celsius
+   #   DP_temps: A vector of dewpoint temperatures in celsius
+   #   base: A character string defining the original temperature scale
+   #         Default is celsius.
+   # Returns:
+   #   The vector of infrared radiation intensity in w/m^2.
+   n <- length (DB_temps)
+   n2 <- length(DP_temps)
+   # Error handling
+   if (n < 1 | n2 < 1){
+     stop ("Argument 'DB_temps' or 'DP_temps' is of zero length.")
```

```

+ }
+ if (TRUE %in% is.na(DB_temps)){
+   stop ("Argument 'DB_temps' must not have missing values.")
+ }
+ if (TRUE %in% is.na(DP_temps)){
+   stop ("Argument 'DP_temps' must not have missing values.")
+ }
+ #Begin Calculations
+ if (base == 'celsius'){
+   HIR <- (.787 +
+           .764*log((DP_temps+273)/273))*(5.6697e-8)*(DB_temps + 273)^4
+ }
+ else{
+   DP_temps <- DegConverter(DP_temps, base = F)
+   DB_temps <- DegConverter(DB_temps, base = F)
+   HIR <- (.787 +
+           .764*log((DP_temps+273)/273))*(5.6697e-8)*(DB_temps + 273)^4
+ }
+ return(HIR)
+ }

> RadiationSplitResults <- function(file = 'solarOutput.txt'){
+
+   RadComponents <- read.table(file)
+   DNI <- RadComponents[[4]]
+   DHI <- RadComponents[[5]]
+
+   comp.df <- data.frame(DNI, DHI)
+
+   return(comp.df)
+

```

+ }

A.1.4 Demo: EPW from online data

This demonstration is designed to demonstrate how to create a basic weather data file in the EnergyPlus Weather (EPW) file format. Testing was completed on a Windows 7 64-bit operating system. To follow along the user will need to download and install three additional items. First, install a version of the statistical software package R R Development Core Team (2012). R-2.14.2 and R-2.15.0 have been used for testing. To calculate the necessary solar data the user must also install DaySIM. Finally, a typical meteorological year file in the EPW format should be saved in the current working directory. This walkthrough will use the Boston, MA TMY3 file from the Department of Energy.

Several functions, previously generated in order to facilitate the generation of the EPW files, are located in Subsection A.1.3. Load these functions prior to attempting the demo. To begin we will add in the necessary packages.

```
> require(lubridate)
> require(plyr)
> require(stringr)
> require(zoo)
```

We will work with the Hanscom Air-Force Base to re-create the KBED EPW file. This function will pull one day's worth of data from the online server. For example:

```
> date <- as.Date(Sys.Date()-1)
> data <- wunder_daily('KBED', date)
> print(data[c(1:3),])
```

Extending this function we can easily gather one year of weather data:

```
> # get data for a range of dates
> date.range <- seq.Date(from=as.Date('2011-01-01'),
+                         to=as.Date('2011-12-31'),
+                         by='1 day')
> # pre-allocate list
```

```

> data.list <- vector(mode='list',
+                     length=length(date.range))
> # loop over dates, and fetch data
> for(i in seq_along(date.range))
+ {
+   data.list[[i]] <- wunder_daily('KBED', date.range[i])
+ }

> # stack elements of list into DF, filling missing columns with NA
> KBED.data <- ldply(data.list)
> KBED.data <- AddIndexColumns(KBED.data)
>
> # # KBED data is characteristically reported on the hour.  Select
> # # only that data recorded on the hour.
> # KBED.data <- KBED.data[grepl(':56', KBED.data[[1]]),]
> # row.names(KBED.data) <- 1:length(KBED.data[[1]])

```

It is a good idea to save this raw data prior to any processing. We will save in the current directory:

```

> # Save to CSV
> # Not Used: raw.path <- paste('~\\path\\to\\',
> #                               'my\\directory\\',
> #                               'KBED.csv',
> #                               sep='')
> # write.csv(KBED.data, file=file(raw.path), row.names=FALSE)
> # rm(data.list, date.range, i, KBED.data)
> # KBED.data <- read.csv(raw.path, as.is = T)
>
> write.csv(KBED.data,
+           file='KBED.csv',

```

```

+         row.names = F)
>

> # Grab the data from the file and put back into workspace
> KBED.data <- read.csv('KBED.csv', as.is = T)
> # Convert the object back into POSIXct class
> KBED.data[[1]] <- as.POSIXct(KBED.data[[1]])
>

> # End raw data grab

```

Now that we have the raw data saved outside of R as well as loaded into the workspace we can choose to process however we like. For this simplified EPW file the processing will occur as described in Fig. A-2

```

> # Begin processing of raw data
>

> # Create merging data frame in order to fill missing values
> # The '00:56' is an artifact of KBED itself
> one.hour.interval <- seq(as.POSIXct('2011-01-01 00:56:00'),
+                          as.POSIXct('2011-12-31 23:56:00'),
+                          by='1 hour')
> x <- as.data.frame(one.hour.interval)
> colnames(x)[1] <- colnames(KBED.data)[1]
> # Merge and remove duplicates
> KBED.data <- merge(KBED.data, x, all.y = T)
> KBED.data <- KBED.data[!duplicated(KBED.data[[1]]), ]
> rownames(KBED.data) <- 1:length(KBED.data[[1]])
> # Data Flags need to be removed. These are -9999.0
> KBED.data <- KBED.data[as.numeric(KBED.data[[2]])>-9999, ]
> KBED.data <- KBED.data[as.numeric(KBED.data[[3]])>-9999, ]
> KBED.data <- KBED.data[as.numeric(KBED.data[[4]])>-9999, ]
> KBED.data <- KBED.data[as.numeric(KBED.data[[5]])>-9999, ]

```



```

> KBED.data[[8]] <- as.numeric(KBED.data[[8]])
> KBED.data <- KBED.data[as.numeric(KBED.data[[8]])>-9999, ]
> KBED.data[[10]] <- as.numeric(KBED.data[[10]])
> KBED.data <- KBED.data[as.numeric(KBED.data[[13]])>-9999, ]
> # Remerge
> KBED.data <- merge(KBED.data, x, all.y = T)
> KBED.data <- KBED.data[!duplicated(KBED.data[[1]]), ]
> rownames(KBED.data) <- 1:length(KBED.data[[1]])
> KBED.data[[10]][8760] <- 0 # Precipitation inches
> #Create zoo object to fill NA's
> KBED.zoo <- zoo(mapply(FUN = as.numeric,
+                       KBED.data[, c(2:5, 8,10, 13)]),
+               KBED.data[[1]])
> KBED.zoo <- na.locf(KBED.zoo,
+                   na.rm = F,
+                   fromLast = T)
> KBED.data[, c(2:5, 8,10, 13)] <- coredata(KBED.zoo)
> # Not Used: processed.path <- paste('~\\path\\to\\',
> #                                     'my\\directory\\',
> #                                     'KBED_processed.csv', sep='')
> #   write.csv(KBED.data,
> #             processed.path,
> #             row.names = F)
>
> write.csv(KBED.data,
+           'KBED_processed.csv',
+           row.names = F)
>
> # Clean up workspace
> # rm(KBED.data,KBED.zoo,x)

```

Once all data except for solar is processed we can alter the respective columns of the base EPW file saved in the directory. Read the stock EPW file into the workspace and convert the necessary units. All variables of the EPW file are in standard international units.

```

> # Create a new data frame that will be used to write the epw file.
> # Not Used: epw.path <- paste('~\\path\\to\\',
> #
> #                                     'my\\directory\\',
> #                                     'USA_MA_Boston-Logan.Intl.AP.725090_TMY3.epw',
> #                                     sep='')
> #
> #     epw.df <- read.csv(file = epw.path,
> #
> #                                     skip=8,header=F)
> #
> #     fill <- readLines(epw.path,n=8)
> #
> #     KBED.data <- read.csv(processed.path)
>
> epw.df <- read.csv(file =
+
+                                     'USA_MA_Boston-Logan.Intl.AP.725090_TMY3.epw',
+
+                                     skip = 8,
+
+                                     header = F)
> fill <- readLines('USA_MA_Boston-Logan.Intl.AP.725090_TMY3.epw',
+
+                                     n=8)
> KBED.data <- read.csv('KBED_processed.csv')
> # convert units of the EnergyPlus required columns:
>
> epw.df[[7]] <- round(DegConverter(as.numeric(KBED.data$TemperatureF),
+
+                                     base = F), 1)
> epw.df[[8]] <- round(DegConverter(as.numeric(KBED.data$Dew.PointF),
+
+                                     base = F), 1)
> epw.df[[9]] <- KBED.data$Humidity
> epw.df[[10]] <- as.numeric(KBED.data$Sea.Level.PressureIn) * 3386
> epw.df[[13]] <- SkyInfraredRadiation(epw.df[[7]],epw.df[[8]])

```

```

> epw.df[[21]] <- KBED.data$WindDirDegrees
> epw.df[[22]] <- as.numeric(KBED.data$Wind.SpeedMPH) * 0.44704
> epw.df[[34]] <- as.numeric(KBED.data$PrecipitationIn) * 25.4
> # Fill Remaining columns with missing values
> # as defined by auxillary programs
> # guide.
> epw.df[,c(11,12)] <- rep(9999, 8760)
> epw.df[[14]] <- rep(9999, 8760)
> epw.df[,c(17:20)] <- rep(99999, 8760)
> epw.df[,c(23,24)] <- rep(99, 8760)
> epw.df[,c(25, 26)] <- rep(9999, 8760)
> epw.df[,c(29, 31, 33)] <- rep(999, 8760)
> epw.df[[30]] <- rep(.999, 8760)
> epw.df[,c(32, 35)] <- rep(99, 8760)
> # Change the year value to 2002 becuae it
> # will be uniform and is arbitrary
> epw.df[[1]] <- rep(2002, 8760)
>

```

Once converted and placed into correct format now simply write the new EPW file. Note that this EPW file still requires observed solar radiation data.

```

> # Not Used: output.path <- paste('~\\research\\uhimodeling\\',
> #                               'rawdata\\epwfiles\\',
> #                               'test_KBED_2011.epw',
> #                               sep='')
>
> output.path <- 'demo_KBED_2011.epw'
> write.table(fill,
+           output.path,
+           quote = FALSE,

```

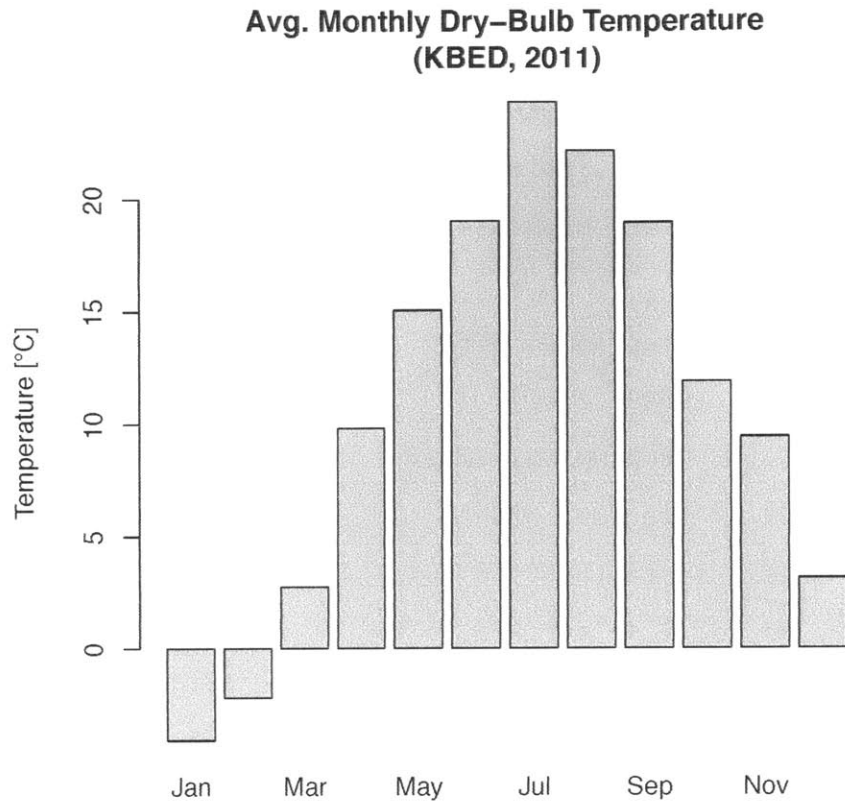


Figure A-3: Average Monthly dry-bulb temperature at KBED in 2011.

```

+         row.names = FALSE,
+         col.names = FALSE)
> write.table(epw.df,
+             output.path,
+             append = TRUE,
+             quote = FALSE,
+             row.names = FALSE,
+             col.names = FALSE,
+             sep = ',')

```

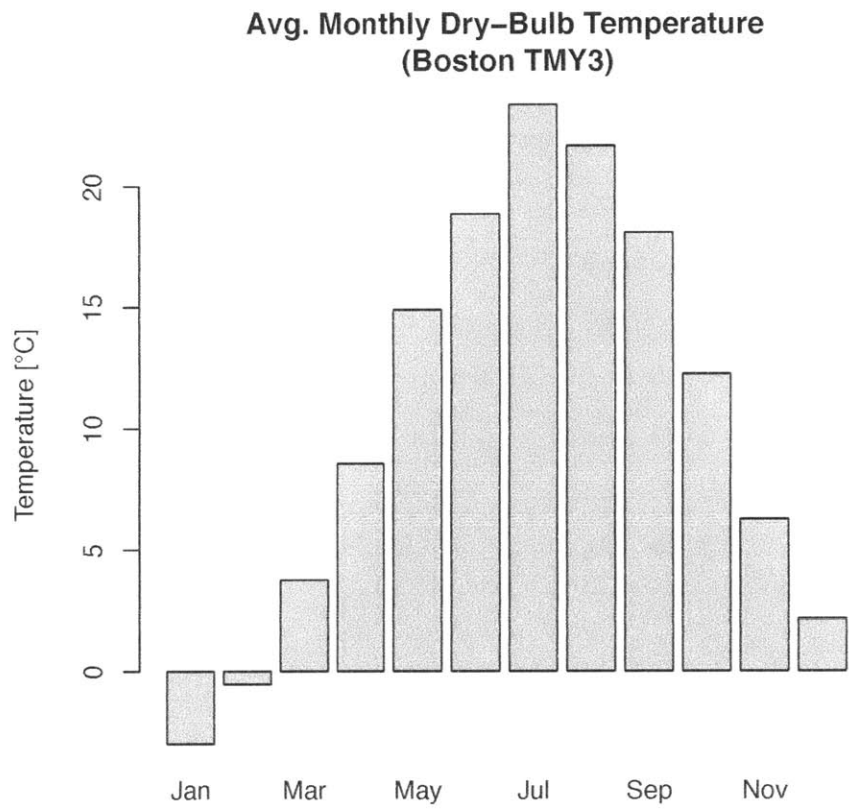


Figure A-4: Average Monthly dry-bulb temperature of the Boston TMY3 file.

Demo: Accessing Sustainable Design Lab @ MIT Data

The Sustainable Design Lab MIT has recently installed an operational weather station within a building canyon on campus. Data is collected and hosted on a public server. Follow the link to the data and save within the current working directory. Once the data is loaded into the workspace we have:

```
> # The data is reported at five minute intervals
```

```
> MIT.df[1:3,]
```

```
Time..Eastern.Daylight.Time Wind.Dir... Wind.Speed...m.s Gust.Speed...m.s
1      2013-02-12 17:20:00          58           0.8           1.5
2      2013-02-12 17:25:00          56           0.8           2.3
3      2013-02-12 17:30:00          51           0.8           2.0
Pressure..mbar Temp...C RH... DewPt...C Batt..V
1      1007.8      5.26 53.6      -3.39  4.19
2      1007.8      5.15 53.7      -3.46  4.20
3      1007.9      5.08 53.9      -3.48  4.21
```

The data spans a period from 2013-02-12 17:20:00 to 2013-05-05 00:40:00 and data is reported every five minutes, which implies that an ideal data set would have 23405 entries. Counting the number of entries, the MIT data has 23405 reported entries as of 2013-05-05. Now we aggregate the data into an hourly format, write to a .csv file, and plot a period of interest.

```
> # Make data frame into a multi-dimensional zoo object
```

```
> MIT.zoo <- zoo(MIT.df[,c(2:length(MIT.df))],MIT.df[,1])
```

```
>
```

```
> # Aggregate the zoo object with the function toHourly
```

```
> MIT.zoo <- toHourly(MIT.zoo)
```

```
> # Write the hourly data to a data frame object and then to csv file
```

```
> hourMIT.df <- data.frame(Time = format(index(MIT.zoo),'%Y-%m-%d %H:%M:%S'),
```

**Hourly Dry-Bulb Temperature
(MIT SDL, 2013-05-05)**

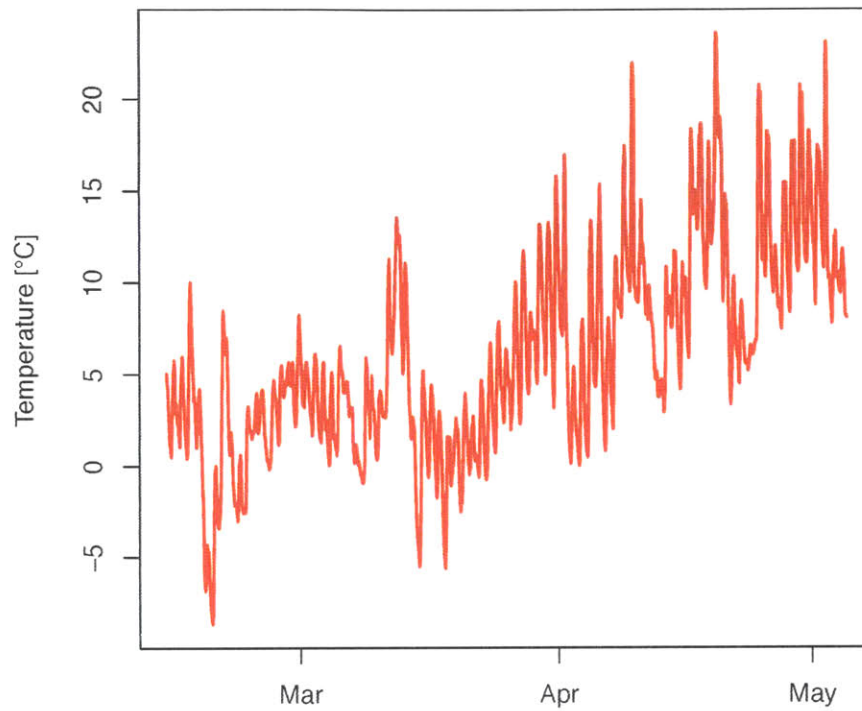


Figure A-5: Hourly dry-bulb temperature recorded at the weather station monitored by the Sustainable Design Lab @ MIT.

```
+           round(as.data.frame(MIT.zoo),2),  
+           stringsAsFactors=F)  
> # plot the data frame for dry-bulb temperature
```

**Avg. Monthly Dry-Bulb Temperature
(MIT SDL, 2013-05-05)**

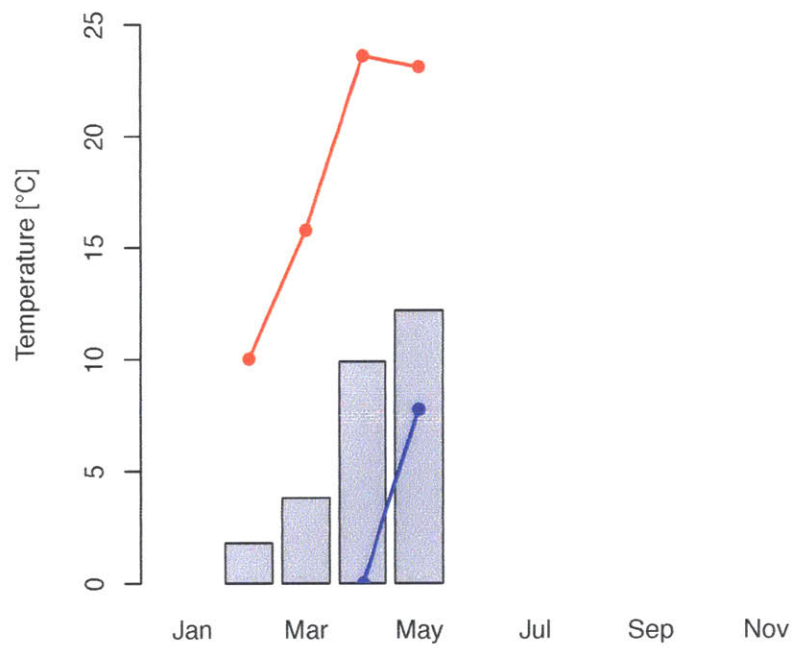


Figure A-6: Average monthly dry-bulb temperature recorded at the weather station monitored by the Sustainable Design Lab @ MIT through 2013-05-05. Monthly maximum and minimum dry-bulb temperatures are identified by the red and blue lines, respectively.

A.1.5 Demo: Solar Data for EPW File

```
> require(solar)
```

Similar to the previous sections we will use first access the solar data from the server.

```
> # get data for a range of dates
> date.range <- seq.Date(from=as.Date('2011-01-01'),
+                         to=as.Date('2011-12-31'),
+                         by='1 day')
> # pre-allocate list
> data.list <- vector(mode='list',
+                     length=length(date.range))
> # loop over dates, and fetch data
> for(i in seq_along(date.range))
+ {
+   data.list[[i]] <- KeneliStation_daily(date.range[i])
+ }
```

Once the data is in the workspace it must be processed

```
> tmp <- ldply(data.list)
> #combine the data from 5min into 1hour intervals
> tmp.zoo <- zoo(tmp$Solar, tmp$Timestamp)
> tmpind.hour <- format(index(tmp.zoo),
+                       '%Y-%m-%d %H')
> tmp <- aggregate(tmp.zoo,
+                  tmpind.hour,
+                  mean)
> index(tmp) <- ymd_hms(str_c(index(tmp),
+                              ":00:00"),
+                       tz = 'EST',
```

```

+             quiet = T)
> one.hour.interval <- seq(as.POSIXct('2011-01-01 00:00:00',
+             tz = 'EST'),
+             as.POSIXct('2011-12-31 23:00:00',
+             tz = 'EST'),
+             by='1 hour')
> x <- one.hour.interval
> x <- zoo(,x)
> t <- merge(tmp,x, all = F)
> t <- merge(t, x)
> tmp.zoo <- t
> tmp.hourly <- data.frame(TimeLocal = index(tmp.zoo),
+             SolarRadiation = coredata(tmp.zoo))
> # Calculate when sun is up and down
> x <- one.hour.interval
> BTd <- fBTd(mode = 'serie',
+             year = 2011)
> sold <- fSold(lat = 42.36,
+             BTd = BTd)
> BTi <- local2Solar(x,
+             -71.03)
> solI <- fSolI(sold,
+             BTi = BTi)
> solI <- as.data.frame(coredata(solI))
> # Pad zeros where sun is down based on solI
> for(i in 1:length(solI$aman)){
+   if(solI$aman[i] == 0) tmp.hourly$SolarRadiation[i] <- 0
+ }
> tmp.zoo <- zoo(tmp.hourly$SolarRadiation,
+             tmp.hourly$TimeLocal)

```

```

> # Now fill the NA values using zoo objects
> tmp.zoo<- na.locf(tmp.zoo,
+                   na.rm = F)
> tmp.hourly <- data.frame(TimeLocal = one.hour.interval,
+                           SolarRadiation = coredata(tmp.zoo))
> tmp.hourly <- AddIndexColumns(tmp.hourly)

```

Now that the radiation data has been processed into hourly values of the total solar radiation we need to prepare a file that can be split into the diffuse and direct components of irradiation. To accomplish this split we will use the Reindl method as noted in Chapter 3 Reindl *et al.* (1990). An executable file is included with DAYSIM entitled `gen_reindl.exe` and the default location on Windows is `C:\DAYSIM\bin\gen_reindl .`

```

> # Build the data frame that will be written to a .txt
> reindl.df <- tmp.hourly[, c('Month',
+                             'Day',
+                             'Hour',
+                             'SolarRadiation')]
> reindl.df$SolarRadiation <- ceiling(
+                               reindl.df$SolarRadiation)
> reindl.df[[3]] <- reindl.df[[3]] + 1
> # Need an output file for the data
> # Not Used: solar.output <- paste('~\path\ ',
> #                               'to\my\directory\ ',
> #                               'test_solarData.txt',
> #                               sep='')
>
> solar.output <- 'demo_solarData.txt'
> write.table(reindl.df,
+             solar.output,

```

```

+         append = F,
+         col.names = F,
+         row.names = F)

> # Path to gen_reindl
> path.to.gen.reindl <- 'C:\\\\DAYSIM\\bin\\gen_reindl'
> # Path to input data
> path.to.input.data <- paste(getwd(),
+                             '\\',
+                             solar.output,
+                             sep='')
> # Path to output file
> path.to.output.data <- paste(getwd(),
+                               '\\',
+                               'demo_',
+                               'solarData',
+                               '_split',
+                               '.txt',
+                               sep = '')
> # Options
> options.for.Boston <- '-m 75 -l 71.02 -a 42.37'
> # String to run via .bat file
> cmd.line.gen.reindl.string <- paste(path.to.gen.reindl,
+                                     '-i',
+                                     path.to.input.data,
+                                     '-o',
+                                     path.to.output.data,
+                                     options.for.Boston,
+                                     sep = ' ')
> # Write the resulting string to a batch file
> fileConn <- file("reindl_call.bat")

```

```

> writeLines(cmd.line.gen.reindl.string,
+           fileConn)
> close(fileConn)
>

```

Run the batch file that was created. The radiation data is now ready to be placed into the EPW file created in Section A.1.4.

```

> fill <- readLines('demo_KBED_2011.epw',n=8)
> epw.df <- read.csv('demo_KBED_2011.csv',skip=8,header=F)
> epw.df[[15]] <- read.table(path.to.output.data,
+                           header=F)[[4]]
> epw.df[[16]] <- read.table(path.to.output.data,
+                           header=F)[[5]]
> write.table(fill,
+            'demo_KBED_2011.epw',
+            quote = FALSE,
+            row.names = FALSE,
+            col.names = FALSE)
> write.table(KBED.2011epw.df,
+            'demo_KBED_2011.epw',
+            append = TRUE,
+            quote = FALSE,
+            row.names = FALSE,
+            col.names = FALSE,
+            sep = ',')
>

```

The KBED EPW file used for simulations described in Chapter 3 is now complete.

Summer Week Irradiation
(KMACAMBR4, 2011)

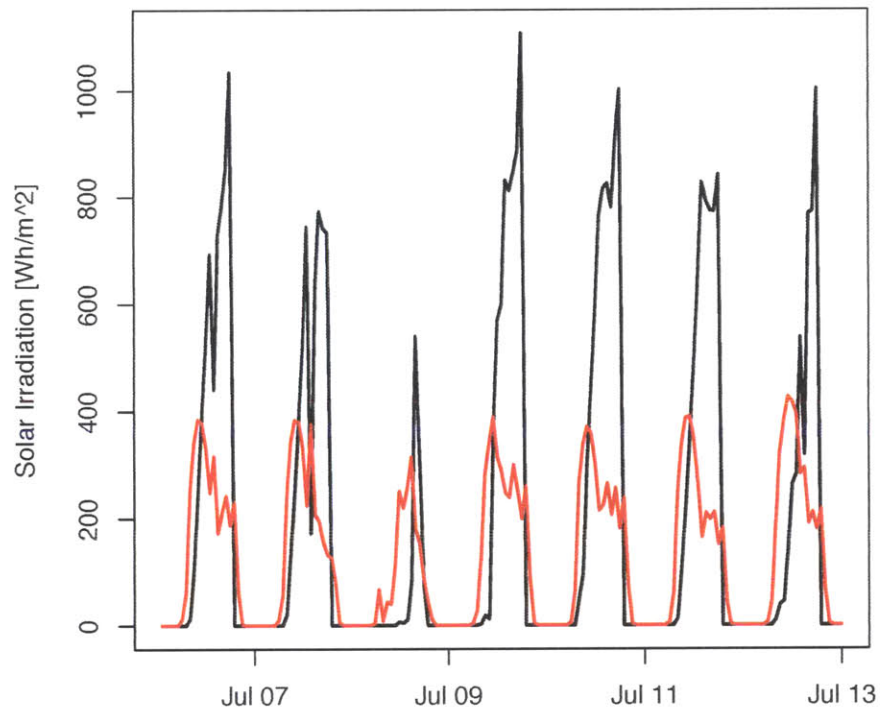


Figure A-7: Hourly Direct Normal Irradiance and Diffuse Horizontal Irradiance for a summer week in 2011 collected from an urban weather station.

Appendix B

Whole Building Models

Urban micro-climates are known to impact building energy use (see chapter 2). Buildings with envelope dominated loads such as residential and low-rise types are more climatically sensitive. To assess the ability of urban micro-climate models to improve predictions of building energy use during the design of urban residential and low-rise buildings this thesis employs whole-building thermal simulation.

To calculate the actual impact of urban climate on energy use predictions each building was simulated using the observed values from the urban and rural stations. Then simulated weather files were used to compare the ability of each model to recreate the urban environment. Descriptions of each building model follows.

B.0.6 Single-Family Building

The single-family building studied is a model constructed to the Building America Benchmark building specification (Hendron and Engebrecht, 2010). Plant and equipment were auto-sized based on the Boston-Logan TMY3 design day data for summer and winter. The ground temperatures are calculated via the Winkelmann method per the Building America building specification (Winkelmann, 2002).

Form

The single-family building is a two story building with a rectangular floor plate (L:W = 6:5). The total conditioned area is 220 m² (2400 ft²) with a 110 m² (1200 ft²) unconditioned attic. The roof is a gable roof at 6:12 pitch and the foundation is slab-on-grade.

Envelope

Opaque envelope components of the single-family building are of light weight construction and built to International Energy Conservation Code 2009 (IECC) Council (2009). A Boston, MA detached single-family home requires a nominally rated R-value of 2.3 W/m²K (13 hft²°F/Btu) with an additional 0.13 m (5 in) of outboard continuous insulation. The wall is modeled as built up layers using a framing factor of 0.23, which is representative of 0.05 m X 0.1 m (2 in X 4 in) construction @ 0.41 m on center (16 in on center). Interior walls are of similar construction, but lack insulation. Attic insulation is required at 6.69 W/m²K (38 hft²°F/Btu) and is laid flat along the attic floor.

Glazed constructions are confined to the exterior walls. The exterior window glazing has a solar heat gain coefficient is 0.245 and the U-factor of the entire assembly is 1.987 W/m²K (0.35 Btu/hft²°F). The window-to-wall ratio is 15%. There are no skylights and no internal glazing.

Mechanical Equipment

The building is sectioned into two thermal zones and an unconditioned attic. A single conditioned zone defines the living space comprised of both stories and a zone defines the return air plenum. All cooling, dehumidification and heating is done mechanically at the zone level.

Each zone is heated by the object 'Coil:Heating:Gas', which is a simplified capacity model of a gas furnace with node connections only in the building's air loop. Nominal capacity of the coil is 1.432E+04 W. Each coil uses a default gas furnace efficiency of

0.78. Gas consumption in the model is a function of the sensible heat load to burner efficiency ratio and a part-load correction.

A packaged electric air-conditioning unit is specified for zone cooling and is modeled with the object ‘Coil:Cooling:DX:SingleSpeed’. The condenser is air-cooled and the default performance curves are supplied. Total cooling capacity [W] rated at $1.13\text{E}+04$, sensible heat ratio rated at 0.74, and air flow rate [m^3/s] is rated at $5.86\text{E}-01$. The rated COP of the unit is 3.95. Power consumption of this object is the sum of compressors and condenser fan power.

Dehumidification of the room air is accomplished locally on the demand side with the zone equipment object ‘ZoneHVAC:Dehumidifier:DX’. At rated conditions the zone dehumidifier has an energy factor of 1.2 L/kWh.

Internal Gains & Schedules

Internal gains are scheduled as a fraction of the design peak gains on a per zone basis. Peak internal gains due to lights, plug loads, appliances, and people are in Table B.1. Infiltration of the unconditioned attic zone is specified by a design effective leakage area. Infiltration of the living zone is calculated via a ‘ZoneInfiltration:FlowCoefficient’ object, which is a function of flow, stack and wind coefficients, schedule fraction, temperature difference, and wind speed. Natural ventilation has a design flow rate of $0.001 \text{ m}^3/\text{s}$, which is modified by the schedule fraction, temperature difference and wind speed. There is no mechanical ventilation and all fresh air is supplied via infiltration and scheduled natural ventilation.

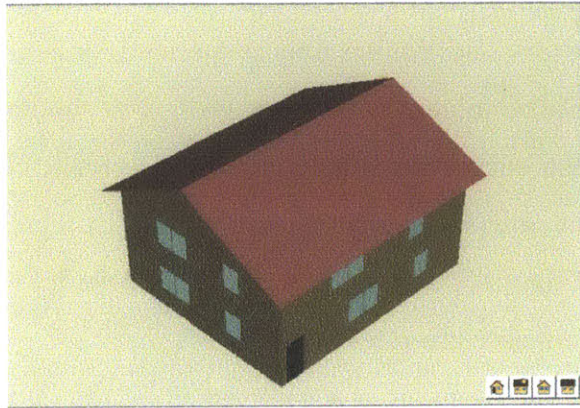


Figure B-1: Single-Family building used for EnergyPlus simulations.

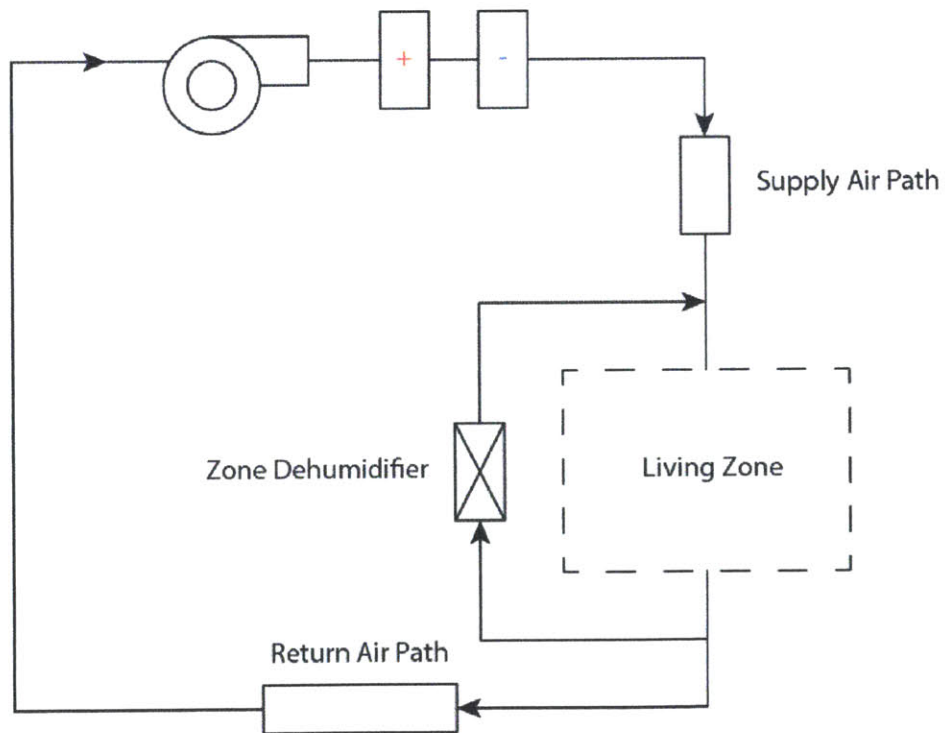


Figure B-2: Schematic diagram of the single zone single family building heating and cooling system. Dehumidification occurs at the zone level and the fan is in a 'blow-through' configuration.

B.0.7 Small Office Building

The small office building studied is a model constructed to the Department of Energy Benchmark building specification (Torcellini *et al.*, 2008). Plant and equipment were auto-sized based on the Boston-Logan TMY3 design day data for summer and winter. The ground temperature at the building is a constant 18°C per the benchmark files.

Form

The small office building is a single story building with a rectangular floor plate (L:W = 3:2). The total conditioned area is 511 m² with an unconditioned attic. The roof is a hip roof and the foundation is a slab-on-grade floor.

Envelope

Each building within the benchmark building set is constructed to meet ASHRAE 90.1-2004 (American Society of Heating Refrigerating and Air Conditioning Engineers, 2004). Therefore the envelope system for this iteration of the small office benchmark building follows the specification for Boston, MA, which is in climate zone 5A. Exterior walls are composed .03 m (1 in.) stucco, .2032 m (8 in.) thick concrete, .05 m (2 in.) continuous insulation, and .015 m (0.5 in.) gypsum board applied to the interior. The floor is 0.1016 m (4 in) of non-insulated, on-grade concrete with a carpet interior modeled as no-mass. Interior walls that divide thermal zones are modeled as two adjacent .015 m (0.5 in) gypsum layers. Separating each thermal zone from the unconditioned attic is the attic floor construction defined by .015 m (0.5 in) gypsum, .24 m (9.5 in.) insulation, and .015 m (0.5 in) gypsum. The final opaque construction is the exterior roof, which is defined as an exterior 0.01 m (0.4 in.) roof membrane and 0.002 m (0.08 in) metal decking on the interior.

Glazed constructions are confined to the exterior walls and a single exterior fully-glazed door. The exterior window glazing and door share identical thermal and optical properties. The solar heat gain coefficient is 0.39 and the U-factor of the each glazing assembly is 3.24 W/m²K (0.57 Btu/hft²°F). The window-to-wall ratio is 21.2%. There

are no skylights and no internal glazing.

Mechanical Equipment

The building is sectioned into five thermal zones and an unconditioned attic. Four zones are defined along the building perimeter and one zone encompasses the building core. All cooling and heating is done mechanically. There is no scheduled natural ventilation and the system operates without an economizer. Cooling and heating are done at the zone level.

Each zone is heated by the object 'Coil:Heating:Gas', which is a simplified capacity model of a gas furnace with node connections only in the building's air loop. Nominal capacity of each coil is auto-sized on a per zone basis. Each coil uses a default gas furnace efficiency of 0.8. Gas consumption in the model is a function of the sensible heat load to burner efficiency ratio and a part-load correction.

A packaged electric air-conditioning unit is specified for zone cooling and is modeled with the object 'Coil:Cooling:DX:SingleSpeed'. The condenser is air-cooled and the default performance curves are supplied. Total cooling capacity [W], sensible heat ratio, and air flow rate [m³/s] are auto-sized on a per zone basis. The rated COP of each unit is 3.67. Power consumption of this object is the sum of compressors and condenser fan power.

Internal Gains & Schedules

Internal gains are scheduled as a fraction of the design peak gains on a per zone basis. Peak internal gains due to lights, plug loads, and people are identical across zones. Infiltration of the perimeter zones is scheduled on a flow per exterior area basis, while infiltration to the attic and core is scheduled as air changes per hour. Mechanical ventilation is auto-sized to meet minimum outdoor air requirements on a per person basis. (Table B.1)

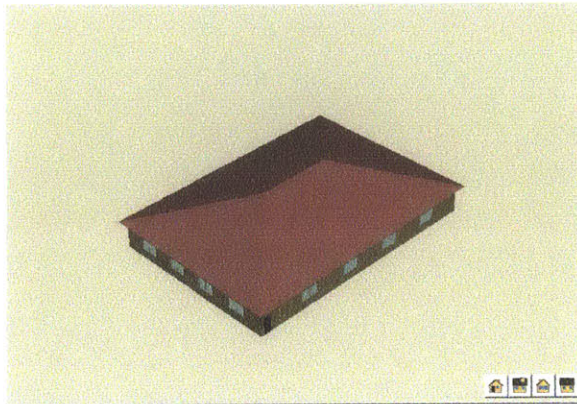


Figure B-3: Small Office building used for EnergyPlus simulations.

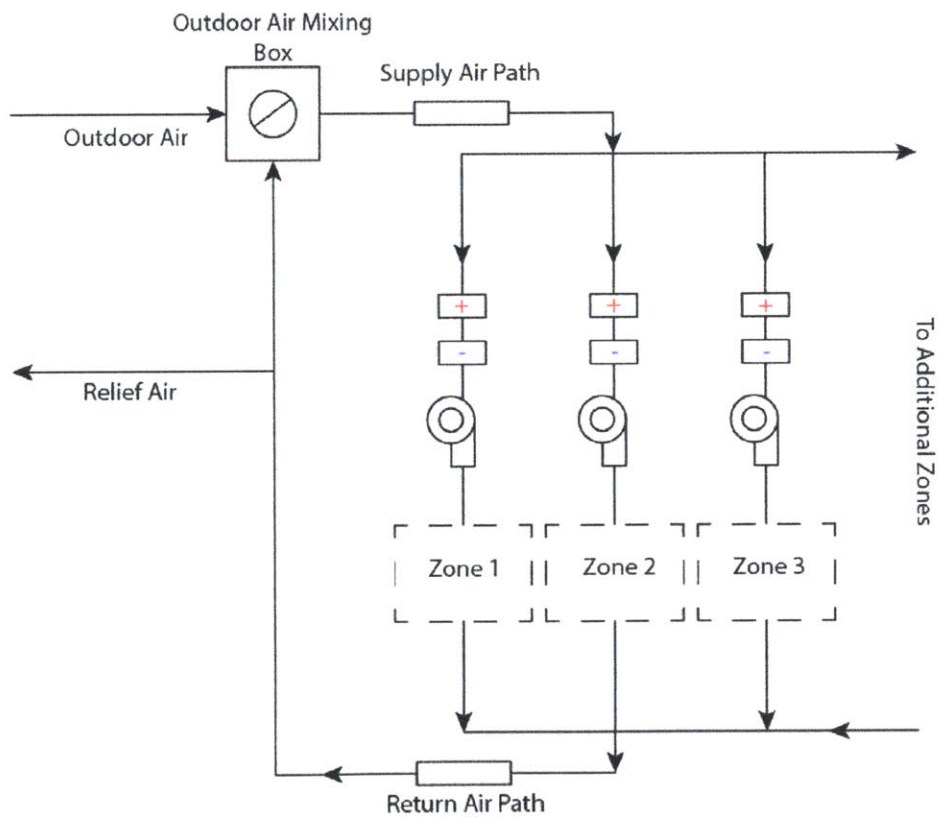


Figure B-4: Schematic diagram of the five zone small office building heating and cooling system. Zone air returns through a shared return path and passes through an outdoor air mixing box prior to being supplied to each zone.

<i>Parameter</i>	<i>Single-Family</i>	<i>Small Office</i>
Conditioned area	211 m ²	511 m ²
Schedules	Typical Building America	Typical office
Lighting power	3.4 W/m ²	11 W/m ²
Elec. Equipment	3.1 W/m ²	11 W/m ²
People	3	28
Infiltration	10.3 ACH @ 50Pa	2.4 ACH
Glazing	15%	15%
Constructions	Stud walls; attic roof; slab-on-grade floor per 2003 IECC	Mass walls; attic roof; slab-on-grade floor per ASHRAE 90.1-2004 5A
Zones	1	5 (4 perimeter + 1 core)
HVAC Objects	Coil:Cooling:DX:SingleSpeed; Coil:Heating:Gas; HVAC:Dehumidifier:DX	Coil:Cooling:DX:SingleSpeed; Zone- Coil:Heating:Gas

Table B.1: Simulation parameters for each EnergyPlus building model used in this study.

Appendix C

References

- Ahmad, K., Khare, M., and Chaudhry, K., 2005. Wind tunnel simulation studies on dispersion at urban street canyons and intersections - a review. *Journal of Wind Engineering and Industrial Aerodynamics*, 93 (9), 697–717.
- AIA, 2012. The American Institute of Architects - AIA 2030 The Commitment, Programs & Initiatives. Accessed from: [http : //www.aia.org/about/initiatives/AIAB079544](http://www.aia.org/about/initiatives/AIAB079544).
- American Society of Heating Refrigerating and Air Conditioning Engineers, Energy Standard for Buildings Except Low-Rise Residential Buildings 90.1-2004. , 2004. , Technical report, American Society of Heating, Refrigerating and Air-Conditioning Engineers, Inc.
- Andolsun, S., Culp, C.H., and Haberl, J., 2010. EnergyPlus vs DOE-2: The Effect of Ground Coupling on Heating and Cooling Energy Consumption of a Slab-on-grade Code House in a Cold Climate. *In: Fourth National IBPSA-USA Conference, New York, USA*.
- Arnfield, A.J., 2003. Two decades of urban climate research: a review of turbulence, exchanges of energy and water, and the urban heat island. *International Journal of Climatology*, 23 (1), 1–26.
- Baklanov, A., *et al.*, 2005. On the parameterisation of the urban atmospheric sublayer in meteorological models. *Atmospheric Chemistry and Physics Discussions*, 5 (6), 12119–12176.
- Bechtel, B., 2011. Multitemporal Landsat data for urban heat island assessment and classification of local climate zones. *In: Urban Remote Sensing Event (JURSE), 2011 Joint, Apr.*. IEEE, 129 –132.
- Bhandari, M., Shrestha, S., and New, J., 2012. Evaluation of weather datasets for building energy simulation. *Energy and Buildings*, (0).
- Bueno, B., Norford, L., Hidalgo, J., and Pigeon, G., 2012. The urban weather generator. *Journal of Building Performance Simulation*, iFirst article, 1–13.

- Chow, D.H.C. and Levermore, G.J., 2007. New algorithm for generating hourly temperature values using daily maximum, minimum and average values from climate models. *Building Services Engineering Research and Technology*, 28 (3), 237–248.
- Committee on Ecological Impacts of Climate Change, N.R.C., 2008. *Ecological Impacts of Climate Change*. The National Academies Press.
- Council, I.C., International Energy Conservation Code. , 2009. , Technical report, International Code Council Accessed from: <http://www.iccsafe.org/content/pages/freeresources.aspx>.
- Crawley, D.B., 2008. Estimating the impacts of climate change and urbanization on building performance. *Journal of Building Performance Simulation*, 1 (2), 91–115.
- Crawley, D.B., Hand, J.W., and Lawrie, L.K., 1999. Improving the weather information available to simulation programs. In: *Proceedings of Building Simulation 99*, Vol. 2, 529–536.
- Department of Energy, 2009. Building Energy Data Book. (1.1.3) Available from: <http://buildingsdatabook.eren.doe.gov/TableView.aspx?table=1.1.3>.
- DOE, 2010. EnergyPlus Manual. *US Department of Energy (DOE)*.
- DOE, 2012. Federal Energy Management Program: Federal Sustainable Building and Campus Requirements. Accessed from: http://www1.eere.energy.gov/femp/program/sustainable_requirements.html.
- Erell, E., 2008. The Application of Urban Climate Research in the Design of Cities. *Advances in Building Energy Research (ABER)*, 2 (1), 95–121.
- for Meteorological Services, F.C. and Research, S., Federal Standard for Siting Meteorological Sensors at Airports. , 1994. , Technical report, U.S. Department of Commerce/National Oceanic and Atmospheric Administration.
- for Meteorological Services, F.C. and Research, S., National Weather Service Instruction 10-1301. , 2010. , Technical report, U.S. Department of Commerce / National Oceanic and Atmospheric Administration.
- Heal, G., Climate economics: a meta-review and some suggestions. , 2008. , Technical report, National Bureau of Economic Research.
- Hendron, R. and Engebrecht, C., 2010. Building America Research Benchmark Definition: Updated December 2009. .
- Hensen, J.L., 2011. *Building performance simulation for design and operation*. Routledge.
- Hsieh, C.M., Aramaki, T., and Hanaki, K., 2007. Estimation of heat rejection based on the air conditioner use time and its mitigation from buildings in Taipei City. *Building and Environment*, 42 (9), 3125–3137.

- Junninen, H., *et al.*, 2004. Methods for imputation of missing values in air quality data sets. *Atmospheric Environment*, 38 (18), 2895–2907.
- Kanda, M., *et al.*, 2007. Roughness Lengths for Momentum and Heat Derived from Outdoor Urban Scale Models. *Journal of Applied Meteorology and Climatology*, 46 (7), 1067–1079.
- Kershaw, T., Sanderson, M., Coley, D., and Eames, M., 2010. Estimation of the urban heat island for UK climate change projections. *Building Services Engineering Research & Technology*, 31 (3), 251–263.
- Kikegawa, Y., Genchi, Y., Yoshikado, H., and Kondo, H., 2003. Development of a numerical simulation system toward comprehensive assessments of urban warming countermeasures including their impacts upon the urban buildings' energy-demands. *Applied Energy*, 76 (4), 449–466.
- Kottek, M., *et al.*, 2006. World Map of the Koppen - Geiger climate classification updated. *Meteorologische Zeitschrift*, 15 (3), 259–263.
- Landsberg, H.E., 1981. *The urban climate*. Vol. 28. Academic press.
- Lee, D.O., 2012. Urban warming? - An analysis of recent trends in London's heat island. *Weather*, 47 (2), 50 – 56.
- Lowry, W.P., 1977. Empirical Estimation of Urban Effects on Climate: A Problem Analysis. *Journal of Applied Meteorology*, 16 (2), 129–135.
- Lun, I., Mochida, A., and Ooka, R., 2009. Progress in Numerical Modelling for Urban Thermal Environment Studies. *Advances in Building Energy Research (ABER)*, 3 (1), 147–188.
- Mallick, J. and Rahman, A., 2012. Impact of population density on the surface temperature and micro-climate of Delhi. *Curr Sci*, 102, 1708 – 13.
- Masson, V., 2000. A physically-based scheme for the urban energy budget in atmospheric models. *Boundary-Layer Meteorology*, 94 (3), 357–397.
- Masters, J., 2012. Weather Forecast & Reports - Long Range & Local | Wunderground | Weather Underground. Accessed from: <http://www.wunderground.com/>.
- Mihalakakou, G., Santamouris, M., and Tsangrassoulis, A., 2002. On the energy consumption in residential buildings. *Energy and buildings*, 34 (7), 727–736.
- Oceanic, N. and Administration, A., 1992. Automated Surface Observing System (ASOS) User Guide. .
- Office of Geographic Information (MassGIS), 2011. Accessed from: <http://www.mass.gov/anf/research-and-tech/it-serv-and-support/application-serv/office-of-geographic-information-massgis/>.

- Oke, T.R., 1974. Review of urban climatology 1968-1973. *World Meteorological Organization*, 383, 152.
- Oke, T.R., 1979. Review of urban climatology 1968-1973. *World Meteorological Organization*, 539, 114.
- Oke, T.R., 1981. Canyon geometry and the nocturnal urban heat island: Comparison of scale model and field observations. *Journal of Climatology*, 1 (3), 237–254.
- Oke, T.R., 1982. The energetic basis of the urban heat island. *Quarterly Journal of the Royal Meteorological Society*, 108 (455), 1–24.
- Oke, T.R., 2006a. INITIAL GUIDANCE TO OBTAIN REPRESENTATIVE METEOROLOGICAL OBSERVATIONS AT URBAN SITES. *Instruments and Observing Methods*, Report No. 81.
- Oke, T.R., 2006b. Towards better scientific communication in urban climate. *Theoretical and Applied Climatology*, 84 (1), 179–190.
- Oke, T.R., 1992. *Boundary layer climates*. Psychology Press.
- Oke, T., 1973. City size and the urban heat island. *Atmospheric Environment (1967)*, 7 (8), 769–779.
- Oxizidis, S., Dudek, A.V., and Aquilina, N., 2007. Typical Weather Years and the Effect of Urban Microclimate on the Energy Behaviour of Buildings and HVAC Systems. *Advances in Building Energy Research*, 1 (1), 89–103.
- Oxizidis, S., Dudek, A., and Papadopoulos, A., 2008. A computational method to assess the impact of urban climate on buildings using modeled climatic data. *Energy and Buildings*, 40 (3), 215–223.
- Patz, J.A., Campbell-Lendrum, D., Holloway, T., and Foley, J.A., 2005. Impact of regional climate change on human health. *Nature*, 438 (7066), 310–317.
- Perpinan, O., 2012. solaR: Solar Radiation and Photovoltaic Systems with R. *Journal of Statistical Software*, 50 (9), 1–32.
- Plate, E.J., 1999. Methods of investigating urban wind fields - physical models. *Atmospheric Environment*, 33 (24 - 25), 3981–3989.
- R Development Core Team, 2012. R: A Language and Environment for Statistical Computing. *R Foundation for Statistical Computing*, [http : //www.R – project.org/](http://www.R-project.org/) (Vienna, Austria) ISBN 3-900051-07-0.
- Reindl, D., Beckman, W., and Duffie, J., 1990. Evaluation of hourly tilted surface radiation models. *Solar Energy*, 45 (1), 9–17.
- Santamouris, M., *et al.*, 2001. On the impact of urban climate on the energy consumption of buildings. *Solar Energy*, 70 (3), 201–216.

- Schneider, T., 2001. Analysis of incomplete climate data: Estimation of mean values and covariance matrices and imputation of missing values. *Journal of Climate*, 14 (5), 853–871.
- Taha, H., Akbari, H., Rosenfeld, A., and Huang, J., 1988. Residential cooling loads and the urban heat island – the effects of albedo. *Building and Environment*, 23 (4), 271–283.
- Tomlinson, C.J., Chapman, L., Thornes, J.E., and Baker, C., 2011. Remote sensing land surface temperature for meteorology and climatology: a review. *Meteorological Applications*, 18 (3), 296–306.
- Torcellini, P., *et al.*, 2008. DOE commercial building benchmark models. 17 – 22 Accessed from: [http : //www.nrel.gov/docs/fy08osti/43291.pdf](http://www.nrel.gov/docs/fy08osti/43291.pdf).
- United Nations, 2011. World Urbanization Prospects, the 2011 Revision. *Department of Economic and Social Affairs, New York, New York* Accessed from: [http : //esa.un.org/unup/](http://esa.un.org/unup/).
- USEPA, U.S.E.P.A., 2012. Heat Island Effect. Accessed from: [http : //www.epa.gov/heatisland/](http://www.epa.gov/heatisland/).
- Weng, Q., 2009. Thermal infrared remote sensing for urban climate and environmental studies: Methods, applications, and trends. *ISPRS Journal of Photogrammetry and Remote Sensing*, 64 (4), 335–344.
- Weng, Q., 2012. Remote sensing of impervious surfaces in the urban areas: Requirements, methods, and trends. *Remote Sensing of Environment*, 117, 34–49.
- Wilcox, S. and Marion, W., 2008. *Users manual for TMY3 data sets*. National Renewable Energy Laboratory.
- Winkelmann, F., 2002. Underground Surfaces: How to get a Better Underground Surface Heat Transfer Calculation in DOE-2.1E.. *Building Energy Simulation User News*, 23 (6), 19–26.
- Yang, X., Zhao, L., Bruse, M., and Meng, Q., 2012. An integrated simulation method for building energy performance assessment in urban environments. *Energy and Buildings*.



mistreet

18.89.0.103
main.pdf

